

POLITECNICO DI TORINO



Collegio di Ingegneria Meccanica, Aerospaziale, dell'Autoveicolo e della Produzione

Degree course of Automotive engineering

Master Thesis

**Online quality control of Resistance Spot Welding
for automotive production**

Candidate:

Mangolini Federico

Matr. s244187

Supervisor:

prof. Paolo Minetola

Company Tutor FCA:

Eng. Alessia Di Marcello

September 18, 2018

This page was intentionally left blank

“Don't be pushed around by the fears in your mind. Be led by the dreams in your heart.”

Roy T. Bennett, The Light in the Heart

Acknowledgements

Questo lavoro nasce a conclusione di una proficua e determinante esperienza di tirocinio in FCA presso l'ente Manufacturing Quality, amministrato dall'Ing. Giovanni Volpes, al quale dedico il mio primo grazie per la sua disponibilità e gentilezza nei miei confronti.

Ringrazio poi l'Ing. Alessia Di Marcello, per aver creduto in me fin dall'inizio, concedendomi la preziosa opportunità di entrare in questa grande azienda e di venire a contatto con una realtà dinamica e stimolante, all'interno della quale ho potuto fare esperienza nel settore della qualità e accrescere le mie conoscenze sui processi industriali dell'autoveicolo. Un grazie sincero va anche a tutti i colleghi conosciuti durante il tirocinio che mi hanno supportato, istruito e consigliato, insegnandomi come affrontare nel migliore dei modi il mondo del lavoro attraverso preziose lezioni di vita e consigli tecnici.

Mi riferisco in particolare a Michele D'Amico, l'autore della ricerca, con il quale ho maggiormente collaborato, e ai capi Errico Steven Vitale e Andrea Visconti.

Ringrazio inoltre il mio relatore Chiar.mo Prof. Paolo Minetola per avermi affiancato con pazienza durante tutta la stesura della mia tesi, dimostrando la sua grande competenza in materia e dandomi numerosi consigli e preziose dritte, che mi hanno permesso di realizzare un elaborato preciso e coerente.

Un riconoscimento speciale va poi a tutti i professori che in questi cinque anni mi hanno insegnato a studiare per diventare un buon ingegnere, con esami spesso difficili ma sempre adeguati al livello del corso di studi.

Passando alle persone a me più care, ci tengo in particolare a ringraziare "i Tonni", che oltre ad essere i miei migliori amici praticamente da una vita, hanno creato insieme a me questo fantastico gruppo grazie al quale condividiamo viaggi, esperienze, risate, e sane distrazioni necessarie per affrontare le fatiche di tutti i giorni.

Grazie anche a Nicoletta, carissima amica a cui sono molto legato che in questi anni mi ha spesso aiutato nelle situazioni più insidiose attraverso saggi consigli.

Grazie ai miei coinquilini, con i quali ho avuto la fortuna di condurre una serena convivenza e con cui ho condiviso un'intensa vita universitaria a Torino, confrontandoci anche nello studio.

Grazie a Carlo, Giorgio, Raquel, Pedro, Federica e a tutti gli altri compagni di corso, con cui sono riuscito subito a creare delle solide alleanze necessarie per affrontare al meglio gli esami e per condividere le gioie e i dolori di questi percorso.

Un grazie d'amore ad Alessia, che più di tutti riesce a consolarmi e ad incoraggiarmi durante i momenti più bui, e ad elogiarmi e gioire con me per gli obiettivi raggiunti.

Il ringraziamento più grande va poi a tutta la mia famiglia, nonni, zii e sorelle comprese, ma in particolare a mamma e papà che in questi anni, nonostante una lontananza sempre più pesante, hanno sempre creduto in me sostenendomi sia psicologicamente che economicamente, dandomi l'opportunità di studiare e di costruirmi un futuro importante .

Per ultimo, un Grazie particolare a chi nelle mattinate più "strette", prima degli esami, aveva la necessità impellente di fare la spesa causandomi una perdita di tempo prezioso per lo studio. Parlo del mitico Nonno Isnardo, che dall'alto della sua esperienza riteneva più importante mangiare che studiare.

Abstract

The aim of this thesis is to provide an integrated real-time control system for resistance spot welding (RSW) in FCA plants, where I began my internship in March. This project is suggested by a colleague of Manufacturing quality who purposed to eliminate statistical ultrasonic and hammer/chisel control, which are both too expensive for the production, due to the fact that they require expert and trained workers. Statistical control is mainly used to evaluate RSW process deviation and to eventually set up the machine in order to correct it. However, this system is not always able to find out all the incorrect points of the vehicles, causing excessive noise and vibration problems during the vehicle test. Therefore, the “online control system” must solve the problem of non-conformity points by increasing the robustness of the process, thanks to the automatic evaluation of the spot-weld by the welding system. In fact, this technology includes spot gun and control system, using the Joule effect to fuse the sheets metal layer and join the parts. This project considers the output parameter of the welding process, in order to find a correlation with statistical control results, which could help to create automatic reports of the spot by the welding tool. The abovementioned analysis has been developed and tested in FCA Melfi plant on a “Jeep Renegade” model by applying the proposed control process for the development of the body-in-white shop.

Table of contents

Chapter 1	Introduction	1
1.1.	Background	1
1.2.	Internship experience	2
1.2.1.	<i>Manufacturing quality</i>	3
1.2.2.	<i>Process Quality</i>	4
1.2.3.	<i>Melfi Plant business trip</i>	11
Chapter 2	Body in White	13
2.1.	B.I.W. welding tecnology	15
Chapter 3	Resistance spot welding	19
3.1.	Resistance spot welding equipment	21
3.2.	Factors and variables affecting spot weld quality	23
3.2.1.	<i>Pressure and force systems</i>	23
3.2.2.	<i>Welding current</i>	24
3.2.3.	<i>Electrode condition and geometry</i>	24
3.2.4.	<i>Welding time</i>	26
3.2.5.	<i>Surface condition</i>	27
3.2.6.	<i>Operator</i>	28
3.3.	Resistance spot welding defect	29
3.4.	RSW welding quality control	42
3.4.1.	<i>Ultrasonic systems</i>	44
3.4.1.1.	<i>Wave path</i>	45
3.4.1.2.	<i>Attenuation</i>	46
3.4.1.3.	<i>Limitations of ultrasonic testing</i>	48
3.4.1.4.	<i>Ultrasonic device</i>	50
Chapter 4	Theoretical background	53

Chapter 5	Case study	91
5.1.	Project reason	91
5.2.	Preliminary	91
5.3.	data collection	94
5.3.1.	<i>Quality Index</i>	97
5.4.	Correlation between welding parameter and U.S. control	105
5.5.	End of Analysis	113
5.6.	Future of project and implementation	114
5.7.	Cost analysis of solution implementation	115
Chapter 6	Conclusion	117
References		118

LIST OF FIGURES

Figure 1. 4M+E+Product	6
Figure 2. PPR table	8
Figure 3. Fiat 500x and Jeep Renegade in Melfi plant	11
Figure 4. B.I.W. schematic division	13
Figure 5. Resistant Spot Welding in automotive production	15
Figure 6. Time sequence of the resistance spot welding cycle.	20
Figure 7. The cutaway view of the location and shape of a weld nugget	21
Figure 8. Resistance Spot Welding gun	22
Figure 9. Deformation of tip face over time	25
Figure 10. Badly pitted tip face	25
Figure 11. Programmed and actual weld time	26
Figure 12. Weld Schedule	27
Figure 13. Missing weld	29
Figure 14. Undersized weld	30
Figure 15. Stuck weld	31
Figure 16. Excessive indentation	32
Figure 17. Expulsion/burn-through	32
Figure 18. Cracks and holes	33
Figure 19. Misallocated/edge welds	33
Figure 20. Sheet metal distortion	34
Figure 21. Extra welds	35
Figure 22. Inconsistent welds	36
Figure 23. Brittle welds	36
Figure 24. Non-round welds	37
Figure 25. Poor class A appearance	38
Figure 26. Stuck electrodes	39

Figure 27. Interfacial separation	40
Figure 28. Hammer and chisel check	44
Figure 29. Ultrasonic pulse echo spot weld tests	46
Figure 30. Ultrasonic probe	51
Figure 31. Ultrasonic scan	52
Figure 32. Schematic of the resistance spot welding process	54
Figure 33. Metal states during the welding process	57
Figure 34. Basic building block of the proposed control system	59
Figure 35. Flowchart of the control system	60
Figure 36. First-order derivative value of dynamic resistance curve	62
Figure 37. Welding machine (63 kVA) and the voltage and current sampling device and their installation	66
Figure 38. RMS value of dynamic resistance	69
Figure 39. Dynamic resistance value using peak value	69
Figure 40. Dynamic resistance using direct division	70
Figure 41. Dynamic resistance value using the proposed method	70
Figure 42. Comparison of dynamic resistances of two methods	71
Figure 43. First-order derivative value of dynamic resistance	71
Figure 44. Ten curves with the same welding conditions	72
Figure 45. Measurement using an optical microscope	75
Figure 46. Scatter figure of coefficient μ (7,000 A)	76
Figure 47. Scatter figure of coefficient μ (7,500 A)	76
Figure 48. Scatter figure of coefficient μ (8,000 A)	77
Figure 49. Scatter figure of coefficient μ (8,500 A)	77
Figure 50. Relation between diameter and energy (7,000 A)	80
Figure 51. Relation between diameter and energy (7,500 A)	81
Figure 52. Relation between diameter and energy (8,000 A)	81
Figure 53. Relation between diameter and energy (8,500 A)	82

Figure 54. Integrated figure of four equations	83
Figure 55. Errors of the model using the uniform equation	84
Figure 56. Dynamic resistance profile when expulsion occurs	88
Figure 57. Viscard Jeep Renegade	93
Figure 58. Ultrasonic report	95
Figure 59. Output parameters	96
Figure 60. Resistance and current pulse analysis	98
Figure 61. Schematization of welding component and circuit	99
Figure 62. Curves of the parameters	100
Figure 63. Oscilloscope analysis	101
Figure 64. Regulator loop	102
Figure 65. Learning phase	103

LIST OF TABLES

Table 1. PPR status graphic	9
Table 2. Process Audit conformity graphic	10
Table 3. Welding Issues and Cause Matrix	41
Table 4. Statistical control frequency.	43
Table 5. Comparison of the dynamic resistance errors at particular points	72
Table 6. Energy used for predetermined nugget diameter using different welding currents	87
Table 7. Experiment results for actual control system using the separate functions	89
Table 8. Experiment results for actual control system using the uniform functions	90
Table 9. Correlation 1	106
Table 10. Correlation 2	107
Table 11. Correlation 3	108
Table 12. Correlation 4	109
Table 13. Correlation 5	110
Table 14. Correlation 6	111
Table 15. Correlation 7	112
Table 16. Correlation 8	112
Table 17. Correlation 9	113
Table 18. Cost analysis	115

Chapter 1

Introduction

1.1. Background

In the automotive field, the market is very hard because there are many competitors that fight to take the leadership and is important to make a product with particular characteristics to distinguish. Another important factor that the customer take into account is the brand, because most of the automotive companies were born a century ago and they have made mistakes and successes that modeled the image of the brand. The buyers evaluate different aspects of the car: first of all the aesthetic value, than the engine characteristic and the overall quality. The last one takes a big increment thanks to new technology that permit a better production and engineering, also the quality of the material increase every year due to bigger investments on research. In the automotive industry, it started to be always more important to measure all the components in the shortest time, nearly real-time, to accelerate defect identification, root cause analysis and to accelerate process adjustment. These requirements have the consequence of reducing costs of the production line and of increasing quality. The quality of the product is one of the most important aspects from the customer point of view and a company must try to satisfy this characteristic. Good material, correct engineering and robust process are three important factors to increase the product quality and with my work, I try to improve the last one. To make a car there are millions of process and I will focus on the body in white sector, more precisely on resistance spot welding (RSW) process. This process is adopted to joint sheets metal to create the frame and vehicle body and the correct welding is necessary to avoid detachment causing issues of security, vibration and noise. The measurements of the welding quality can be done off-line or in-line. The former means that only a sample of production is taking from line production and measured in a controlled environment, the latter, instead, means that the 100% of production is controlled because the measurement system is located along the production line, for example, between two stations of the production line (in-line control system). Today, these measurement systems are mainly off-line. In an off-line system, only a tiny percentage of the production is

withdrawn and analyzed off-line. Usually external labs are needed, extra equipment and, obviously, skilled operators to use the necessary machines. The In-line or Off-line control is chosen considering the importance of the component and from the difficulty of the control. Example: a critical screw must be tightened with high-cost screwdriver that permits to control the torque and the angle. Than no critical screw use, a simple screwdriver that controls only the torque and it cost 1/20 less. The quality of the paint is controlled for every car because it is an aesthetic value and must be perfect, the quality of the welding process is controlled with a frequency defined in the control plan. The resistance spot welding (RSW) quality check is an off-line control and can be done in a different way and it depends from the type of RSW and its classification that is Q- for a non-important point and Q+ for an important point. Q- points are controlled with a hammer/chisel, Q+ points are controlled with an ultrasonic sensor. The first problem is the frequency of the control that can start from 1 to 3 components each turn, taking into account that a mass market segment produces 400 cars each turn, it follows that an anomaly found during the check causes a line escalation necessary to control and eventually repair more or less 100 cars causing loss of time and money. The second problem is caused by the cost of this control due to the necessity of skilled operators to use the necessary machines. Thanks to the project analyzed in this thesis it is possible to remove this off-line RSW control with the objective to save money and increase the robustness of the control process thanks to a 100% inspection with a correlation between the spot-gun output parameter and the anomaly.

1.2. Internship experience

I have begun my experience in the first week of March in the manufacturing quality department until the end of September 2018. This sector is perfect to increase the competence in the automotive field because it is continually in communication with other departments like: CRF (Fiat Center of Research), PD (Product Development), Manufacturing, Logistic, Powertrain, Supply Chain and European production plant. I have been to Melfi plant in the south of Italy to take data for the project and learn about the different process of a plant, I have also visited the Mirafiori and Grugliasco plants where Maserati makes his products.

I've worked also for "special cars preparation" with the task of following the tune-up of the vehicle involved in the "Parco del Valentino exhibition" and "Geneva International Motor Show".

1.2.1. Manufacturing quality

Manufacturing quality department has the aim to guarantee the good quality of the product through a high-quality process thanks to different teams that collaborate to find the perfect setup and rules for a good production.

- Control Plan: evaluate for each process what must be controlled and how;
- Geometry and Measurement System: evaluate the measure of the control and the system to use;
- Vehicle layout and safety: verify the correct disposition of wiring and evaluate the safety of the disposition;
- Special car: verify the quality of the car with peculiar preparation like armored cars for the police or motor show;
- Customer Product Audit: evaluate the correct operation for the final product quality control;
- Quality system: creates and define the documents that provide requirements, specifications guidelines or characteristics that must be used to ensure materials, processes and product are fit for their purpose such as ISO, ASME and similars;
- Manufacturing Quality engineering: evaluate the technologies adopted in the process for the quality control;
- Plastic quality: Verify all the control concerning the plastic production, bumpers and interiors;
- Process quality: certify and control the correct execution of the production process during the new production of a vehicle and verify the control status of the plant during the normal production.

Manufacturing quality department operate for all EMEA plant (European region) and collaborate with worldwide FCA plants with learning session and line-up of standards. The world plants are divided in four main regions:

- EMEA region has 9 assembly plant distributed in Italy, Poland, Serbia and Turkey. In Italy there are AGAP in Grugliasco where Maserati makes Ghibli and Quattroporte, Mirafiori where Maserati Levante and Alfa Romeo Mito are produced, Sevel Plant in Abruzzo for Fiat Ducato, Sata plant in Melfi for 500X and Jjeep Renegade, Pomigliano for Fiat Panda and Cassino for AlfaRomeo Giulia, Giulietta and Stelvio. Tychy plant in Poland produce Fiat 500 and Lancia Y, FAS in Serbia for 500L and Tofas in Turkey for Fiat Doblo and Tipo;
- LATAM in south America with Goiana and Betim plant in Brazil and Cordoba Plant in Argentina;
- APAC operates in the Asian continent with a joint venture in India in Ranjangaon and China in Shanghai;
- NAFTA region operates in North America with plants in Michigan (U.S.A.), Toronto (Canada) and Toluca (Mexico).

1.2.2. Process Quality

My position in the company deals with supporting and learning what concern the process quality, that start from WPI “Work Place Integration”, PPR “Plant Process readiness” and process audit.

- ❖ WPI follows the start of a new project involving manufacturing engineering and defines the groundwork for the PPR phase. It is divided in Loops with a different target:

VIRTUAL stage

LOOP -1 - Preparation phase;

LOOP 0 - Design phase in a virtual environment, where the focus is on product analysis, macrocycle delivery (set of the line), first design of the workstation (Cross-sheets).

LOOP 1 - Product refinement (Component test analysis), detailed design of workstation: saturation analysis, ergonomic analysis, quality readiness, WCM (world class manufacturing) check-list, logistic activities;

PHYSICAL stage

LOOP 2 - First physical check of the workstation in a Training Area («Pilotino» and Line), coinciding with Tooling phase;

LOOP 3 - Validation and Workstation Readiness activities during Process Verification, coinciding with VP (Process Validation) and PS (pre-series);

LOOP 4 – Ramp-up management.

- ❖ The Plant Process Readiness (PPR) is the methodology used to evaluate the "readiness" of the production processes of a plant's technological units, in compliance with the required quality standards. It starts before the VP until the conformity status is reached and the first sellable car is made (job 1).

The core activity of the Plant Process Readiness is the verification, audit, of every single process of each technological unit involved in the development phase (BIW, painting, assembly and plastics).

The process audit is the objective verification, on the production processes, to establish the correspondence with the project requirements and the current company regulations. The auditor, or evaluator, is an appropriately trained process specialist in order to evaluate quality standards.

To support the auditor, to perform the process verification activities in development, we use the PPR Questionnaire Guide Line (QGL), a guideline consisting of a series of

questions to be applied for the verification of the arguments inherent to a given process, in order to evaluate it entirely.

The QCL is divided in six groups defined by method, machine, material, man, Environment, Product.

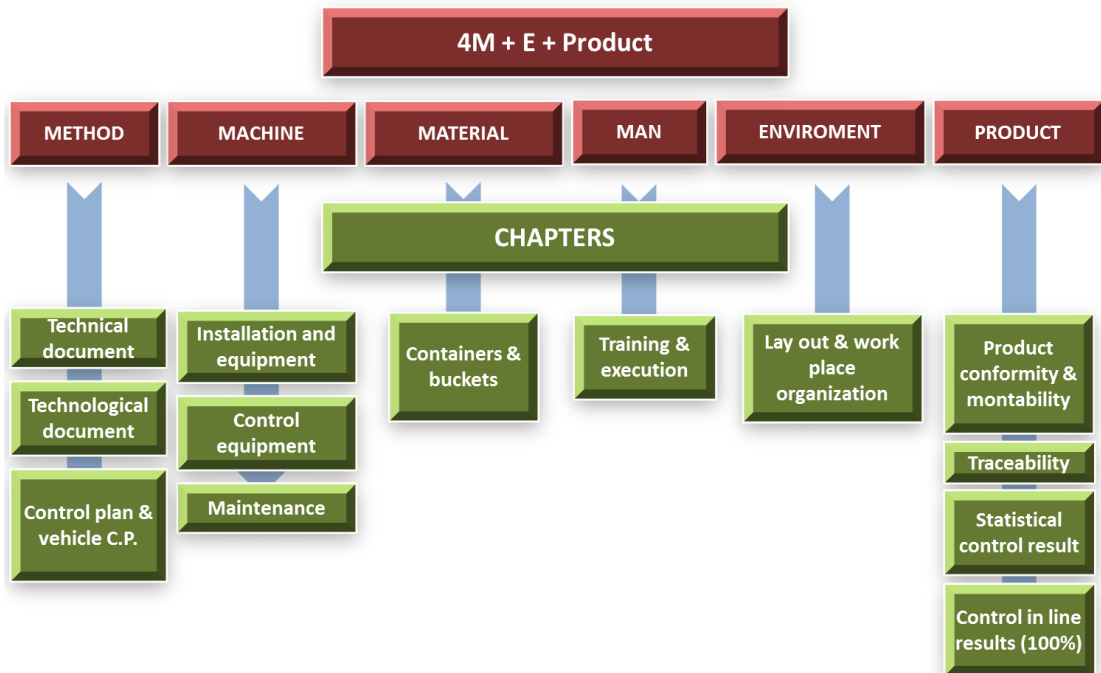


Figure 1. 4M+E+Product

For each point if the verification has a negative result, an anomaly or non-conformity is opened and a relative "weight" is attributed, depending on the severity.

The severity level assigned to each individual anomaly is called **PRIORITY** and can assume a value from 1 to 3.



High risk anomalies:

Missing the standards and / or process that generates a **significant** qualitative risk for internal and / or external customers:

- Impact on safety / legislative / homologation features;
- impact on the final product and / or on the repeatability of the process.

PRIORITY 2

Medium risk anomalies:

Missing the standards and / or process that generates a **middle** quality risk for internal and / or external customers:

- impact on the final product and / or on the repeatability of the process;
- Priorities 1 managed with robust provisional action that guarantees product compliance and process reliability.

PRIORITY 3

Low-risk anomalies:

Deficiencies / insufficiencies compared to the standards that do not have direct qualitative impacts on the process:

- document updating / standardization;
- improvements.

The list of priority goes on a table where the overall conformity is calculated and an intervention program can be tuned up to solve the priority.

		METHOD			MACHINE				MATERIAL		
PROCESSES		Technical Doc.	Technological Doc.		Vehicle Control Plan	Equipment & Tool		Control equipment	Maintenance	Container	
			Certification operation sheet (certification)	VSOP/Tightening book/Red&Black book, ecc		Production	Handling / conveyor	Operator terminal/Scanner /s niffer		External	Internal
Item 1				NA				NA			
Item 2		NA		NA	NA					NA	NA
Item 3			NA					NA	NA	NA	
Item 4							NA			NA	NA
Item 5			NA	NA	NA			NA	NA		NA
Item 6				NA			NA	NA		NA	NA
Item 7			NA			NA		NA	NA		
Item 8			NA	NA			NA	NA		NA	
Item 9			NA		NA		NA		NA	NA	
Item 10						NA		NA		NA	

MATERIAL		MAN	ENVIROMENT	PRODUCT						
Container		Training and execution	Lay-out and WO	Product, Part Assembly	Traceability		Statistical Control Result			Control in Process 100%
External	Internal				Operation (equipment man)	Component s u MES	Torque capability REPORT	Torque capability NO REPORT	Other (specific for operative unit)	
		NA			NA				NA	
NA	NA	NA	NA	NA	NA			NA		
						NA		NA		NA
NA	NA		NA			NA	NA	NA	NA	
NA			NA					NA	NA	NA
NA	NA	NA		NA	NA		NA	NA	NA	
		PR1	NA						NA	NA
NA			NA			NA		NA	NA	
NA					NA	NA	NA		NA	NA
NA		NA		NA				NA		

PR1=high risk anomaly NA=not applicable

Figure 2. PPR table

The target percentages are fixed: 70% for Pre-series and 90% for DaP (Deliberate to production) and the dates are defined by Product Planning.

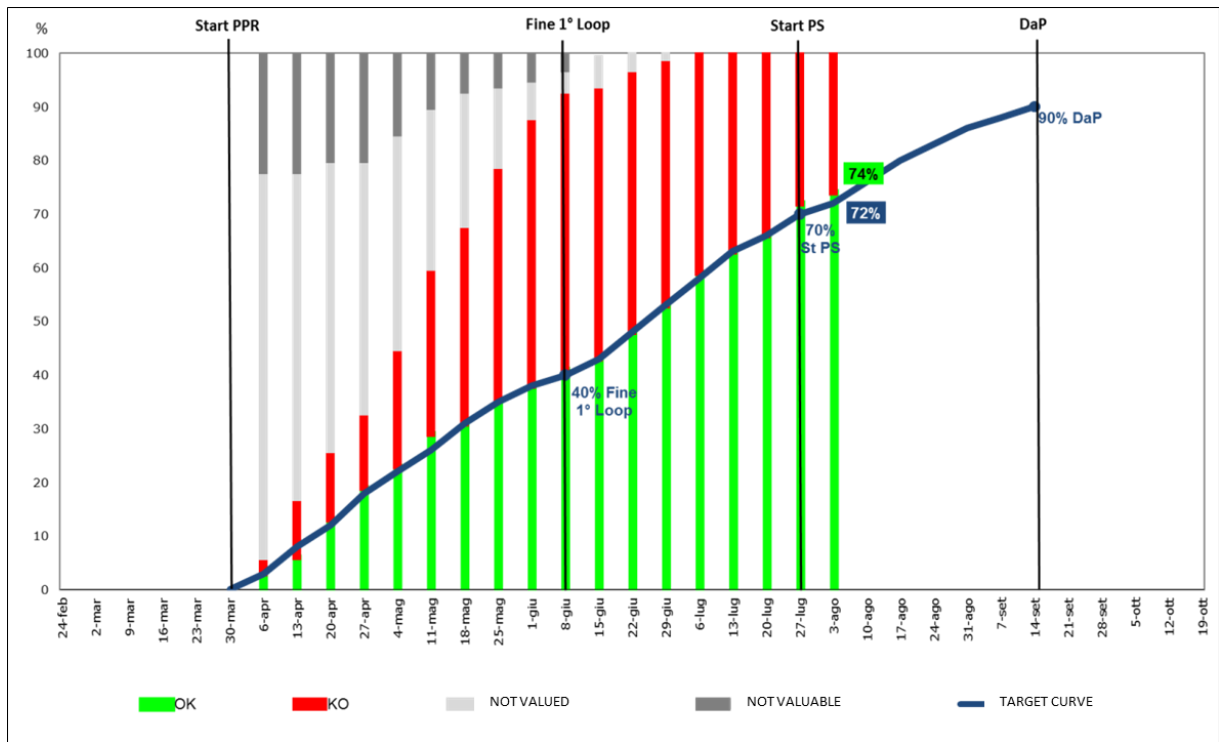


Table 1. PPR status graphic

After the DaP, the process audits are assigned to the plant quality with the aim to close all the priorities.

- ❖ The Process Audits are made both from Manufacturing Quality and the Plant Quality. Manufacturing Quality conducts audits about cross-cutting themes and on all Plants. These audits are also used to check the alignment of the method among central Auditors and Auditors of Plant and to carry out possible training on the job. Plant Quality, with its function of Process Quality, plans and performs "standard" audits at intervals agreed with Manufacturing Quality, as well as audits about emerging themes.

The audit task has the following phases:

- Plan the process audits;
- Prepare the verification;
- Conduct the process audit;

- Prepare a report of the audit, at the end of the verification, attributing to processes the relative responsibilities and including the interventions aimed at resolving critical issues, decided by the concerned departments.

The auditor verifies that the planned corrective actions were implemented and are effective on the date resigned and, in case of failure, he/she promotes the re-planning with the appropriate departments. The verification of the effectiveness of the corrective actions implemented and their certification can be made during the next audit. The audit plan is generally annual, but may be delayed as a result of changes in process and/or emerging issues.

The Audit is made in the same way of PPR but with an annual target that is important to respect to guarantee a good quality of the process.

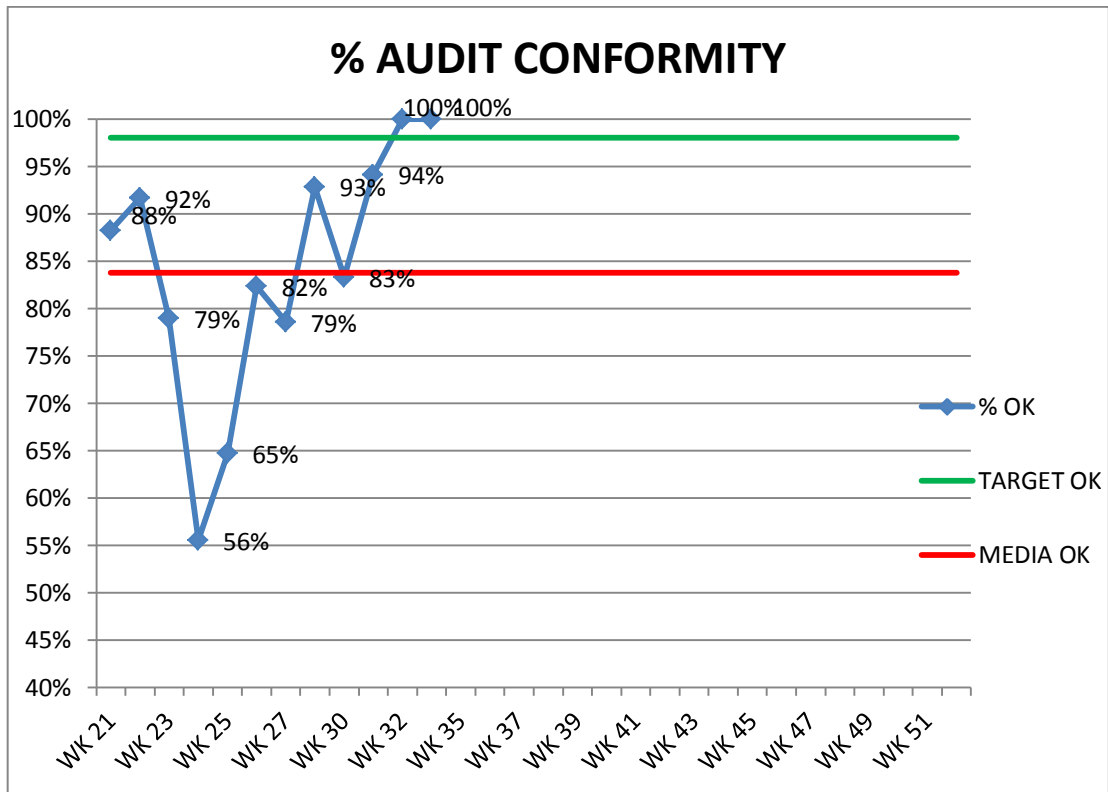


Table 2. Process Audit conformity graphic

1.2.3. Melfi Plant business trip

Following completion in 2014 of an investment program of more than €1 billion , FCA Melfi is today one of the most advanced automotive plants in the world. Innovative technologies and best practices developed at Group plants worldwide have been leveraged to ensure every vehicle produced at Melfi meets the highest standards of quality. The plant currently produces the new Fiat 500X and Jeep Renegade, which represent the Group's entry into the rapidly-expanding Small SUV segment.

Covering a total area of approximately 1.7 million square meters, the plant employs nearly 8,000 people and has a total production capacity of 400,000 vehicles per annum. A further 3,300 people are employed by suppliers and logistics providers operating at the adjacent supplier park.



Figure 3. Fiat 500x and Jeep Renegade in Melfi plant

In the second half of April, I went to Melfi plant SATA to analyze data from the welding process of the car body line. Renegade (520) and 500x (334) have the same frame and use the same line with different tools for the different part and different welding process. I took

data from both processes to increase the effectiveness of the experiment and make a comparison for the welding points with the same thickness.

In this experience, I learnt how a plant works and I saw all the processes that concern the assembly of a vehicle starting from the B.I.W. (body in white) process to the assembly shop through the paint shop. I also took the contact with the people involved in the project to simplify the communication of data.

This project is about a new solution of quality control of resistance spot welding (RSW) and it is important to analyse the process of B.I.W. (body in white) shop to understand where the solution can be applied for investment and money saving. B.I.W. unit has the task to join the metal parts of the vehicle which are stamped previously in Stamping unit. The unit is divided in four main zones: Chassis, Body, Movable parts and fitting; the metal parts can be joint with different technology: welding, screw, rivet, bonding and hamming. The quality of a chassis is important for the passive safety during the crash test. It must always guarantee the right behavior during impact.

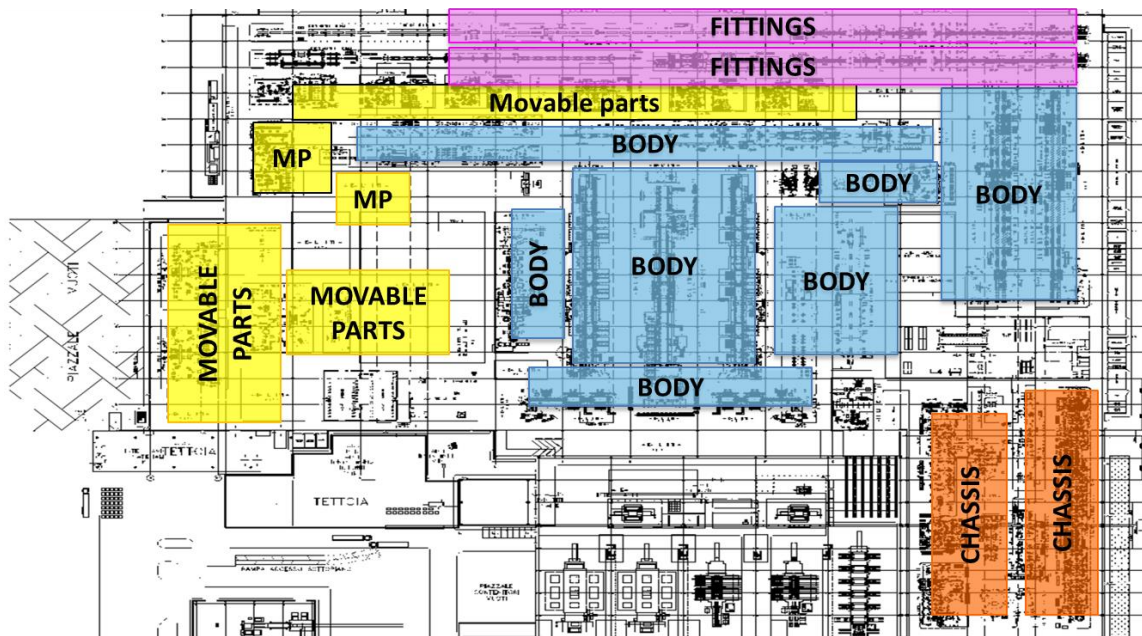


Figure 4. B.I.W. schematic division

The car is born in the chassis zone. There are three different areas where the front frame, the rear floor and the central floor are made. After they are joined together in another station, then chassis embedding and chassis completion end the chassis line.

The Body zone starts with two different lines for the left and the right body sides, also divided in model. Then the body sides are joined with the underbody frame in the basted body line and are finished in the body completion with the roof.

Movable part zone makes the doors, bonnet, tailgate and front fenders. This zone uses a specific glue plus the roller hammering to join the frame and covering together. This technique doesn't leave signs on the surface for an aesthetic reason. Another viscous material is put between the sheet layer that in the e-coat oven increase the volume with the aim to avoid vibration.

In the end, movable parts and body are fit together in the fitting line. First of all, the hinges are screwed. Then starting from the rear door to the front fender in this line is important to make a right setup of G&P (gap and flush) with a high-sophisticated control system.

Chassis:

- Front frame
- Rear frame
- Central floor
- Sub-frame Completion

Body

- Body Side preparation (L/R)
- Body side completion (L/R)
- Basted body line
- Body line completion

Movable parts

- Rear doors (L/R)
- Front doors (L/R)
- Bonnet
- Tailgate

- Front fenders (L/R)

Each of this line is also divided in OP (operation) that are numbered in 10, 20, 30, [...], 100, 120 and for each operation there are different robots (R01, R02,...) with a different function (welding, control, spreading, clamping, placement of part).



Figure 5. Resistant Spot Welding in automotive production

2.1.B.I.W. welding technology

Welding is the joining technique with which the continuity of the metallic material is realized between two pieces to be welded. The result of the operation is the so-called "welded joint", more simply called "welding". Continuity can essentially be achieved in two ways:

- by contact and liquid-liquid connection, by melting the two materials of the joint;
- by solid-solid contact, without fusion: in this case the connection is obtained by mutual diffusion among the materials, which always remain in the solid state.

The behavior modalities of the various materials, in welding operations, are defined by their "weldability", which expresses their ability to be welded.

The most utilized welding processes in B.I.W. are:

- **Resistance spot welding:** Process of autogenous welding by pressure, in which heat necessary to bring the surfaces to be welded to the melting temperature is provided by Joule effect, through the electrical resistance of the area to be joined.
- **Projection welding:** Modification of spot welding. In this process, the weld is localized by means of raised sections, or projections, on one or both of the workpieces to be joined. Heat is concentrated at the projections, which permits the welding of heavier sections or the closer spacing of welds. This technology is used to join nuts, screws and bushes on the sheet metal.
- **Gas Metal Arc Welding (GMAW):** Welding with equipment which automatically feeds a continuous wire electrode to a holder or torch. A protective atmosphere is provided by a gas typically supplied through the torch nozzle. Argon and carbon dioxide are the typical shielding gases. This process is sometimes referred to as Metal Inert Gas (MIG) or Metal Active Gas (MAG) welding.
- **Flux-Cored Arc Welding (FCAW):** A process similar to GMAW. The continuous wire electrode is a metal tube filled with flux and metal powders. The flux provides the protective atmosphere and leaves the weld covered with a thin slag coating. Electrodes designed for use with an externally supplied shielding gas are also available. This process enables the efficient welding of zinc, iron-zinc coated steels with a specifically compounded ferrous filler metal electrode.
- **Gas Tungsten Arc Welding (GTAW):** Welding where fusion is produced by heating with an arc between a non-consumable tungsten electrode and the workpiece. Filler metal may be added if required. An inert shielding gas is directed through the electrode holder. The Process is sometimes referred to as TIG welding. This process shall not be specified for welding coated steels because the zinc vapors poison the tungsten electrode.

- **Plasma Arc Welding (PAW):** An arc welding process similar to the GTAW process. Coalescence is produced by heating with a constricted arc between an electrode and the work-piece or between the electrode and the constricting nozzle. Filler metal may or may not be added. This process shall not be specified for welding coated steels as the coating may poison the tungsten electrode.
- **Pulsed Gas Metal Arc Welding (GMAW-P):** A variation of GMAW using a special power source providing a "pulsed peak" current superimposed upon a background current. An advantageous process for welding zinc, iron-zinc coated and thin bare sheet steel, and for welding aluminum alloys with aluminum alloy filler metal. There is a derivative of GMAW-P that runs in the short circuit mode of transfer. The process relies upon feedback from information obtained at the arc which results in changes in the character of the arc making the process advantageous for solid steel wires on thin gauge assemblies.
- **Laser welding:** Laser beam welding (LBW) is a welding technique used to join pieces of metal or thermoplastics through the use of a laser. The beam provides a concentrated heat source, allowing for narrow, deep welds and high welding rates.
- **Laser brazing welding:** Brazing is a joining process whereby a filler metal or alloy is heated to melting temperatures above 450°C and distributed between two or more close-fitting parts, without actually melting the base material. The laser is used to heat up the wire material, which will then flow in between the two closely fitted joining materials. In contrast to welding, the joint materials are held together due to wetting by the molten wire (filler) material. Therefore, the joint materials do not necessarily need to be of the same material. Brazing also allows the joining of dissimilar materials with considerable strength.
- **BETAMATE™** structural adhesives deliver cutting-edge solutions in similar and dissimilar material bonding, closure bonding, and body structure bonding, enabling improved load carrying capabilities, vehicle stiffness and durability, design flexibility, and weight reduction. BETAMATE™ structural adhesives offer high-performance adhesion to automotive substrates such steel, aluminum, magnesium, and composites, innovatively replacing welds and mechanical fasteners, reducing fatigue and failure

commonly encountered with traditional processes – substantially increasing manufacturing efficiencies.

Chapter 3

Resistance spot welding

Spot welding is the welding method that uses the heat generated by the resistance of the material to the electrical current together with the gripping pressure simultaneously. There is no extra external heat source. Heat is produced only on the parts to be welded and pressure is applied by the rocker arms or electrode arms. The high current density is provided by the transformer and the pressure is provided by the hydraulic and pneumatic equipment. It is the most common form of electric resistance welding as its method is very easy, practical and easeful. Although it seems to be very basic, its process is very complex and requires the continuous control of specified parameters. The method may be used for joining sheet to sheet, sheets to rolled sections or extrusions, wire to wire, for sundry special applications using combinations of the above. By far the widest application in industry is the spot welding together of sheet-metal parts, as in the hollow-ware industry (handles to kettles and saucepans) or the automotive industry. For example, the typical car body contains about 5000 spot welds joining a mixture of sheet metal material types and thicknesses. This welding method is very advantageous corresponding to its high speed of operation, hence its adaptability to mass production, its cleanliness, no need for welding rods, and its high degree of control possible by electrical means (i.e., reducing the necessity for a degree of operational skill). The process spot welding involves the joining of two or more pieces of sheet metal in localized areas (spots) where the melting and coalescence of a small volume of material occurs from heating caused by resistance to the passage of an electric current. The electric current is carried to the sheets via electrodes that are also used to clamp the workpieces together. The heat H in joules delivered to the weld zone is determined by the equation :

$$H = I^2 R t \quad (1.1)$$

Where I is the current through the weld zone, R is the effective resistance in the current carrying circuit, and t is the time during which the current flows through the weld zone.

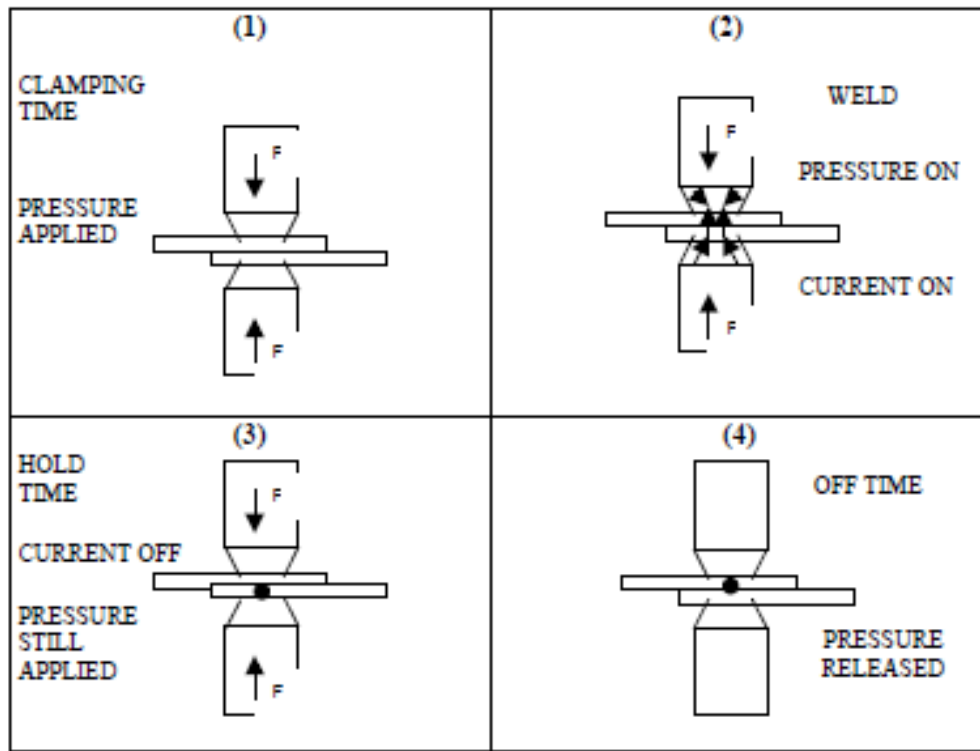


Figure 6. Time sequence of the resistance spot welding cycle.

The sequence in a complete welding cycle comprises clamping the workpieces with the electrodes (at a controlled clamping force) and the passage of the weld current for a specified period, followed by holding the pieces clamped for a specific time period with the weld current off, and finally releasing the clamping pressure and the workpiece. This sequence is illustrated in Figure 6.

As the weld current flows through the clamped workpieces, the highest resistance will be at their contacting surface. The heat develops at this side, causing a rapid rise in the temperature. The temperature rise culminates in melting of the metal starting at the center of the current path. Thus, a pool of molten metal from the workpieces begin to grow outward for the duration of the current flow. When the weld current is turned off, this volume of molten metal cools down and solidifies.

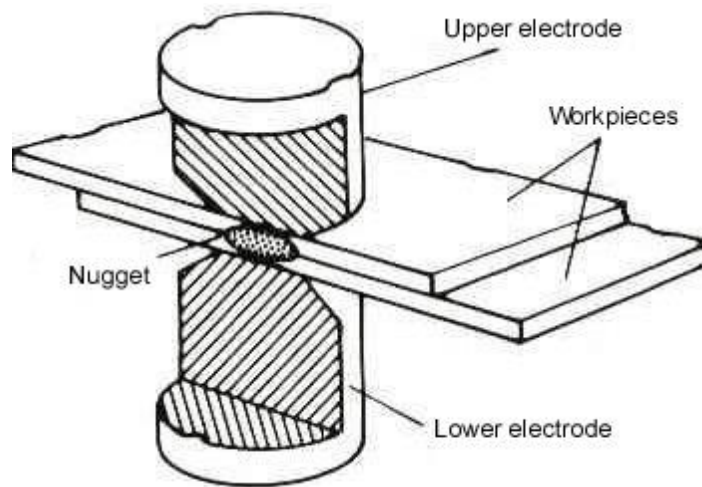


Figure 7. The cutaway view of the location and shape of a weld nugget

The volume of metal from the workpieces that has undergone heating, melting, fusion and solidification is called the weld nugget. The cutaway view of a typical spot weld nugget is given in Figure 7. The weld nugget forms at the faying surfaces, but does not extend completely to the other surfaces. In a cross section, the nugget in a properly formed spot weld is round or oval in shape; plan view it has the same shape as the electrode face and approximately the same size.

3.1. Resistance spot welding equipment

The equipment needed for resistance spot welding (RSW) can be simple and inexpensive or complex and expensive, depending on the degree of automation. Spot welding machines are generally composed of three principal elements :

- Electrical Circuit: It is composed of a welding transformer, tap switch and a secondary circuit.
- Control Circuit: It initiates and times the duration of current flow and regulates the welding current.

- Mechanical System: This system consists of the frame, fixtures and devices that hold and clamp the workpiece and apply the welding pressure.

Welding operations in highly automated production lines are based primarily on multiple spot welders and robotic cells. In addition, manual welding operations can be used to manufacture either subassemblies, which are fed into the main production/assembly lines, or in many instances, finished products. These differing end uses require machines of varying designs and characteristics. RSW machines can be divided into three basic types :

- Pedestal-type welding machines;
- Portable welding guns;
- Multiple welding machines incorporating lightweight gun welding units.



Figure 8. Resistance Spot Welding gun

Another fundamental parts for Resistance spot welding are electrodes, they should be made of the materials having high thermal and electrical conductivities and sufficiently low contact resistance to prevent burning of the workpiece surface or alloying at the electrode face. In addition, the electrode should have adequate strength to resist deformation at operating pressures and temperatures. Electrode materials for resistance spot welding have been classified by RWMA and in International Standards Organization (ISO) standard ISO 5182. Using the proper electrodes for the spot welding application is necessary in order to achieve

the best results in any spot welding operation. Selection of the alloy is important since this can help modify the heat balance or reduce the tip wear. The tip face diameter and contour must also be considered since these factors control the welding pressure and current density which must be within an acceptable range for satisfactory results. Incorrect tip face geometry will also result in increased surface marking. Although there are many alloys, types, sizes and shapes of electrodes commercially available, there are six standard nose configurations and, of these, there are three that are most frequently used for spot welding. There are: flat, radiuses and domed. Most of the welding schedules are based on these three shapes. Other sizes and shapes are often required to conform to the contour of the weldment or to suit other conditions. Each of the electrodes are manufactured using a number of different alloys to provide the best combination of electrical and mechanical properties for a particular welding operation.

3.2. Factors and variables affecting spot weld quality

The qualities of resistance welds are affected by many variables, including the properties of the material to be welded, the surface smoothness and cleanness, the electrode size and shape, and the welding-machine settings that determine welding time, pressure, and current. Successful welding depends on consistent weld properties, which in turn require uniform welding conditions. Experience has shown that a change in any single variable of more than 10% is sufficient to make the weld unacceptable. Unacceptability may represent failure to meet a specified property limit, such as a minimum tensile or impact strength, or it may define actual fracture of the weld. There are numerous factors occurring during production which influence end weld quality. An understanding of these factors and their effect on quality is most important to individuals concerned with production, maintenance, manufacturing engineering and quality control. Some factors and variables affecting the spot weld quality are described below.

3.2.1. Pressure and force systems

Weld force brings the metal between the electrodes together and provides electrical continuity, the required welding pressure, and forging force, so that a weld may be generated. The

welding equipment pressure systems are normally either hydraulic or pneumatic. Mechanical systems are encountered, but to a lesser degree. With a hydraulic or pneumatic system the electrode force, or welding force, is generated by the pressure of the media acting over the area of the piston of the cylinder to which the movable electrode is attached. The effect of an improper electrode force can be illustrated relative to the basic heat equation used in resistance welding; i.e. $H=I^2Rt$. Low electrode force will increase the resistance factor R of this equation. While a high resistance caused by a low force will generate more heat, the negative effects of metal expulsion, porous welds, surface whiskers of sharp metal spikes, sticking electrodes, poor electrode life and low strength welds will be encountered. On a microscopic scale, the surfaces of electrodes and workpieces consist of peaks and valleys. When subjected to low force, the metal-to-metal contact will be only at the contacting peaks. The resulting contact area is less than that produced by an appropriate force. Contact resistance will therefore be higher, causing a greater amount of heat to be generated.

3.2.2. Welding current

If the current passed during the weld time is too high for the combination of electrode caps in use, their condition and contact area, the weld time, the weld force, and the materials being welded, it will generate more heat as described in the previous section resulting in excessive indentation, cracks and holes, expulsion/burn through, sticking electrodes, rapid electrode cap wear and “brassy” appearance to weld surface on galvanized steels.

3.2.3. Electrode condition and geometry

A complete weld schedule must include a recommended electrode shape and geometry. The loss of this shape, either through mushroomed electrodes or a change in electrode shape, can have disastrous effects on weld quality. The actual contact area of an electrode tip on the material to be welded will determine the weld current density and the electrode force density, or pressure. When electrode tips are allowed to mushroom (Fig. 9), the pressure and current density decrease in an exponential fashion, since the area is proportional to diameter squared.

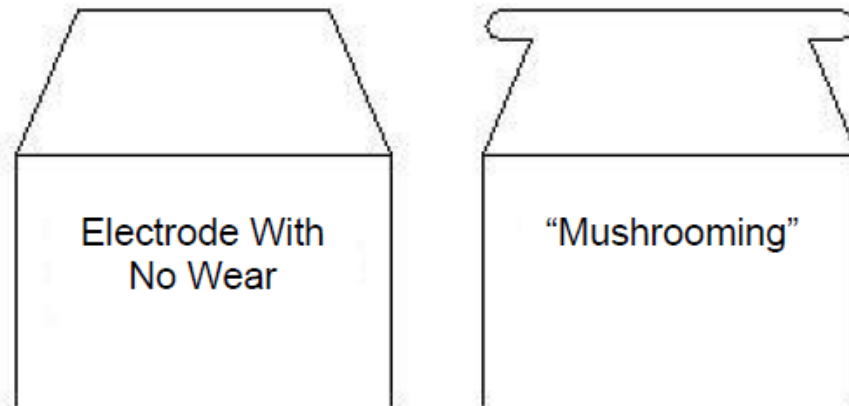


Figure 9. Deformation of tip face over time

Electrode wear can also occur by the pitting of the tip face (Fig. 10). In severe cases, localized current flow may result, potentially causing non-round welds.

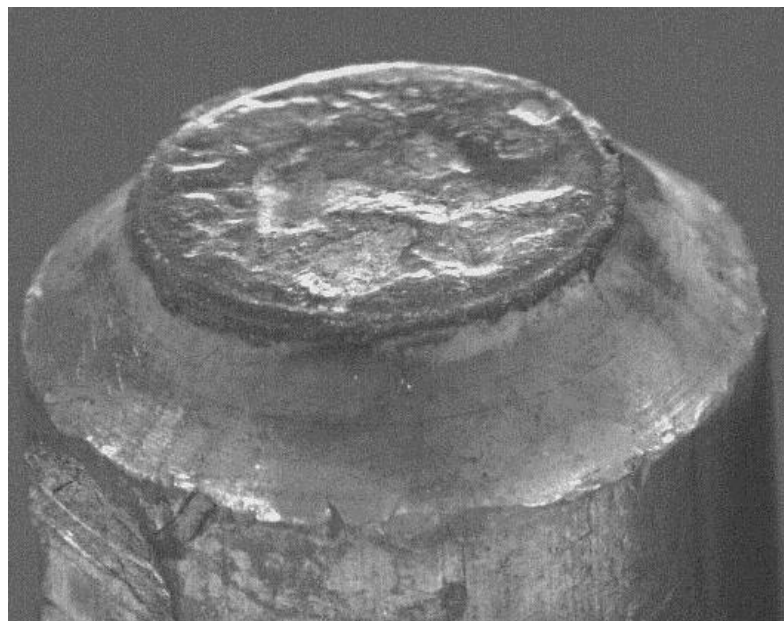


Figure 10. Badly pitted tip face

A full appreciation of actual electrode tip contact area relative to quality welds is of extreme importance. Tips should be redressed whenever the slightest amount of mushrooming or pitting is noted.

3.2.4. Welding time

For a typical weld, weld time is the amount of time welding current flows through the metal. Since electrical power arrives at the weld control as alternating current, at a 60-cycle per second rate (50 in some areas), weld time is usually measured in cycles. This has become a convenient measuring standard for the duration of weld heat. One cycle equals 1/60th of a second, for a 60-cycle per second supply and 1/50th of a second, for a 50-cycle per second supply. For Direct Current (DC) welders, weld time is usually measured in cycles as a convenience. In some instances, however, with mid- and high-frequency DC welding, milliseconds are often used to measure weld time. However, with DC welders, there is some difference in programmed weld time and actual weld time as the Fig. 11.

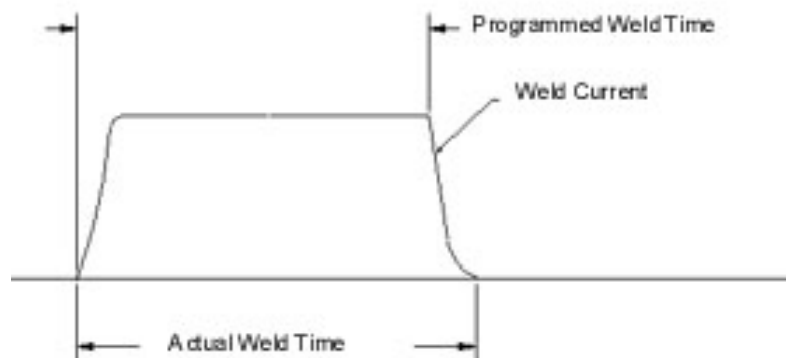


Figure 11. Programmed and actual weld time

In a typical single-pulse weld the metal between the electrodes is heated from room temperature to welding temperature and rapidly cooled. The growth and shape of the weld nugget are governed by the heat/cool cycles of the weld schedule (Fig. 12). When weld time is

too long, high indentation, excessive expulsion, and electrode sticking can occur. Worst case produces "burn-through" where metal between the electrodes is completely melted, producing a hole in the parts to be welded. The electrodes penetrate through this molten metal and may contact each other. On the other hand, when weld time is too short, a small nugget will result. Worst case will result in a missing weld, or a stuck weld can occur.

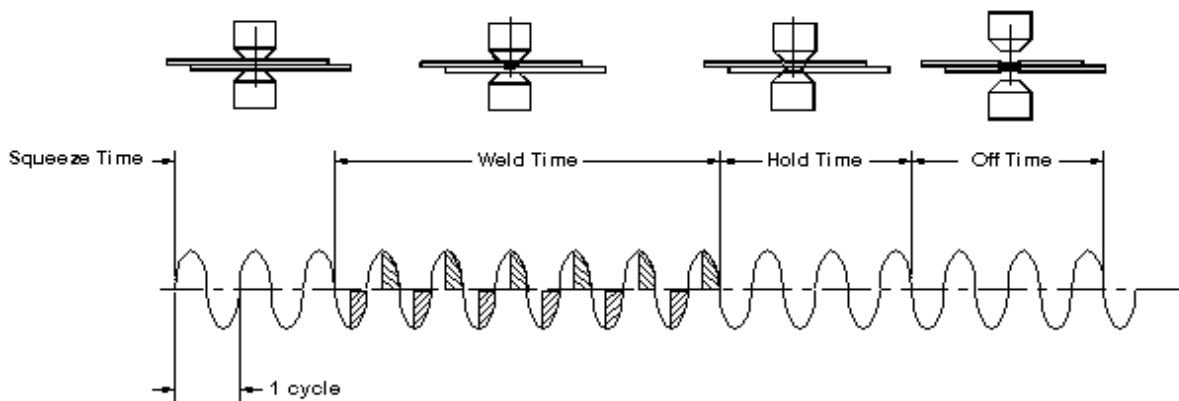


Figure 12. Weld Schedule

3.2.5. Surface condition

A workpiece surface that is not free of substances that will degrade the welding operation. Since most surface contaminants have high electrical resistance, excessive heat is generated at the area of electrode contact and at the faying surface. This results in partial welding of the tip surface to the material, producing short tip life and degraded surface appearance. At the faying surface, metal expulsion may occur and slag inclusions or voids are frequently found in the fusion zone. The conditions described above are usually not consistent over all the work surface and will produce variations in the welding results. When required, the material should be cleaned by suitable chemical or mechanical means.

3.2.6. Operator

Securing adequately trained personnel and utilizing their skills most efficiently is one of the greatest problems. The personnel problem includes all individual departments involved in the fabrication of the finished part from its design to its final acceptance. The operation of a resistance spot welding machine requires a proper training in this welding method. A proper training comprises, for example, adequate knowledge of the theory of the resistance welding, surface preparation, resistance welding equipment, and experience on the selection of the parameters, such as welding force, welding current and welding time.

3.3. Resistance spot welding defect

The RSW can generate different defect with different causes. Some defects are more severe than other and can cause problems during the use of the vehicle. Others are less important because the spot holds the parts but with less resistance than the ideal one. There are also aesthetics defects which are important in a visible part like the door and the tailgate. In this section all the defect that can occur during the welding process are illustrated.

➤ **Missing weld**

A weld is missing when there is no fusion of parent metal or coatings at the intended weld location. Missing welds can occur either because:

- The welding equipment never contacted the workpiece at the intended weld location;
- Inadequate heat was developed at the intended location.

Missing welds may be the result of operator placement mistakes, or the result of machine errors in performance or settings.

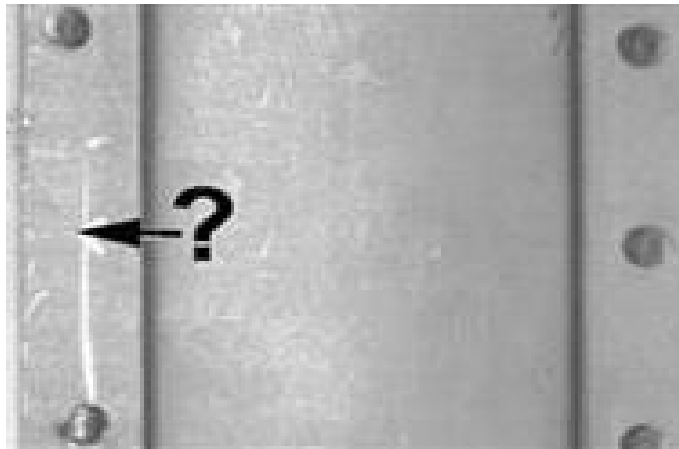


Figure 13. Missing weld

➤ **Undersized weld**

The weld button/nugget diameter does not meet applicable specifications. (The weld nugget is the fused volume that joins the workpieces. The button is the material remaining attached to the fused area after destructive sheet separation.) Undersized welds can be the product of dirty or damaged parts and materials, or of incorrect welding setups.

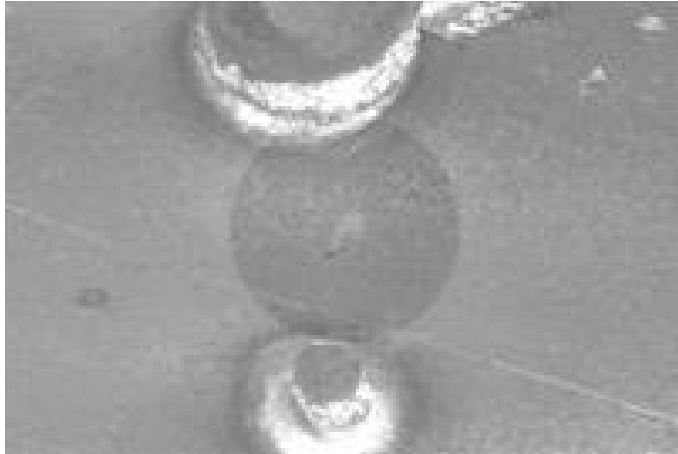


Figure 14. Undersized weld

➤ **Stuck weld**

Workpieces are held together by localized fusion at the welding interface, but no weld button is formed. Stuck welds occur when there is insufficient heat at the welding interface to bring about nugget growth. Instead, fusion occurs only between point contacts between the sheets. With coated materials, coatings can melt and refreeze, effectively soldering the parts together. The resulting bonds are strong enough to hold the workpieces together under light loads, but reasonable force will pull them apart. Electrode wear, low weld current and high weld force may cause “stuck welds,” when only a slight, weak bond is formed.

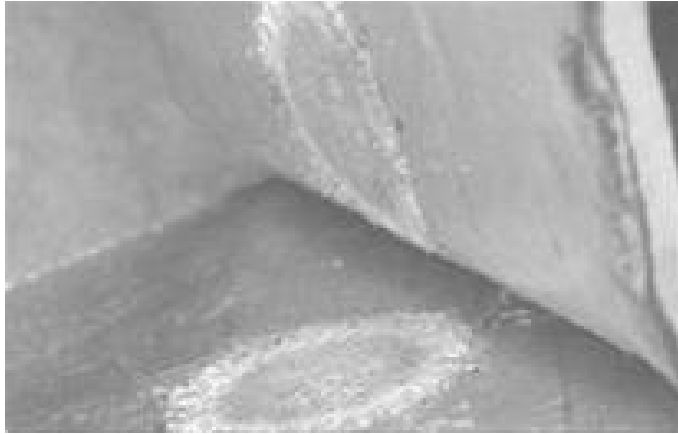


Figure 15. Stuck weld

➤ **Excessive indentation**

Excessive Indentation occurs when the depression left by the electrode on the workpiece exceeds the manufacturer's specification. Indentation on at least one side of the workpiece is an essential part of resistance welding. Acceptable indentation and the method of measurement may vary among manufacturers. The weld classification (Class A, Cosmetic, Common, etc.) may also influence the acceptable indentation. Acceptable indentation may be different on each side of the workpiece. Some electrode configurations may produce nonsymmetrical indentations (e.g. truncated cone with a flat cap). High weld current, high weld force and long squeeze and hold times may cause deep indentations that do not meet specifications.



Figure 16. Excessive indentation

➤ **Expulsion/burn-through**

Issues with high electrode follow-up, high current and welds too close to the edge may cause the expulsion of molten metal during welds.



Figure 17. Expulsion/burn-through

➤ **Cracks and holes**

Discontinuities within the weld nugget and/or surrounding area caused by metallurgical changes resulting from welding. Same as fissures (cracks), voids (holes), pores (holes). Holes may be contained within the nugget at the weld center, or distributed around the edge at the sheet interface, as is sometimes caused by interfacial expulsion. Holes may also be surface cavities such as those formed by heavy surface

expulsion. Surface cracks usually radiate from the approximate center of the nugget, and in extreme cases may pass through the entire thickness of the weld zone. Cracks may also exist in the material surrounding the nugget. High current, low force, expulsion and other systematic problems may cause cracks and holes in welds.

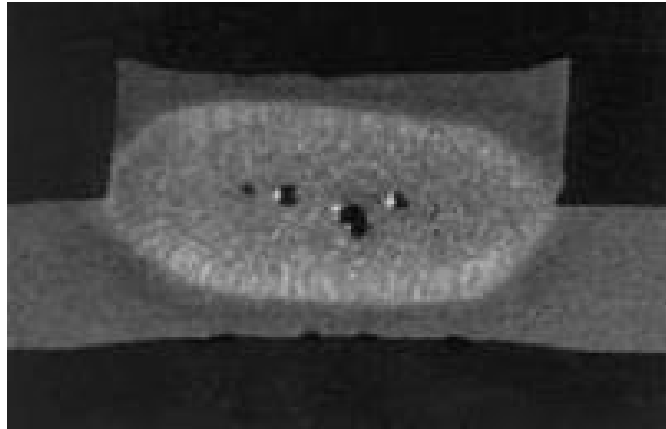


Figure 18. Cracks and holes

➤ **Misallocated/edge welds**

A weld that is incorrectly positioned compared to current workpiece design. Edge welds are those welds that touch or extend beyond the edge of the workpiece. Edge welds are often the result of electrode misplacement, trouble with access to weld areas, or part defects.

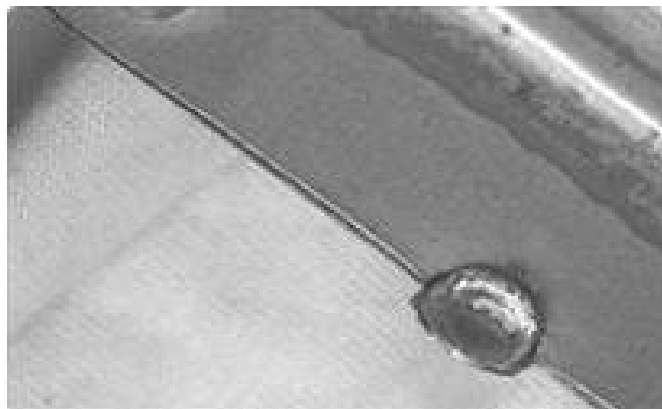


Figure 19. Misallocated/edge welds

➤ **Sheet metal distortion**

The sheet metal is distorted if it is deformed such that the weld interface is out of the plane of the sheet metal, or if any of the sheets are displaced from their original plane. The weld is not in the plane of the surrounding metal. This condition is caused by the electrode faces not being parallel to the workpiece. Therefore, the application of welding force and current cause the weld to be made at an angle to the plane of the interface (out of plane condition). The metals being welded do not have an intimate contact in the area to be welded. The application of welding force and current causes one or both sheets to distort toward one another. Problems with weld force, fixture placement and access to weld areas may cause distortion in workpieces and stampings.

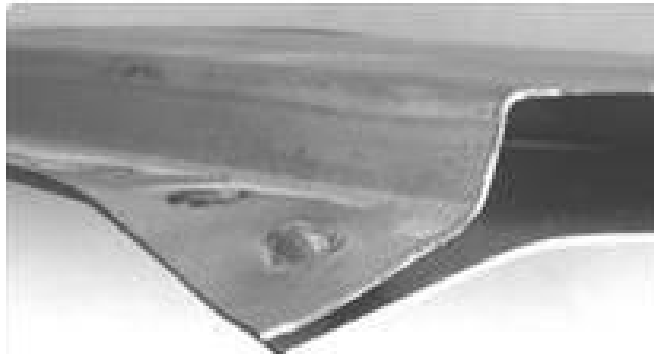


Figure 20. Sheet metal distortion

Extra welds

Additional unintended welds are usually the result of incorrect stampings or operator, robot or fixture error.

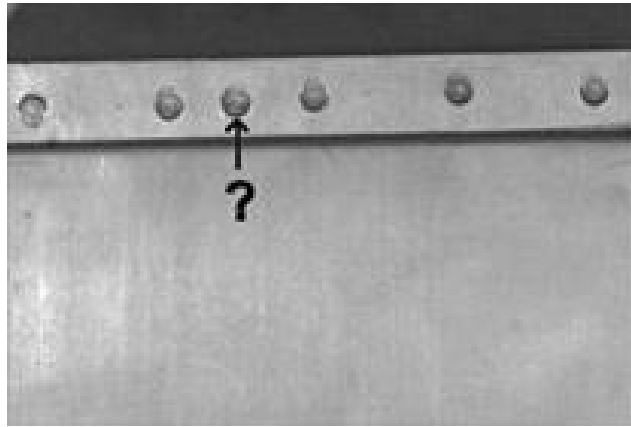


Figure 21. Extra welds

Inconsistent welds

Weld quality varies with some welds failing to meet applicable quality standards.

Quality may vary as a result of a trend or in a more random pattern. A gradual decrease in weld quality can occur because of an increase in the face diameter of the tips. Random variation about this trend may eventually fall below the minimum standards. Countermeasures to address the trend may include current steppers, tip-dressing, etc. More random variation may occur due to intermittent factors such as voltage sag and spike, workpiece surface variation, etc. Further system analysis may be required to determine the root cause of the variation. Variances in stampings and uneven electrical or mechanical connections may cause inconsistent resistance welds.

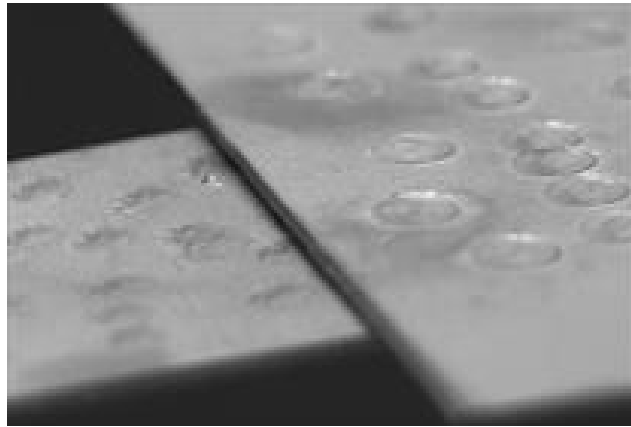


Figure 22. Inconsistent welds

Brittle welds

A resistance spot weld that fractures with little or no plastic deformation in either the weld or the surrounding metal. The measurement of spot weld brittleness depends upon the test method. The size and shape of the welded structure under test, the rate of load application, the weld's microstructure and surface conditions, and the ambient temperature all influence the amount and location of plastic deformation prior to fracture. Each must be considered when evaluating welds. Brittle welds often fracture interracially. A weld that fractures with little plastic deformation may be caused by long hold times or problems with the stamping alloy chemistry.

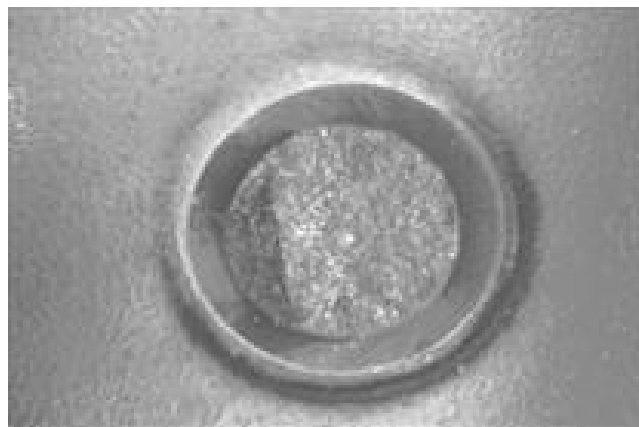


Figure 23. Brittle welds

Non-round welds

Welds or weld buttons are not circular. Non-round welds may be caused in several ways. Typically they are the result of using worn electrode tips, improperly aligned welding equipment, or insufficient weld energy. Reference should be made to appropriate company standards to determine whether any non-round conditions are acceptable. Non-round welds may be caused by electrode wear, issues with tip alignment, or dirty workpieces.



Figure 24. Non-round welds

Poor class A appearance

Visible weld features do not conform to the requirements of the applicable standard. Spot welds are typically classified both in terms of their functional requirements and their surface appearance. The most stringent cosmetic stipulation is for the appearance of a surface (usually customer-visible) to be free from markings or imperfections such that a weld is not visible after painting. Other requirements may limit the displacement, indentation, or distortion of the parent metal. These criteria are normally specified as a percentage of the governing metal thickness. Weld flash may also be specified as unacceptable. Issues with required Class A appearances are often concurrent with a number of other issues, such as weld consistency and quality.



Figure 25. Poor class A appearance

Stuck electrodes

Sticking is a term that refers to the tendency of the electrode tip to adhere to the workpiece. Elevated temperature at the electrode/workpiece interface can produce alloying conditions. Zinc coating allows a zinc-copper alloy to develop at the electrode tip, promoting adhesion. When bare steel is welded, a carbon layer forms on the tip. This layer acts as a barrier to the fusion of electrode and workpiece, thereby minimizing sticking. Sticking may also result from melting and refreezing of the workpiece coating [e.g. zinc], prior to tip removal from the workpiece. Electrodes, stampings or fasteners may weld together unintentionally after long hold times, incorrect materials or stamping coatings.



Figure 26. Stuck electrodes

Interfacial separation

The weld nugget splits along the original welding plane, rather than pulling a button. The weld zone shows evidence of adequate fusion between the parent materials. Interfacial separation may occur with heavy stack-ups or certain materials such as aluminum and high strength steels. With stack-ups involving thick gages, the workpiece may be stronger than the weld nugget. Therefore during peel testing, chisel testing, etc., the crack that starts at the edge of the nugget will meet less mechanical resistance by growing through the nugget, rather than through the thickness of the workpiece. Normally during destructive testing the crack starting at the nugget's edge travels through the thickness of the sheet, forming the button. With thicker or stronger stack-ups, or with certain materials, the crack may encounter less resistance by passing through the nugget. Such welds may be acceptable if the fused area exceeds the minimum button size, and the surrounding material shows evidence that the weld had adequate strength, for example, the flanges may be distorted during testing. (Refer to the appropriate company standards). Extra care should be taken with interfacial separations in high strength steel, since these might be indicative of brittle weld failures (see Brittle Welds). Separation along the original weld plane (rather than tearing at a weld button) occur when stampings are stronger than the weld nugget.

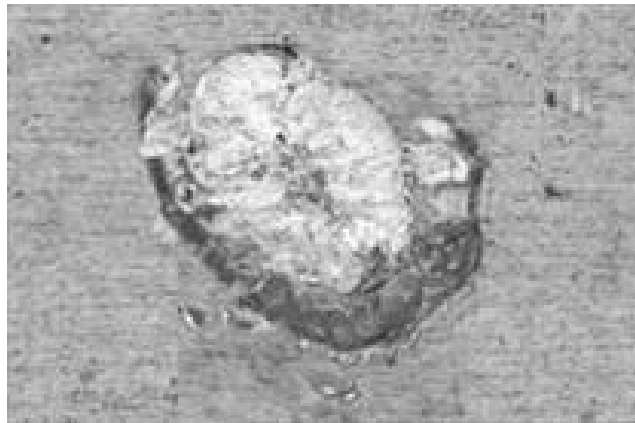


Figure 27. Interfacial separation

Welding Issue and Cause Matrix

relationships between issues and causes:
S » Strong
W » Weak

Caus	Issues														
	Missing Weld	Undersized Weld	Stuck Weld	Excessive Indentation	Expulsion/Burn-Thru	Cracks and Holes	Mislocated or Edge Welds	Sheet Metal Distortion	Extra Welds	Inconsistent Weld Quality	Brittle Weld	Non-Round Weld	Poor Class A Appearance	Sticking or Stuck Tips	Interfacial Separation
Weld Current Low	S	S	S									S			
Weld Current High				S	S	S							S	S	
Weld Force Low					W	S							W	S	
Weld Force High		S	S	S									S		
Weld Time Short	S	S	W									S			
Weld Time Long				S	W								W	W	
Squeeze Time Short					W	S							W		
Hold Time Short					W	S					W		S		S
Hold Time Long											S			S	W
Wrong Tips		S	S	W	W	W	S	W				S	W	S	
Inc. Tip Alignment		S			W	W	S	W				S	S		
Electrode Wear	W	S	S		W							S	W		
Electrode Skidding		S		W	W			W		S		S	W		
Inc. Tip Dressing	W	W	W	W	W	S				W	W	S	S	W	
Wrong Shank	W	W	W	W	W	W	W	W				W	W		
Insufficient Cooling		S	W			S				W				W	
Poor Mech. Connect		S	W		W	W				S			W		
Inc. Air/Hydraulics		S	W	W	W	S				W				W	
Incorrect Cylinder		S	W	W	W	W				W		W	S	W	
Incorrect Hoses					W	W		W					W	W	
Poor Elec. Connect	S	S	W							S		S			
Wrong Transformer	W	W	W	W	W	W				W		W	W	W	
Wrong Cables/Shunts	W	W	W				W	W		S		W	W	W	
Poor Weld Access		S	W				S	S					S		
Shunting Guns/Parts		S	W							S		S	S		
Incorrect Material		S	W		W	W				W		W	W	S	
Dirty Material		S	W		W	W				S		S	S		
Excessive Sealer	S	S	W	S	S	W				S		S		W	
Poor Part Fit-Up	W	S	W	S	S	W	S	S		S		S	S		
Damaged Part		S			W	W	W	S		W		W	S		
Weld Flange Small					S	W	S								
Welds Mislocated	S			W	W		S	S	S	S			S		
Tips Not Parallel		S		S	W			W				S	S	S	
Inc. Gun Equalization				W				S					S		
Incorrect Tests	W	S		W			W	W	W	W	S	S	W		S
Incorrect Workpiece	S	W	W	W	W	W	S	S	S	W	W	W	W	W	W
Poor Tip Follow-Up		W			S					S		W	S	W	

Table 3. Welding Issues and Cause Matrix

3.4.RSW welding quality control

Each operation of the process must be controlled to guarantee the quality, 100% control in line is the better solution but it is not always possible because same control operation has needed time and would cause a slowdown in production. For this reason, statistic controls are made to evaluate the progress of process compliance, the frequency of this checks is defined in the control plan and depends on the number of vehicles produced in a work shift. This part of the thesis is focused on RSW and BETAMATE quality control. The first one is important for the project and during the internship I worked on the vision control of BETAMATE spreading.

The spots are divided into four categories with different control plans:

- Report spots;
- Q+ spots with and without interposed adhesive;
- Q- spots with interposed adhesive;
- Q- spots without interposed adhesive.

There are three types of control:

- Visual check;
- Ultrasonic check;
- Check with hammer/chisel

CHECKS ON ELECTRIC RESISTANCE SPOTS WELDING (SDPE)												
TYPE OF POINT AND TYPE OF CHECK				CHECK FREQUENCY IN FUNCTION OF PRODUCTION NUMBER (N° CHECK/SHIFT)								
				PRODUCTION ≤75 CARS/SHIFT			PRODUCTION AT 76 TO 199 CARS/SHIFT			PRODUCTION ≥200 CARS/SHIFT		
TYPE AND POINT CLASSIFICATION	VISUAL CHECK	ULTRASONIC CHECK	CHECK WITH HAMMER / CHISEL	VISUAL CHECK	ULTRASONIC CHECK	CHECK WITH HAMMER / CHISEL	VISUAL CHECK	ULTRASONIC CHECK	CHECK WITH HAMMER / CHISEL	VISUAL CHECK	ULTRASONIC CHECK	CHECK WITH HAMMER / CHISEL
REPORT SPOTS	X	X (MANDATORY)	X (Destructive Check)	1	1	1	2	2	2	3	3	3
Q+ SPOTS WITH AND WITHOUT INTERPOSED ADHESIVE	X	X (MANDATORY)	*	1	1	*	2	2	*	3	3	*
Q- SPOTS WITH INTERPOSED ADHESIVE	X	X (MANDATORY)	*	1	1	*	1	1	*	1	1	*
Q- SPOTS WITHOUT INTERPOSED ADHESIVE	X	X (alternative to hammer / chisel)	X (Not destructive check in alternative to ultrasonic check)	1	1	1	1	1	1	1	1	1

Table 4. Statistical control frequency.

Visual check: The correct quantity and distribution of welding spots (according to the specific operation sheet and spots layout). Absence of defects on welding, namely: excessive marks, weld sprays, blowing, double welds, weld spots with excessive diameter, burnt-cold-perforated weld spots, spots applied to the edge of tab or too close to a fold.

Mechanical check (hammer and chisel): Carry out an element detachment test on each welding spot section. Weld section refers to a set of spots applied using the same equipment. The test must be carried out at least on the first, central and final spot of the section checked if the cycle time does not allow more spots to be checked, and also in accordance with criticality relating to the machining process e.g.: welding of panels in several thicknesses, positioning of critical welding tongs, etc. When applying force near any weld spot, if the spot becomes detached, it should be considered (KO), if the panel only buckles, the spot may be considered (OK).



Figure 28. Hammer and chisel check

3.4.1. Ultrasonic systems

Ultrasonic inspection is a nondestructive method in which beams of high-frequency sound waves are introduced into materials for the detection of surface and subsurface flaws in the material. The sound waves travel through the material with some attendant loss of energy (attenuation) and are reflected at interfaces. The reflected beam is displayed and then analyzed to define the presence and location of flaws or discontinuities. The degree of reflection depends largely on the physical state of the materials forming in the interface and to a lesser extent on the specific physical properties of the material. For example, sound waves are almost completely reflected at metal/gas interfaces. Partial reflection occurs at metal/liquid or metal/solid interfaces, with the specific percentage of reflected energy depending mainly on the ratios of certain properties of the material on opposing sides of the interface. Cracks, laminations, shrinkage cavities, bursts, flakes, pores, and other discontinuities that produce reflective interfaces can be easily detected. Inclusions and other inhomogeneities can also be detected by causing partial reflection or scattering of the ultrasonic waves or by producing some other detectable effect on the ultrasonic waves. Ultrasonic inspection is one of the most widely used methods of nondestructive inspection. Its primary application in the inspection of metals is the detection and characterization of internal flaws: it is also used to detect surface flaws, to define bond characteristics, to measure the thickness and extent of corrosion, and (much less frequently) to determine physical properties, structure, grain size, and elastic

constants. The primary functional requirement from a nondestructive technique for spot weld inspection is the capability to assess and classify the spot weld quality into acceptable, undersize and unacceptable categories. Other requirements include cost-effectiveness of the inspection method and suitability for implementation and in the production environment without the requirement of highly skilled operators. The category of unacceptable welds is mostly comprised of "stick" welds, where the mating surfaces are weakly bonded in the weld zone because of shallow heating and melting. "Stick" welds are a predominant failure mode of the spot welding process. These welds have the same appearance as the acceptable welds, but will not produce a weld nugget when the sheets are peeled apart. In other words, the weld tears rather than the parent metal around it. The method described in this section is based upon an ultrasonic pulse-echo technique. By using transit time and attenuation of the ultrasonic energy, it enables detection of the presence and size adequacy of a weld in the weld zone. Early works pointed toward the probable success of the ultrasonic pulse-echo method applied through the thickness of the weld nugget. The technique has been successfully applied to heavier-gage sheet metal automotive parts for several years.

3.4.1.1. Wave path

The ultrasonic wave must be a beam directed perpendicularly to the faces of the sheets metal and through the center of the nugget. The width of the sound beam must be approximately equal to the smallest allowable weld diameter. In general, an ultrasonic wave is reflected when it impinges on an interface where a change in acoustic impedance occurs. In Figure 29 reflections are shown to occur at the outer surfaces of the two sheets. Reflections can also occur at the interface (air) between the two sheets if the nugget is small as in Figure 29. The nugget-to-parent metal boundary does not produce perceptible reflections, refraction or scattering because changes in density and velocity are a tenth of a percent or less (air-to-steel difference exceeds 99.9 %).

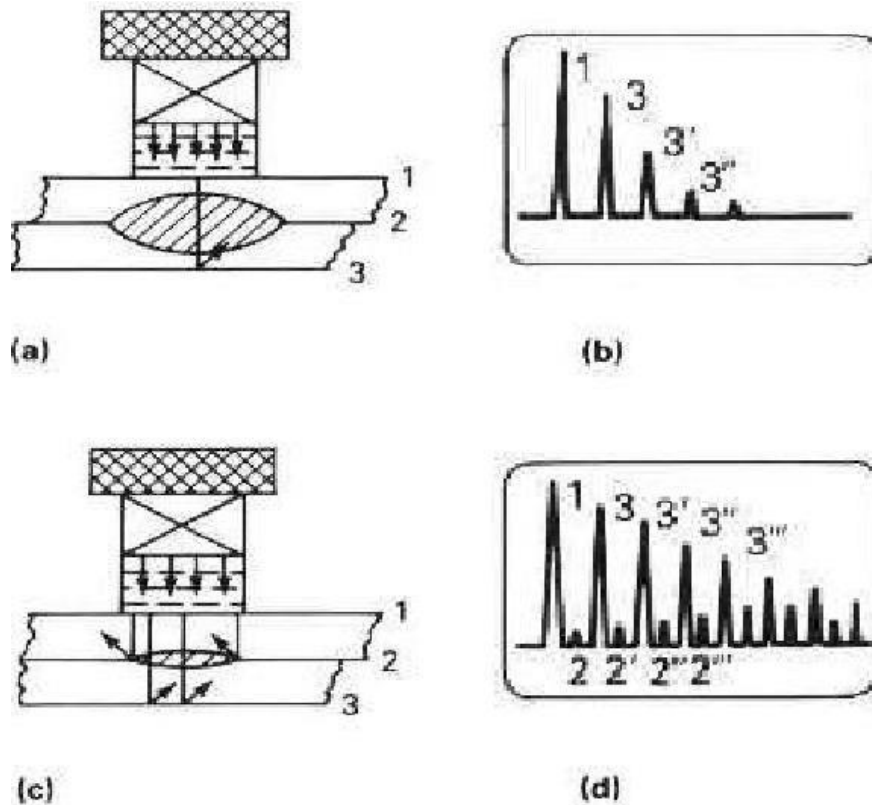


Figure 29. Ultrasonic pulse echo spot weld tests: wave paths in a satisfactory weld (a), echoes from the satisfactory weld (b), wave paths in an undersized weld (c) and echoes from the undersized weld (d).

Theoretically, one potential problem with testing spot welds is the slight curvature in the metal surfaces left by champing the welding electrodes. Empirically, this is found to have little effect on the ultrasonic test result. Typical oscilloscope displays showing the pulse-echo patterns for the two nugget-to-beam diameter ratios are shown in Fig. 29c (ultrasonic beam narrower than the weld) and Fig. 29a (ultrasonic beam wider than the weld). The difference in these echo patterns permits the ultrasonic method to distinguish between adequate and undersize welds.

3.4.1.2. Attenuation

Measuring the thickness of a weld nugget can only be done indirectly because the thickness gaging function determines just the thickness between the other faces in the nugget area. The nugget itself is measured by the effect of its grain structure on the attenuation of the ultrasonic

wave. As the wave reflects back and forth between the outer faces the weld sheets, its amplitude A is attenuated approximately exponentially with the distance as:

$$A = A_0 \exp(-2\alpha x)$$

The attenuation (rate of decay) α of the ultrasonic wave depends on the microstructure of the metal in the beam. In spot welds, the attenuation is caused principally by grain altering. The grains scattering ultrasonic energy out of the coherent beam causing the echoes to die away. In most metals, coarse grains scatter more strongly than the fine grains. For the Rayleigh scattering of interest here, the attenuation coefficient α attributable to scattering is approximated by:

$$\alpha = B V f^4$$

Where :

f = frequency (megahertz) ;

V = a variable approximately proportional to grain volume ;

and

B = a coefficient accounting for factors such as the preferred orientation of grains and anisotropy of individual grains.

A weld nugget is a cast microstructure with coarser grains than the adjacent cold rolled parent metal (still, though, in the Rayleigh region). For this reason, a nugget scatters more strongly than the remaining parent metal. It follows that a nugget produces higher attenuation than the parent metal and that a thick nugget produces higher attenuation than a thin nugget. Therefore, a thin nugget can be distinguished from a thick nugget by the echoes rate of decay for nuggets of equal diameter. A stick weld is zero reflectivity interface with minimal prior melting and effectively zero thickness nugget. It can be distinguished from a thicker nugget by the ultrasonic pulse echo rate of attenuation observed on an oscilloscope. Typical echoes from a good weld nugget and from a stick weld are compared in Figure 29.1.

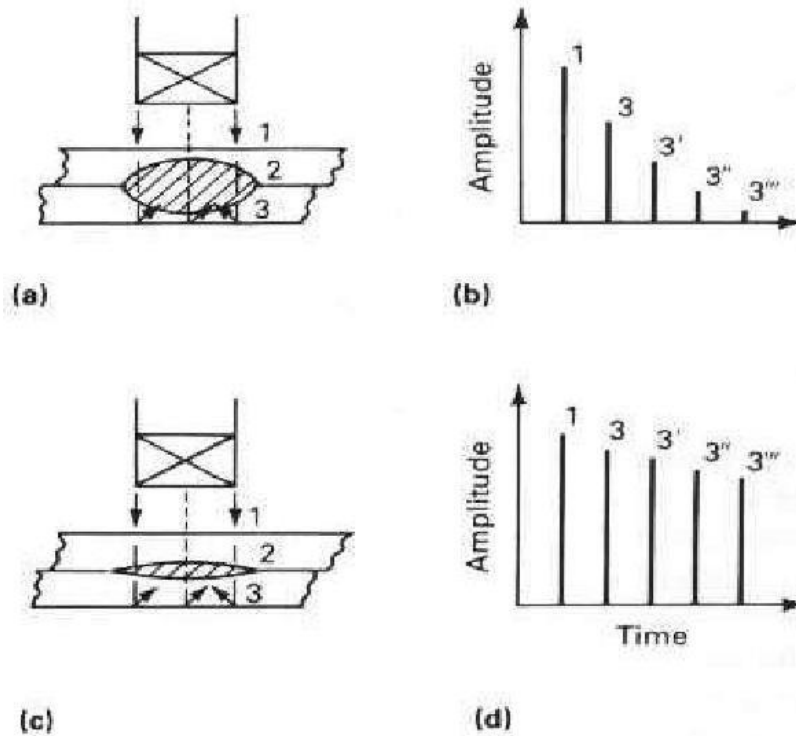


Figure 29.1. Ultrasonic attenuation from two spot welds: diagram of a satisfactory weld (a), (b) echo pattern from the satisfactory weld(b), diagram of a stick weld (c) and echo pattern from the stick weld (d).

It is possible to differentiate between the two welds on the basis of decay patterns. For this reason, the pulse echo ultrasonic method at normal incidence can be expected to perform the required measurements on spot welds in metals with coarse grained nuggets and fine grained parent sheet metal.

3.4.1.3. Limitations of ultrasonic testing

The information obtained from ultrasonic tests only refers to those parts of the test object which are covered by the sound beam of the probe used. The sound beam can be completely reflected from boundary surfaces within the test object so that flaws and reflection points lying deeper remain undetected. It is therefore important to make sure that all areas to be tested in the test object are covered by the sound beam. In present-day test practice, there are principally two different methods of flaw evaluation: If the diameter of the sound beam is smaller than the extent of flaw, then the beam can be used to explore the boundaries of the

flaw and thus determinate its area. In this method, the smaller the diameter of the probe's sound beam, the more accurately the boundaries (and therefore the flaw area) can be determined. Therefore, care should be taken to select a probe which will give a sufficiently narrow beam at the position of the flaw. If, however, the diameter of the sound beam is larger than the size of the flaw, the maximum echo response from the flaw must be compared with the maximum echo response from an artificial flaw provided for comparison purposes. In this method, the echo from a small, natural flaw is usually smaller than the echo from an artificial comparison flaw, e.g. circular disc flaw of the same size. This is due, for instance, to the roughness of the surface of a natural flaw, or to the fact that the beam does not impinge on it at right angles. If this fact is not taken into account when evaluating natural flaws, there is a danger of underestimating their magnitude. In the case of very jagged or fissured flaws, e.g. shrink holes in castings, it may be that the sound scattering occurring at the boundary surface of the flaw is so strong that no echo at all is produced. In such cases, a different evaluation method should be chosen, e.g. by using the back-wall echo attenuation in the evaluation. The distance sensitivity of the flaw echo plays an important part when testing large components. Attention should be paid here to choosing artificial comparison flaws which are as far as possible governed by the same "distance laws" as the natural flaws to be evaluated. The ultrasonic wave is attenuated in any material. This sound evaluation is very low, e.g. in parts made of fine-grained steel, likewise in many small parts of other materials. However, if the sound wave travels larger distances through the material, a high cumulative sound attenuation can result even with small attenuation coefficients. There is then a danger that echoes from natural flaws appear too small. For this reason, an estimate must always be made of the effects of the attenuation on the evaluation result and taken into account is applicable. If the test object has a rough surface, part of the incident sound energy will be scattered at its surface and is not available for the test. The larger this initial scattering, the smaller the flaw echoes appear, and the more errors occur in the evaluation result. It is therefore important to take the effect of the test object's surfaces on the height of the echo into account (transfer correction). All ultrasonic wall thickness measurements are based on a time-of-flight (TOF) measurement. Accurate measurement results require a constant sound velocity in the test object. In test objects made of steel, even with varying alloying constituents, this condition is mostly

fulfilled: the variation in sound velocity is so slight that it is only for importance for high-precision measurements. In other materials, the sound velocity variations may be even larger and thus affect the measuring accuracy. If the test object's material is not homogeneous, the sound may propagate at different sound velocities in different parts of the test objects. In this case, an average sound velocity should be taken into account for the range calibration. This is achieved by means of a reference block whose sound velocity corresponds to the average sound velocity of the test object. If substantial sound velocity variations are to be expected, then the instrument calibration should be readjusted to the actual sound velocity values at shorter time intervals. Failure to do so may lead to false thickness readings. The sound velocity within the test object also varies as a function of the material's temperature. This can cause appreciable errors in measurements if the instrument has been calibrated on a cold reference block and is then used on a warm or hot test object. Such measurement errors can be avoided either by warming the reference block to the same temperature before calibrating, or by using a correction factor obtained from tables. The measurement of the remaining wall thickness on plant components, e.g. pipes, tanks and reaction vessels of all types which are corroded or eroded from the inside, requires a perfectly suitable gauge and special care in handling the probe. The inspectors should always be informed about the corresponding nominal wall thickness and the likely amount of wall thickness losses.

3.4.1.4. Ultrasonic device

Ultrasound device consists of a "device for ultrasound tests" with a valid calibration certificate and having the following characteristics:

- Possibility of making use of the reflected echo procedure;
- Supported frequency field equal to 20 MHz at least;
- Automatic freezing of the image when the thresholds set by the user are achieved;
- Automatic assessment of the weld point: good point, cold weld, glued, small core, not welded, burnt;
- Internal database with the possibility of assigning the weld points to assembly, sub-assembly, component, weld point, each one with the relevant ultrasound parameters;
- Compatibility with firm Network;

- Possibility of saving the echograms and relevant parameters;
- Possibility of detailed reports;
- Statistic function.

There are special transducers, with internal water column, having a frequency of 15 or 20 MHz, according to the needs, and diameters fit for the diameter of the weld point to be tested. The probe shall have a diameter corresponding to the minimum diameter accepted by the weld point.

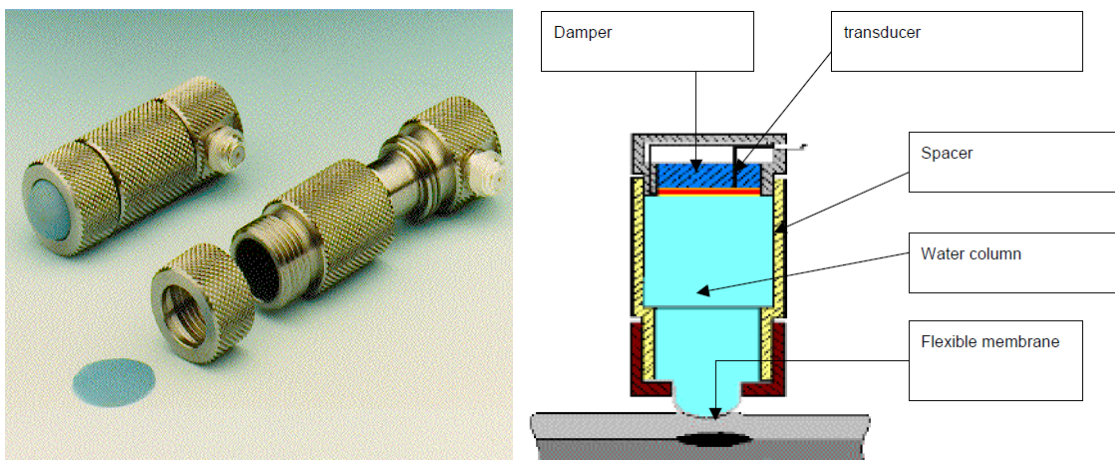


Figure 30. Ultrasonic probe

Thanks to its flexible membrane, the transducer fits for the various shapes of the weld point, then allowing the execution of a correct coupling. After mounting the membrane on the transducer and filling it with water, the membrane shall protrude for 4 to 7 mm in order to ensure a sufficient coupling. In case it does not occur, the transducer shall be filled with water again and the membrane shall be replaced with a new one. When filling the transducer with water, check that no air bubbles generate, for they could distort the test. In this case, the operation shall be repeated. During the execution of the test, the operator shall carry out periodical checks of the protrusion of the elastic membrane of the transducer and replace it when necessary.

Execution of detection In order to give an assessment of the tested joint, by means of the ultrasound method, the positioning of the transducer on the point surface is particularly useful. Due to the possible deformation of its membrane, the transducer has no well-defined support surface. As a consequence, in order to get optimal results when carrying out the assessment, a correct positioning is required imperatively.

Anomalies considered when allocating KO at the measurement stage are as follows:

- weld spot inefficient (e.g. see figure 31.2)
- small nugget diameter (e.g. see figure 31.3)

Figure 1: scan representing a "good spot"

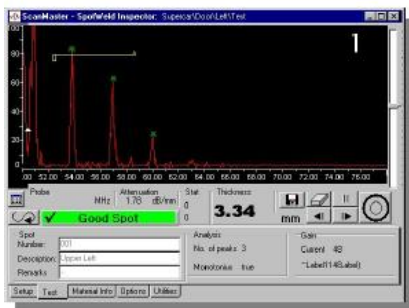


Figure 2: scan representing an "unwelded spot"

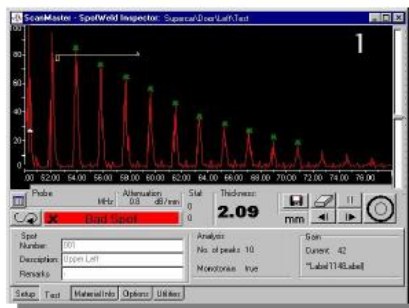


Figure 3: scan representing an "undersized spot"

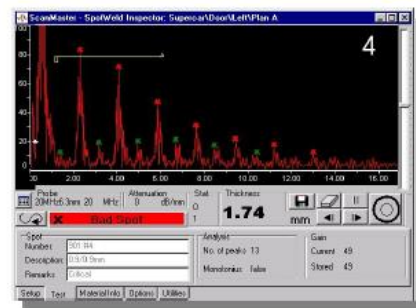


Figure 31. Ultrasonic scan

If a check is carried out on a weld section, the test must be carried out at least on the first, central and final spot of the section checked if the cycle time does not allow more spots to be checked, and also in accordance with criticalities relating to the machining process e.g.: welding of panels in several thicknesses, critical positioning of welding tongs, etc.

If a KO is obtained during the spot measurement, the measurement may be repeated, optimizing probe positioning by means of circular movement and/or repositioning.

The spots with interposed adhesive and inaccessible spots must be checked with the ultrasonic test.

1. Analysis and control of the RSW process

The RSW process is a metal-absorbing energy and then melting process. External electrical power is applied on the workpieces, and heat is initially generated at the interface of two separate sheet metal, and then gradually spreads to nearby zones. In general cases, the electrode force applied on the RSW system is controlled with air pressure in a pneumatic cylinder, its value using a predetermined setting during the welding process. On the other hand, the external energy can be applied through an electrical system of RSW machine. The most commonly used RSW machine utilizes two silicon controlled rectifiers (SCRs) to control the energy input, which uses individual firing angle to control the amount of energy delivered into the workpieces for each control cycle. The power source is usually an alternating current (AC) type, and one sine wave of the power source includes two control cycles of the operation of the RSW machine. This type of RSW is called single-phase AC RSW. Although there is another type of RSW machine, a three-phase medium frequency direct current (MFDC) RSW, deemed advantageous in some certain practical applications, the single-phase AC RSW is predominantly used in the modern automotive industry. The heat generated in the weld during the welding process follows the basic Joule heat generating formula:

$$Q = \int_{T_1}^{T_2} I(t)^2 R(t) dt,$$

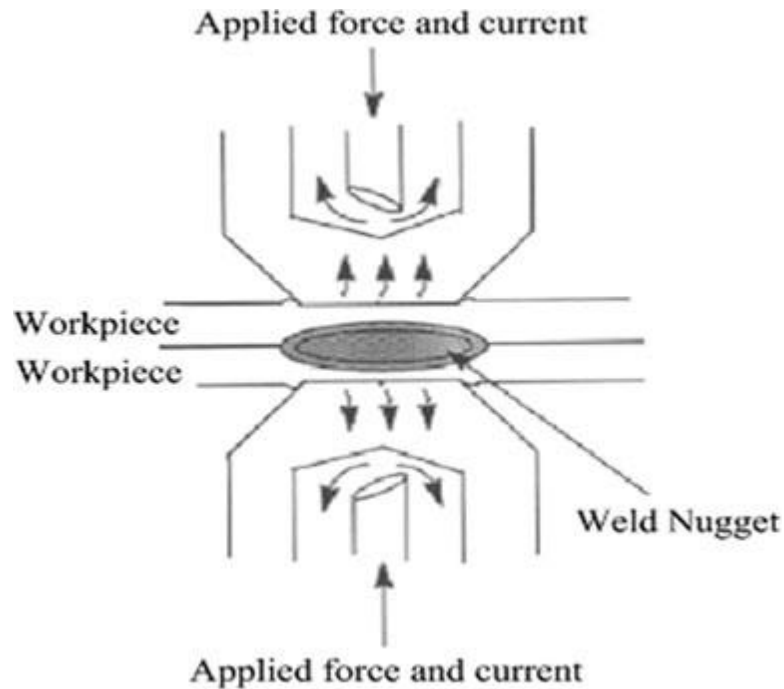


Figure 32. Schematic of the resistance spot welding process

where Q is the amount of heat energy generated in the weld, $I(t)$ is the welding current, $R(t)$ is the dynamic resistance of the sheet metals, T_1 and T_2 denote the beginning and ending times of the operation, respectively. The heat energy generated in the weld, which is also the heat energy absorbed by the weld, depends on the welding current, dynamic resistance, and welding time. The characteristics of dynamic resistance should be considered carefully in advance. During the welding process, the dynamic resistance undergoes a series of different variations. One integrated RSW process has been divided into six stages. The dynamic resistance in general, at stages I, II, and III, consists of the contact resistance, caused by the surface roughness and contaminants, and the bulk resistance of the weld, which is common metal resistance. At the beginning of the process, the surface contact resistance is much larger than the bulk resistance. Hence, the heat energy absorbed by the weld would be concentrated at the surfaces of the weld. As a result, the surface contaminants would break down and surface asperity would be softened. Therefore, at stage I, due to the temperature being increased, the contact resistance decreases very fast, while the contact area increases.

On the other hand, the bulk resistance keeps increasing from stage I to III because its resistivity increases with the rising temperature. Its value can maintain the changes following the certain rule of the metal resistance, which is the Ohm's law, during the whole welding process. The overall dynamic resistance begins to rise at stage III, when the contact resistance has been mostly eliminated and the bulk resistance is almost contributed by purely solid metals. At the beginning of stage IV, the metal starts melting. Then, the molten liquid metal appears and the nugget begins to grow, and the workpiece will be a mixture of solid and liquid metals. As a result, this point, which is also the first melting point of the weld, should be the starting point for establishing the model for the relation between heat energy and nugget diameter. After this point, the solid and liquid metals may share the same temperature because of the existence of latent heat or enthalpy of fusion, but they do not share the same electrical resistivity. Thus, if the energy delivered into the workpiece can make the nugget formation and growth process consistent, the overall dynamic resistance would have different variation tendency at the time when the first melting point appears, due to the changing composition of the weld. This feature can be used to online detect the first melting point. After the time when the first melting point appears, the molten liquid metals increase and solid metals decrease. Because liquid metal has a lower resistivity, its increase makes the integrated dynamic resistance decrease. On the other hand, the resistance of the solid metal is still increasing because of the increasing temperature. After a short while, the dynamic resistance will decrease from a peak.

In the proposed control system, the energy controller should be chosen appropriately to guarantee the consistency of the nugget formation and growth. Then, the online nugget diameter estimator can be designed after online detection of the time when the first melting point appears. The online nugget diameter can accurately supply the real-time value of nugget diameter to the control system. The integrated control system design should be based on the physical characteristics of the RSW process.

1.2 Control strategy of the proposed control system

The first step is to select the most appropriate energy closed-loop controller for the proposed control system. There are three control strategies used in the modern welding industry: constant current control (CCC) strategy, constant heat control (CHC) strategy, and constant voltage control (CVC) strategy. Currently, CCC is the most common type of strategy used in the industry due to its simplicity, reliability, and performance. However, which strategy should be chosen depends on how the strategy affects the nugget formation. The weld is a mixture of solid metal and molten liquid metal after the first melting point. The liquid metal is in the middle of external solid metals and surrounded by solid metals; these parts are in series connection. In order to analyze and model the process conveniently, the nugget growth should have a smooth and consistent rate during the welding process. To achieve this goal, an appropriate energy control strategy is needed. After the time when the first melting point of the weld appears, the heat energy generated in the weld is latent heat, which is a constant and cannot increase the temperature significantly. The temperature at the interface layer between the solid and liquid part can be considered the same as the temperature in the liquid nugget, and the resistivity of the liquid part near the interface layer would also be the same because they share the same temperature. In fact, the temperature of the liquid weld can be considered the same during the welding process because of the existence of latent heat. Then, assuming the weld is divided into a uniform small unit volume, to convert one volume from solid into the liquid state would cost the same amount of heat energy. In addition, the resistance of each volume is also the same. Under this circumstance, CCC should be adopted since it guarantees constant heat energy is provided to generate new liquid units continuously, despite the fact that the heat energy delivered into the entire solid part is not constant due to the variation of the dynamic resistance in the different stages of the welding process. Hence, during one certain period, there are constant amounts of unit volume of the solid part near the interface layer converted into a liquid nugget. In other words, no matter what the value of resultant dynamic resistance changes, the nugget growth rate would be approximately constant, if CCC is used. On the other hand, if CHC is used, when the total dynamic resistance increases at the initial stages, the welding current would decrease. As a

result, the heat energy generated for converting solid part to liquid part would be reduced since the resistance of each unit volume near the interface layer is approximately the same at any given time. Although the heat energy generated in the total weld is constant, the decreasing welding current leads to decreased nugget growth during the dynamic resistance ascending phase. On the other hand, if the resultant dynamic resistance is decreasing after peak β , the welding current would increase based on CHC. Therefore, the nugget growth increases. Hence, the CHC strategy leads to the nugget growth changing rather than maintaining a constant rate. In addition, when the welding current is increasing after the dynamic resistance passes the peak β , the increasing nugget growth based on CHC strategy may lead to possible expulsion or over-weld rather than keeping the nugget size approaching its limit gradually as it should be. Moreover, CVC may cause the same results as CHC: the variation tendency of the welding current opposes the variation tendency of dynamic resistance. Hence, as far as nugget growth is concerned, CCC is the sole control strategy for establishing a consistent relation because the heat energy absorbed by the total weld can be allotted rationally during an integrated welding process.

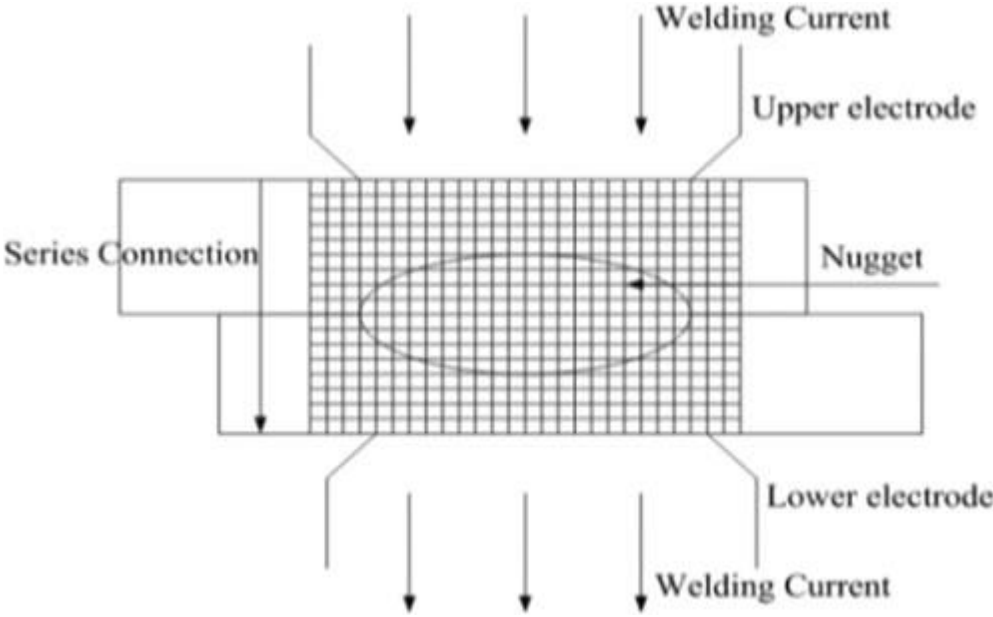


Figure 33. Metal states during the welding process

1.3 Control of welding time during one operation

In conventional CCC welding operations, the welding time is a predetermined value for a given weld. Therefore, the nugget diameters of the welds cannot be the same due to the different initial surface conditions of the welds even from the same batch. To obtain the desired nugget size for given welds, the welding times should differ even if the CCC strategy is used. Hence, welding time is not a predetermined value in the proposed control system. In practice, the actual welding time should be decided by the online calculation of the nugget diameter, which is obtained by an online nugget diameter estimator. To achieve online nugget diameter control, a precise model should be established. Assuming that such a model can be obtained, the proposed control system is depicted schematically. The proposed online nugget diameter estimator can be considered as a nugget diameter sensor. The welding time can be determined according to the error between the desired nugget diameter and the calculated nugget diameter from the online nugget diameter estimator. If the calculated value of nugget diameter approaches that of the predetermined goal within the given tolerance, welding action should be terminated immediately; otherwise, welding action will continue, and the nugget size will continually increase. The actual welding time is determined online according to the preliminary goal and the result of the estimator. In addition, a three-phase MFDC RSW and a single-phase AC RSW have the same working principle for nugget formation. Even though the control system was developed based on a single-phase AC RSW machine, the framework proposed in this paper can be also applied in a three-phase MFDC RSW machine. In this work, the controller combines a nonlinear controller and a PI controller that adjusts the input of the nonlinear controller. Because the input and output of the PI controller are welding currents with the same units, the confirmation of the parameters in the PI controller is easier than other common PID controllers. The mathematical description of the controller is:

$$\begin{cases} e_i = I_R^d - I_{R,i}^a \\ I_{R,i}^c = I_{R,i}^a + K_p e_i + K_i \sum_{j=1}^i e_j \\ \alpha_{i+1} = \frac{\arccos \left[\frac{I_{R,i}^c}{I_{R,i}^a} [\cos(\omega \alpha_i) - \cos[\omega (1/(2f) + \psi_i)]] + \cos[\omega (1/(2f) + \psi_i)] \right]}{\omega}, \end{cases} \quad (2)$$

where the subscript i denotes the value in the i th control cycle, the control process is a recursive process. The welding current is evaluated using RMS values; I_R^d is the desired welding current, while $I_{R,i}^a$ is the actual welding current in the i th control cycle and K_p , K_i are parameters in the PI controller. After the PI adjustment, the welding current $I_{R,i}^c$ is the input of the nonlinear controller. f is the frequency of the AC machine, ω is the corresponding angle frequency, its value is $2\pi f$; α_i denotes the firing angle in the i th control cycle. Equation (2) is to obtain the firing angle α_{i+1} after i th control cycle. The corresponding control flowchart is shown in Fig. 35. After the energy control strategy is confirmed, the online nugget diameter estimator should be designed to supply the real-time value of nugget diameter to the control system.

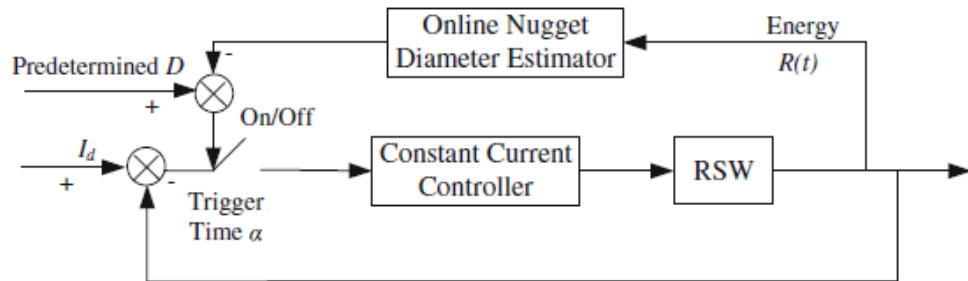


Figure 34. Basic building block of the proposed control system

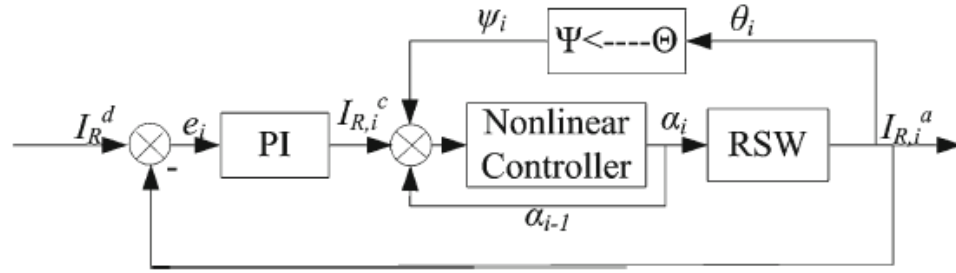


Figure 35. Flowchart of the control system

2 Proposed online nugget diameter estimator

The online nugget diameter estimator is the most important part of the proposed control system. It will be capable of providing real-time information about the nugget diameter of a weld during the welding process. As described in the preceding sections, the nugget diameter can be described by heat energy absorbed by the weld after the time when the first melting point appears during the welding process:

$$D = f(E), \quad (3)$$

where D denotes the nugget diameter, and E denotes heat energy absorbed by the weld. To establish the mathematical model for the online nugget diameter estimator, the time when the first melting point of the weld appears during the RSW process should be considered first. Because before the time when the first melting point appears, even if a certain amount of heat energy input has been absorbed by the weld, there is no formation of the nugget. In other words, there is a time delay or dead zone between the energy input and nugget formation. The model to be developed, which relates the heat energy and nugget diameter, should be established from when the first melting point appears.

2.1 Principle of online detecting the time when the first melting point of the weld appears during the RSW process

The exact time when the first melting point of a weld appears cannot be directly measured because the nugget formation process cannot be directly gauged effectively with current technology. The particular time can only indirectly be gauged based on analysis of the characteristics of nugget formation and growth. The first melting point being generated, the workpiece is total solid metal; while after the first melting point, the workpiece is a mixture of solid and liquid metals. Due to the latent heat, the temperature of the liquid part will roughly remain the same, but the temperature of the solid part can keep increasing until it reaches the temperature of the melting point and then melts. If the constant current control scheme is used during the welding process, the increasing rate of the temperature of the weld before the first melting point will be larger than that after the time when the first melting point appears. In other words, the increasing rate of the temperature of the weld has a sudden drop when the first melting point appears. This is because the heat energy delivered into the weld before the time when the first melting point appears will be all used to increase the temperature or dissipated, but after that time, part of the heat delivered into the weld will be used to generate the latent heat. Since the dynamic resistance of the weld is temperature dependent, the variation of the temperature will be reflected in the variation of the dynamic resistance of the weld during the welding process. Hence, it is possible to detect the first melting point according to the increasing rate or slope of the dynamic resistance curve of the weld. Moreover, liquid metal has a lower electrical resistivity than solid metal. Before reaching the first melting point, the workpiece is one integrated solid metal; when this particular point is reached, it becomes a mixture of solid and liquid metals. Based on these two reasons, the increasing rate or the slope of integrated dynamic resistance curve should have a clear drop immediately after the time when the first melting point just appears, under the condition of a constant current control. Hence, when the first melting point appears, the slope of dynamic resistance has a different variation tendency. This feature can be used to online detect the time when the first melting point appears. The first-order derivative value of the dynamic resistance with respect to time is employed to calculate the slope of the

dynamic resistance. When the first melting point appears, its value should have a sudden drop. This drop can be detected easily using the second order derivative value of dynamic resistance. Since the slope of the dynamic resistance curve near the first melting point should be positive, the sign of the second order derivative value of the dynamic resistance should change from positive to negative when the first melting point appears. As a result, the first melting point should correspond to the peak of the first-order derivative value of the dynamic resistance. Therefore, the time when the first melting point appears is the time when the first-order derivative value of the dynamic resistance achieves the peak and the second-order derivative value changes its sign from positive to negative. The principle of online detecting the first melting point can be shown in Fig. 36,

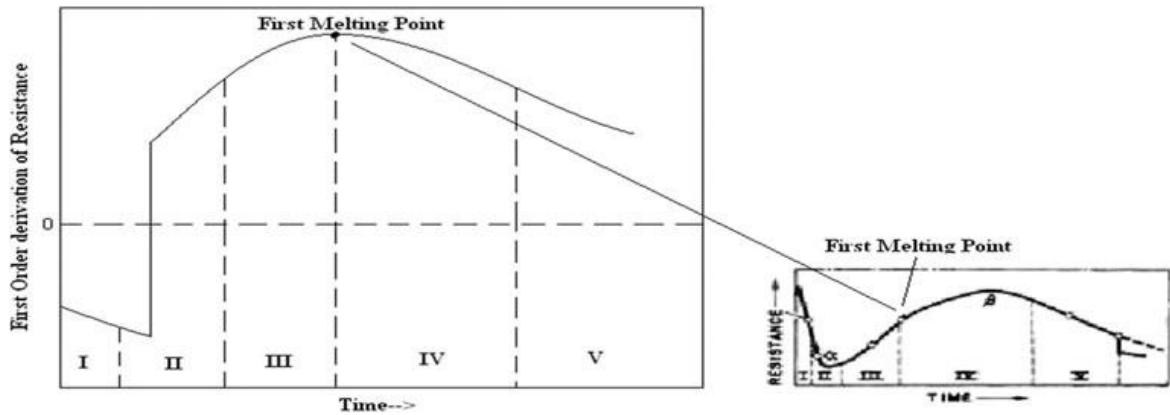


Figure 36. First-order derivative value of dynamic resistance curve

which presents an approximate first-order derivative value of a dynamic resistance curve. Hence, the first melting point can be obtained online according to the slope change of the dynamic resistance curve. In summary, the time when the first melting point appears can be obtained as follows, let

$$dy'(i-1) = \frac{dy(i) - dy(i-1)}{\Delta t}, \quad (4)$$

where dy_0 denotes the first-order derivative value of the dynamic resistance, dy is the original value of dynamic resistance, Δt is the data calculating cycle, and i is the index of calculating data. Then:

$$\begin{cases} t_{\text{first melting point}} = i_{\text{max}} \cdot \Delta t \\ i_{\text{max}} = i \text{ when } dy'(i) = dy'_{\text{max}} \end{cases}, \quad (5)$$

where $t_{\text{first melting point}}$ denotes the time when the first melting point appears, $dy_{0 \text{ max}}$ denotes the maximum of first-order derivative value of dynamic resistance, i_{max} is the data index of $dy_{0 \text{ max}}$, whose time corresponds to $t_{\text{first melting point}}$. In order to precisely estimate when the first melting point appears, the dynamic resistance must be measured online with a very high resolution in advance. Although there is some previous work on calculating dynamic resistance, only one value of dynamic resistance can be obtained during each control cycle. Generally, the frequency of the power source is 50 Hz, which means that the frequency of the dynamic resistance sampling system was merely 100 Hz. Since more detailed information about the dynamic resistance is required for detecting this particular point, an alternative method for obtaining dynamic resistance values with a high resolution in real time is required. Dynamic resistance of RSW is supposed to be easily obtained based on the measured values of electrode voltage and welding current using Ohm's law. However, during the welding process, the phases of positive and negative power supplies may not match entirely, and the differences of the phases between positive and negative trigger circuits may not be consistent cycle by cycle. The electrical system of RSW is low voltage–high current; the values of electrode voltage and welding current cannot be obtained with the same devices at the same time. The electrode voltage can be measured by common devices because the value is small. On the other hand, the value of the welding current is very large; hence, a special device is required for this measurement. To measure very large alternating current, a Rogowski current transducer is often used. The original sampling value of the transducer is the product of the deviation of the welding current and induction coefficient of the transducer. The welding current can be obtained using some necessary data transformations through special hardware design and corresponding mathematical algorithms. Hence, though the data sampling facilities for electrode voltage and welding

current use the same sampling frequency and central processor, obtaining the dynamic resistance by directly using Ohm's law can cause serious problems. Considering there is noise in the welding system, the electrode voltage can be written as:

$$U(t) = RI(t) + \Delta U(t), \quad (6)$$

where $U(t)$, $I(t)$, R denote the electrode voltage, welding current and dynamic resistance, respectively. $\Delta U(t)$ denotes the random error. For eliminating the negative effects resulting from $\Delta U(t)$, Eq. (6) can be processed through multiplying $I(t)$ during one integrated cycle of AC power supply, which includes two control cycles of RSW operation. Hence, Eq. (6) can be written as:

$$\sum_{\text{two continuous cycles:}} U(t)I(t) = R \sum_{\text{two continuous cycles:}} I^2(t) + \sum_{\text{two continuous cycles:}} \Delta U(t)I(t). \quad (7)$$

During two control cycles of RSW operation, welding current follows an approximately symmetrical pattern with the opposite polarities because the properties of the workpiece do not undergo significant changes during two neighboring control cycles, $\Delta U(t)$ is a random value, which is much lower than that of the welding current, the last element in the Eq. (7) can be neglected. Therefore, the dynamic resistance R can be written as:

$$R = \frac{\sum_{\text{two continuous cycles:}} U(t)I(t)}{\sum_{\text{two continuous cycles:}} I^2(t)}. \quad (8)$$

In this equation, the numerator and denominator are the sums of products during two continuous control cycles, which include one positive trigger and one negative trigger. During the actual calculating process, the corresponding data [numerator and denominator in Eq. (8)] in the two control cycles preceding the current one are stored and updated for later use point by point. Using this new processing method, a corresponding dynamic resistance value can be obtained for each sampling point from the third control cycle. The resolution of

the proposed method is significantly increased in comparison with the conventional method, which only obtains one measurement per control cycle. Each value of dynamic resistance based on Eq. (8) is a processed result using electrode voltage and welding current from two control cycles. Furthermore, because the dynamic resistance values can be obtained with a high resolution, it is possible to pick up a lot of noise during the process. To eliminate the noise, a simple online filter was used. In general, the dynamic resistance curve should be smooth and monotone of time. A special filter based on the Jensen inequality was designed as follows:

$$R(i) = \begin{cases} R(i) & \text{if } i = 1 \\ R(i) & \text{if } i = 2 \text{ and } R(i) > 0.5(R(i+1) + R(i-1)) \\ 0.5(R(i+1) + R(i-1)) & \text{if } i = 2 \text{ and } R(i) < 0.5(R(i+1) + R(i-1)) \\ R(i) & \text{if } i \geq 3 \text{ and } R(i) > 0.25(R(i+1) + R(i+2) + R(i-1) + R(i-2)) \\ 0.25(R(i+1) + R(i+2) + R(i-1) + R(i-2)) & \text{if } i \geq 3 \text{ and } R(i) < 0.25(R(i+1) + R(i+2) + R(i-1) + R(i-2)) \end{cases} \quad (9)$$

This filter utilized the neighboring values to balance out the values at each point. As a result, the filter can generate a smooth external envelope of original data. After obtaining sufficient data regarding dynamic resistance, the first melting point of the weld can be found by carefully processing the data based on the Eqs. (4–5).

2.2 Experiment for dynamic resistance measurement and detecting the first melting point of the weld during the RSW process

The effectiveness of the proposed method for online measurement of the time when the first melting point of the weld appears should be experimentally verified. The experiment was conducted on a 63 kVA single-phase AC RSW machine. The electrode force was determined by the pressure differential of the two air pressure gauges. The air pressure applied was 0.18 MPa. The particular electrode geometry used in this work was a truncated cone with a 160° angle and a 5-mm face diameter. The corresponding controller was implemented by the dsPIC6014, which is a digital signal processor (DSP) manufactured by Microchip Technology Inc. The realization of the algorithm achieved in the experiment was written using C language. The welding workpiece used was mild steel sheet with a thickness of 1.5 mm. In addition, the

electrode voltage was obtained by a tip voltage detection cable, while the welding current was detected by a Rogowski current transducer. The welding machine together with electrode voltage and welding current sampling devices and their installations are shown in Fig. 37.

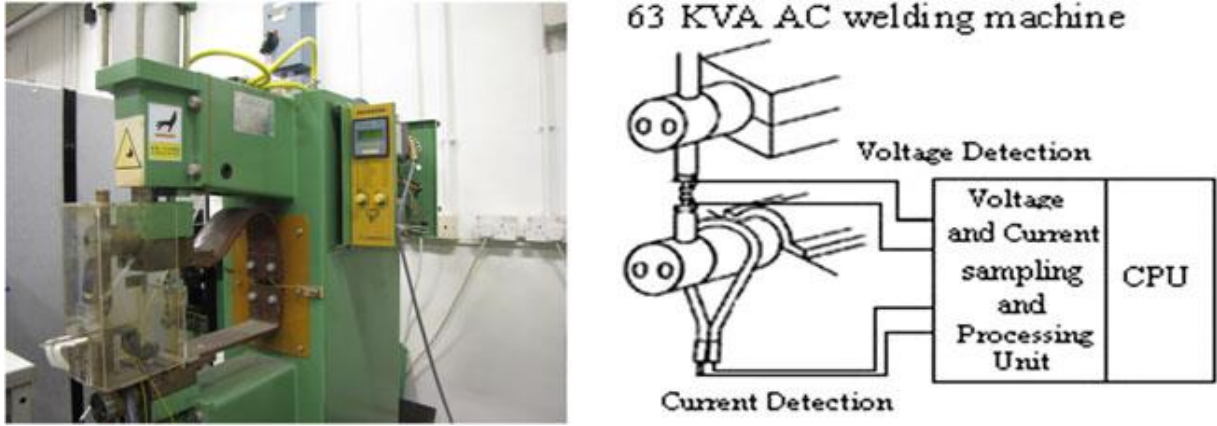


Figure 37. Welding machine (63 kVA) and the voltage and current sampling device and their installation

To validate the accuracy of the dynamic resistance measurement obtained using the new processing method, the RMS value of dynamic resistance is introduced for comparison.

$$R(n) = \sqrt{\left(\sum_{j=1}^{N_R} u_j^2\right) / \left(\sum_{j=1}^{N_R} i_j^2\right)}, \quad (10)$$

where n denotes the number of control cycles, N_R denotes the number of sample points in the n th control cycle, and u and i are the values of electrode voltage and welding current. The first step is to use the open-loop control to check whether the RSW circuit has the inductive noise, even though the electrode voltage is measured between upper and lower electrodes. For eliminating the inductive noise, peak value of each control cycle was used in previous work, the method uses the formula: $V=Ri+L di/dt$, when the welding current achieves the peak value in each control cycle, di/dt equals to zero; hence, one value of dynamic resistance can be

obtained. Figure 38 shows the RMS value of the dynamic resistance, while Fig. 39 shows the values of the dynamic resistance using the peak value of each control cycle. The firing angle in the experiment is 126° . Comparing the two figures, they show an approximate pattern. This shows that the inductive elements in the circuit are very small. In addition, the RMS value can be used to describe the dynamic resistance values. The errors between the two calculating methods are from the different data processing methods. Because the peak values of electrode voltage and welding current are hard to precisely locate, and many experiment results show that the curves may not be smooth enough when the peak value method is used, the RMS value of dynamic resistance, which utilizes more data acquisition information, is used in this work. Then, to check the effectiveness of the proposed measurement method of dynamic resistance, two comparisons were conducted. Figure 40 shows the experiment results which use $R(t)=V(t)/I(t)$ directly. Figure 10 shows the experiment results, which are obtained from the method shown in Eqs. (8–9); also, the RMS value and the value using the proposed method are depicted together. It shows that the direct division cannot obtain a satisfactory result of dynamic resistance because electrode voltage and welding current do not match. However, the proposed method can obtain a more reasonable result of dynamic resistance. In Fig. 41, the curve has no initial drop because the dynamic resistance calculation begins from the third control cycle using the proposed new method. The lateral axis is the actual current effective time of the welding process. The effective time during one control cycle indicates the duration when the welding current is not zero and one SCR is turned on. Hence, the effective time during one control cycles is <0.01 s. In the experiments, its value is <0.005 s during one control cycle because the majority of conduction angles θ are $<90^\circ$. In addition, the effective time begins from the third control cycle to coincide with the proposed new method of dynamic resistance measurement shown in Eqs. (8–9). According to the comparison in Fig. 41, the values obtained from the proposed method have patterns approximating to the curves of RMS values of dynamic resistance, which have lower resolution. Then, the experiment was conducted to online detect the time when the first melting point appears. In this experiment, CCC strategy in Eq. (2) was used. After fine tuning the constant current controller, the optimum value of parameters of the PI controller are $K_p=0.75$ and $K_i=0.3$. The predetermined welding current was set to be 7500 A; the welding time was 12 cycles of power source, which

had a frequency of 50 Hz. The number of control cycles was 24; hence, the number of RMS values of the dynamic resistance was also 24. The data sampling frequency was 6.4 kHz, and dynamic resistance calculation was executed after collecting four sets of sampling data, showing that the calculating frequency was 1.6 kHz. The following figures show the experiment results. Figure 42 shows the corresponding dynamic resistance curve using the proposed method, with the lateral axis as the actual current effective time. Figure 43 shows the corresponding first-order derivative value of dynamic resistance. The time when the peak value occurs in Fig. 43 can be easily determined, as it corresponds to the time when the first melting point of the weld appears. As demonstrated in the figure, the first melting point appeared at 0.0228125 s, which corresponded to the seventh control cycle. The RMS value of the dynamic resistance for this control cycle, which included the first melting point of the weld was $1.7036 \times 10^{-4} \Omega$. Experiment results confirmed that the proposed method of dynamic resistance measurement can be employed for highly accurate online detection of the time when the first melting point of the weld appears. With this information, revealing the relation between the nugget diameter and the heat energy absorbed by the weld in real time becomes possible. In order to evaluate the variations of the dynamic resistance of the welds under the same welding condition, an additional ten experiments were conducted. The experiment conditions were the same as in the previous experiment. Figure 44 shows the experiment results with 10 curves. Each curve consists of 24 RMS values of dynamic resistance. The maximum differences between these 10 curves at particular locations are shown in Table 5; the unit of resistance is $10^{-4} \Omega$.

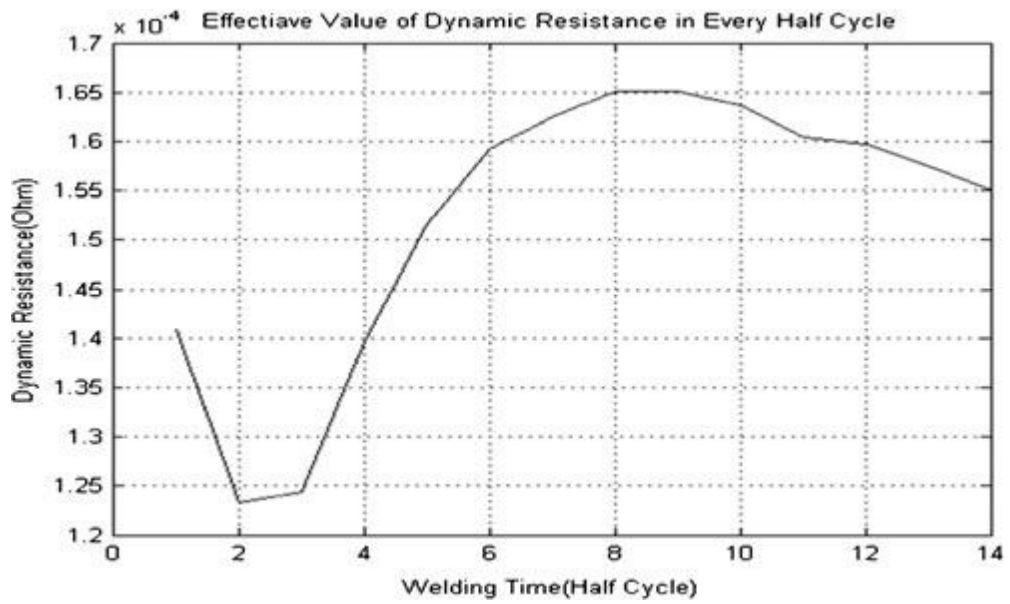


Figure 38. RMS value of dynamic resistance

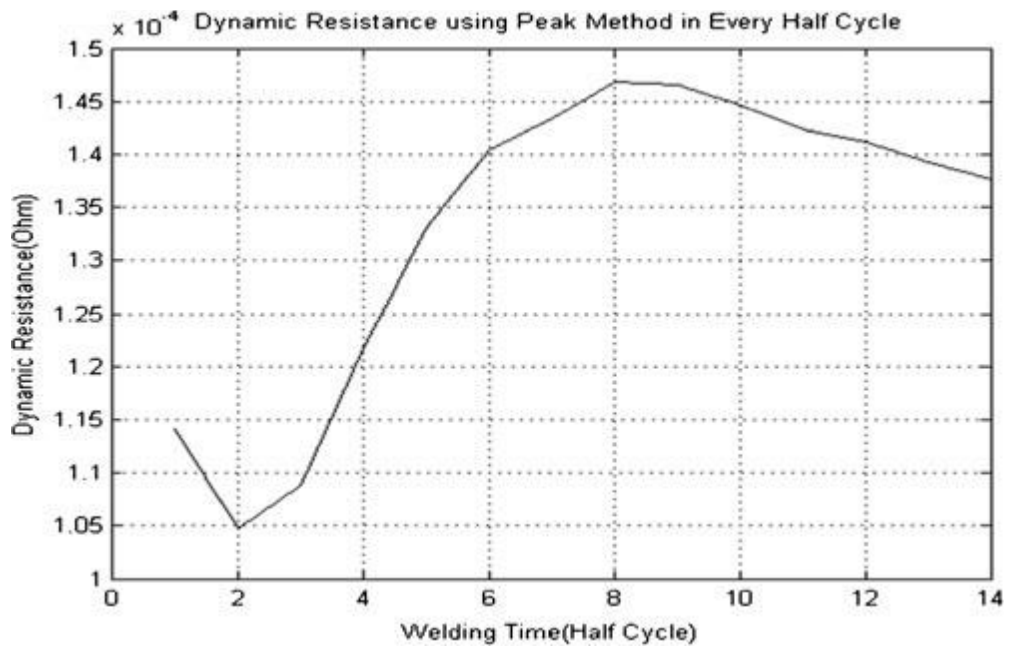


Figure 39. Dynamic resistance value using peak value

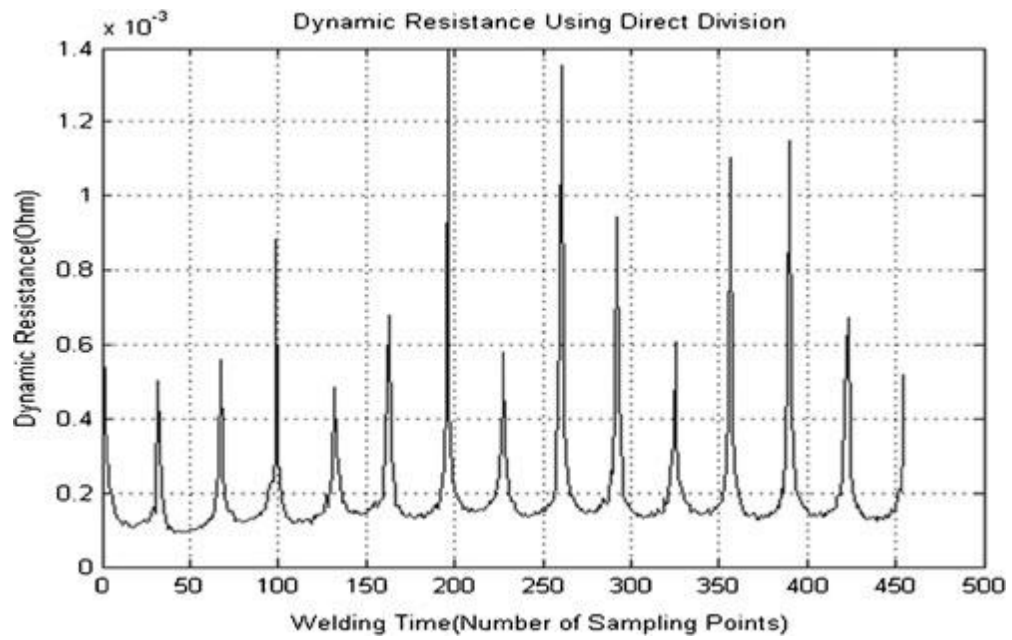


Figure 40. Dynamic resistance using direct division

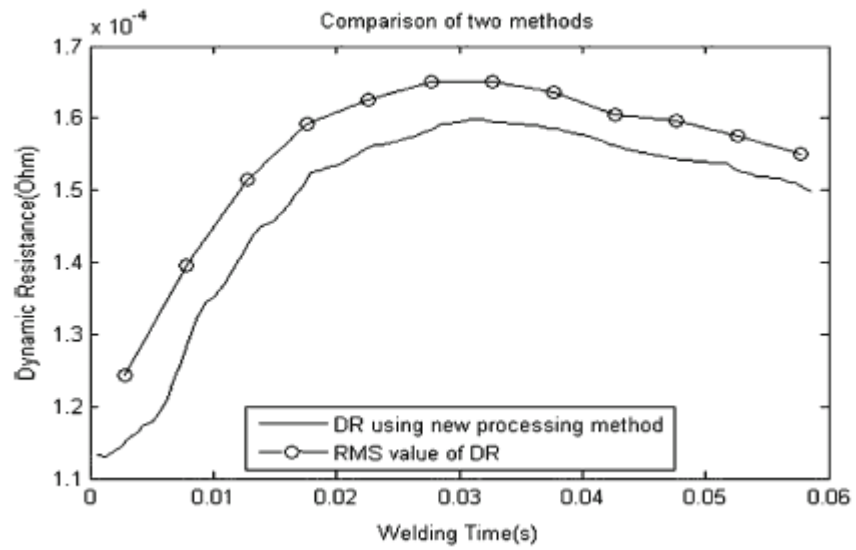


Figure 41. Dynamic resistance value using the proposed method

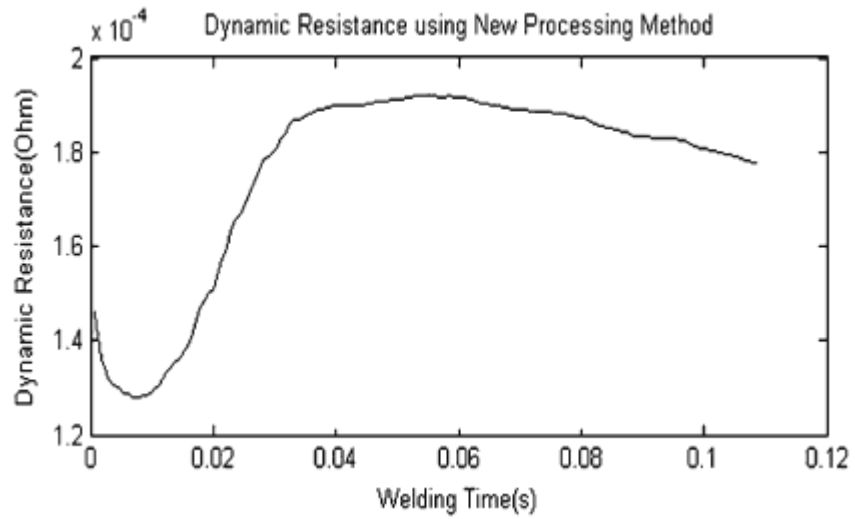


Figure 42. Comparison of dynamic resistances of two methods

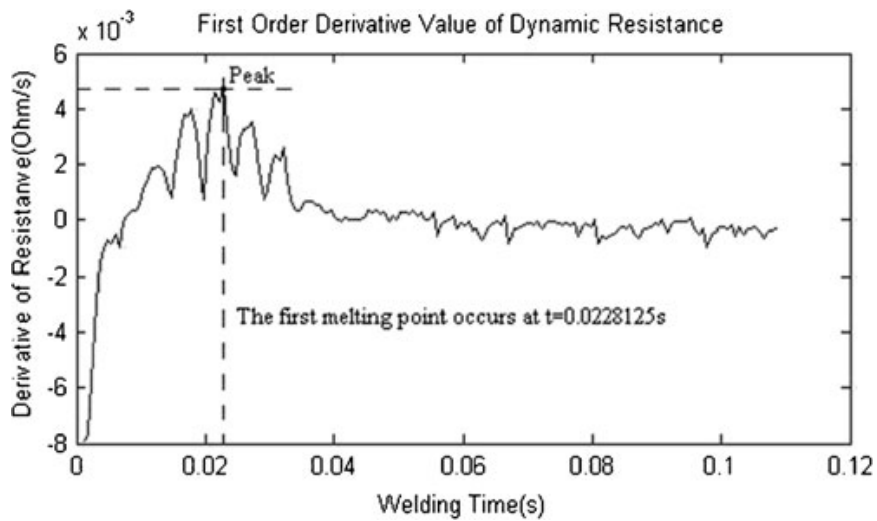


Figure 43. First-order derivative value of dynamic resistance

As observed in Fig. 44 and Table 5, the 10 curves have large differences in dynamic resistance values, even under the same welding condition. The largest difference usually occurred at the beginning while the contact resistance dominated the total dynamic resistance before the nugget was formed. Then, the differences decreased gradually as the welding time increased.

The above experiment results demonstrate the importance of selecting an optimum initial starting point to obtain a precise model for estimation of the nugget diameters using the value of heat energy absorbed by the weld.

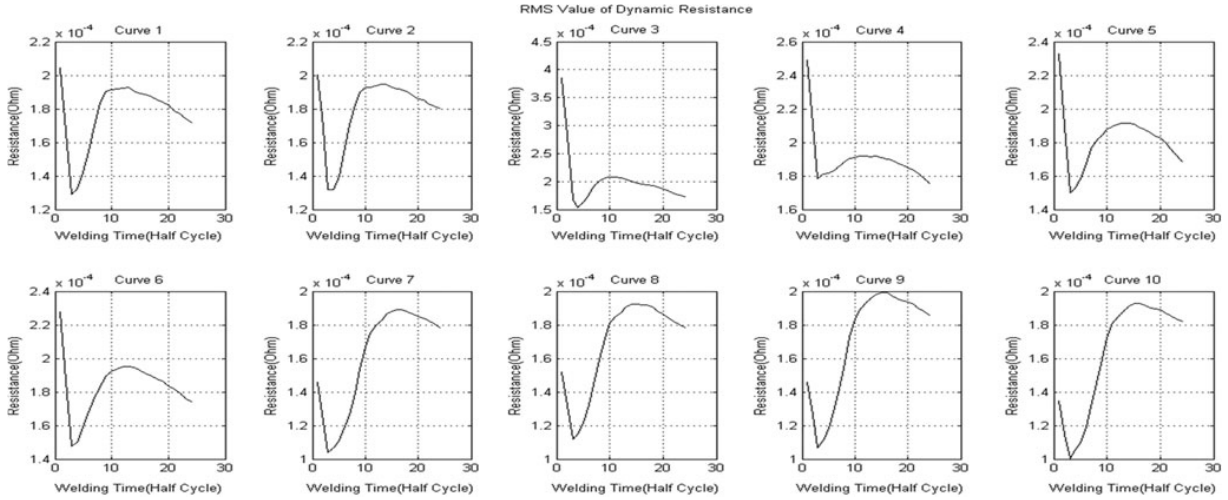


Figure 44. Ten curves with the same welding conditions

Particular locations	Dynamic resistance ($/10^{-4} \Omega$) at			
	First point	Minimum point	First melting point	Peak
Maximum difference	2.1521	0.7548	0.3759	0.1940

Table 5. Comparison of the dynamic resistance errors at particular points

2.3 Mathematical model of the relation between nugget diameter and heat energy absorbed by the weld

After online detection of the time when the first melting point appears, the actual model of the relation between the nugget diameter and heat energy absorbed by the weld can be established. The nugget is formed due to the weld absorbing the externally delivered heat energy. In addition, in the interface layer between solid and molten liquid parts, the temperature is

approximately the same because of the existence of latent heat. Hence, one specific nugget volume should be generated by one specific amount of heat energy because the heat energy that contributes to phase transition and metal melting is latent heat, a constant for a specific material. Then, a specific mathematical model of the relation between the nugget volume and heat energy that contributes to phase transition can be described as:

$$V \cdot C_1 = E_1, \quad (11)$$

where V denotes the nugget volume, E_1 is the heat energy which contributes to form V , and C_1 denotes the transition coefficient. However, in practical applications, only the total heat energy absorbed by a weld can be monitored and measured because there is no effective method of distinguishing the solid metal and the molten liquid metal. Assuming there is a time-varying ratio between the total heat energy absorbed by the weld and the heat energy that contributes to the nugget formation, this can be described as:

$$E \cdot C_2(t) = E_1, \quad (12)$$

where $C_2(t)$ is the time-varying ratio, and E is the total heat energy absorbed by the weld. In addition, the detailed expression of the nugget volume is difficult to precisely obtain. However, it can be approximated as a cubic function of nugget diameter. There is also a coefficient λ between the cubic function of the nugget diameter and nugget volume. Hence, combining Eqs. (11) and (12), and using the coefficient λ , the mathematical model of the relation between the nugget diameter and the heat energy absorbed by the weld can be written as:

$$\lambda D^3 C_1 = E \cdot C_2(t). \quad (13)$$

Hence, Eq. (13) can be rewritten as:

$$D = \left(\frac{C_2(t)}{\lambda \cdot C_1} \right)^{1/3} E^{1/3}. \quad (14)$$

The ratio between D and cubic root of E can be replaced by a time-varying ratio $\mu(t)$. Moreover, according to the analysis above, the heat energy E should be calculated from the time when the first melting point appears in practical applications. It can be calculated using the following equation:

$$E(t) = \sum_{j=j_1}^{j_2} \sum_{i=1}^N U(i)I(i) \times t, \quad (15)$$

where N denotes the number of sampling values within one control cycle, and j_1 and j_2 denote the beginning and ending control cycles of the energy calculation, respectively; t is the calculating cycle of dynamic resistance values, and U and I are the actual values of electrode voltage and welding current. Nugget diameter D is also a time-varying value during the welding process. Hence, a simple mathematical model that can be used for the online nugget diameter estimator is described as:

$$D(t) = \mu(t)E(t)^{1/3}, \quad (16)$$

where the coefficient $\mu(t)$ can be obtained experimentally. Notice that the structure of the model would remain the same for different welds of different materials and sizes, and even produced by different welding currents when CCC strategy is used. Those differences can be reflected in the difference of $\mu(t)$. The CCC strategy was used to conduct these experiments. To obtain satisfactory welds, the welding current should be properly chosen. An excessive welding current can easily induce expulsion, while too low a welding current may induce an undersized weld or no weld at all, or lead to poor efficiency. Different welding currents, from 7,000 to 8,500 A with 500-A intervals, were used in the experiments. For each selected welding current, different welding durations were used to obtain welds with different nugget diameters. To ensure a measurable nugget diameter, each welding operation must at least reach the peak value of the dynamic resistance. In general cases, the first melting point of the weld must appear prior to the peak of the dynamic resistance curve. In these experiments, the first melting point of the weld can be detected online using the proposed method given in the

previous section. The nugget diameters can be obtained by destructive test after each experiment. To obtain precise and reliable nugget diameters, after cutting off the weld using a low-speed diamond wheel saw, the specimen was mounted using a cold mounting method with a polymer resin to cast a mold. Then, the specimen was ground and polished carefully to obtain a smooth surface. Finally, the nugget diameter was monitored and measured using an optical microscope combined with the computer. An example of measuring a nugget diameter is shown in Fig. 45.

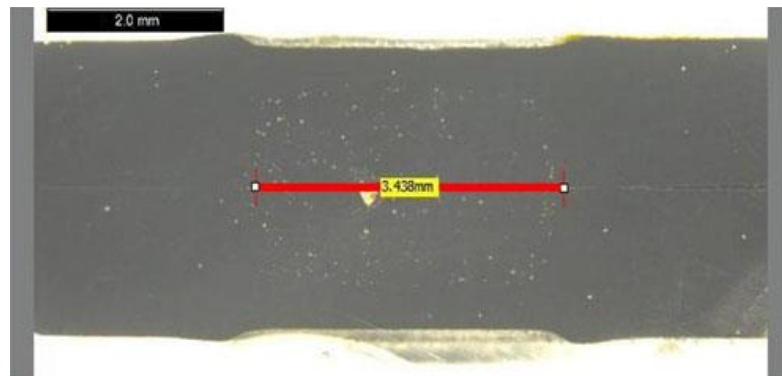


Figure 45. Measurement using an optical microscope

The unit of nugget diameter measurement was mm, and the unit of heat energy calculation was kJ; therefore, the unit of $\mu(t)$ was mm/kJ^{1/3}. After each experiment, the corresponding coefficient $\mu(t)$ can be calculated using Eq. (16). The corresponding scatter figures of coefficient $\mu(t)$ when the welding currents are 7,000, 7,500, 8,000, and 8,500 A can be shown in Figs.46, 47, 48, and 49, respectively.

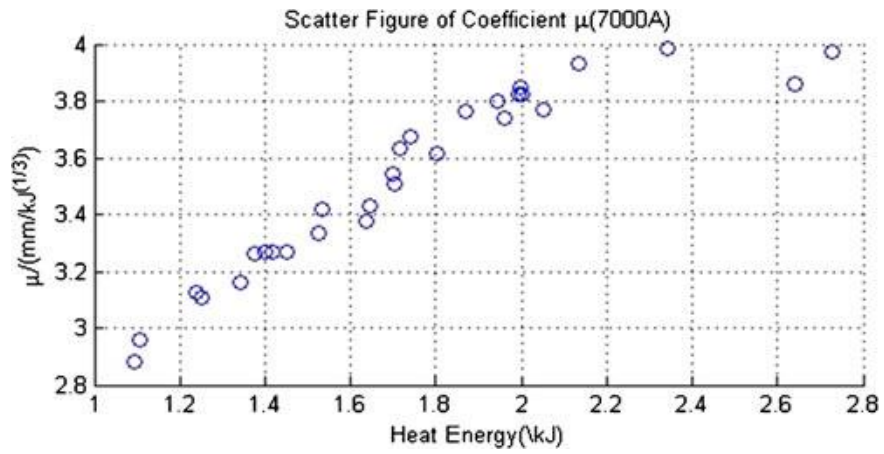


Figure 46. Scatter figure of coefficient μ (7,000 A)

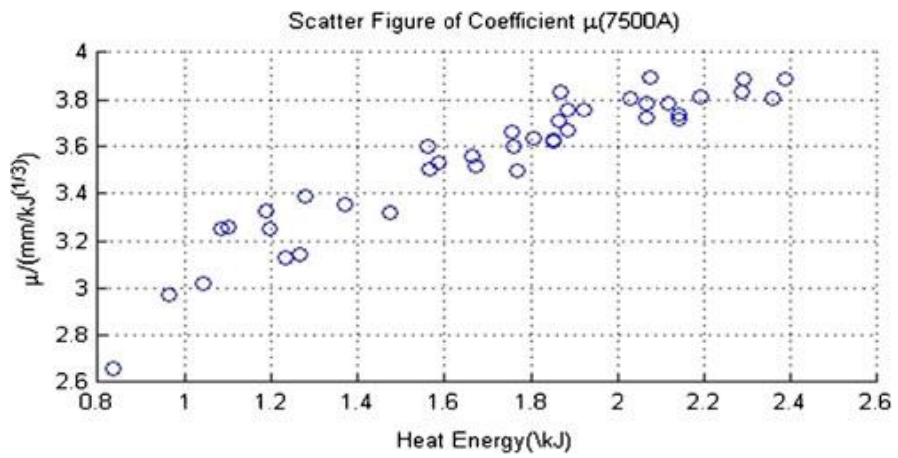


Figure 47. Scatter figure of coefficient μ (7,500 A)

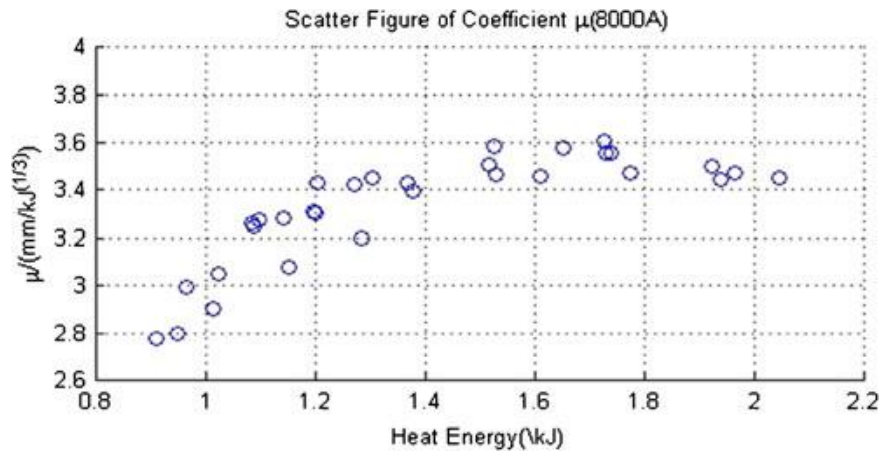


Figure 48. Scatter figure of coefficient μ (8,000 A)

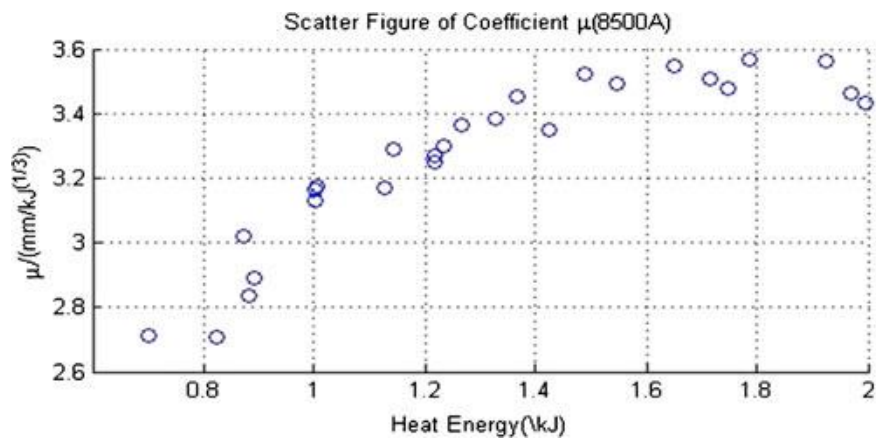


Figure 49. Scatter figure of coefficient μ (8,500 A)

The above four figures follow a similar pattern: the value of coefficient μ linearly increased with the heat energy when the heat energy value was small, but when the heat energy reached a saturation value, the coefficient μ had no significant changes even though the heat energy was still increasing. Because the heat energy absorbed by the weld from the time when the first melting point appears is a measurable variable as shown in Eq. (15), the coefficient $\mu(t)$ can be expressed in terms of $E(t)$. Curve fitting was employed to find out the correlation between the heat energy absorbed by the weld from the time when the first melting point

appears and the coefficient μ for each welding current. According to the characteristics of coefficient μ shown in the Figures 46, 47, 48, and 49, the result of curve fitting should be a segmented function, consisting of a quadratic linear curve and a constant straight line, which describe the rising part and the saturation part, respectively. When the welding current was 7,000 A, the result of curve fitting for the data in Fig. 46 can be shown as being:

$$\mu(t) = \begin{cases} 0.9614E(t) + 1.898 & E < 2.1136 \\ 3.93 & 2.1136 \leq E < 2.8 \end{cases}, \quad (17)$$

where $E(t)$ denotes the heat energy calculated from the time when the first melting point of the weld appears to the time t using Eq. (15). Then, Eq. (16) can be expressed analytically based on the result of $\mu(t)$. In addition, for each welding current, the beginning point of Eq. (16) should be the origin of the nugget diameter-heat energy axis, which corresponds to the time when the first melting point of the weld appears in each experiment. Hence, the integrated mathematical model of the relation between nugget diameter and heat energy absorbed by the weld from the time when the first melting point appears for when the welding current was 7000 A can be expressed as:

$$D(t) = \begin{cases} (0.9614E(t) + 1.898)E(t)^{1/3} & 0 < E < 2.1136 \\ 3.93E(t)^{1/3} & 2.1136 \leq E < 2.8 \end{cases}, \quad (18)$$

where $D(t)$ denotes the nugget diameter at the time t . The maximum error between this model and the actual experiment nugget diameters was 0.1265 mm. Figure 50 shows this relation using the type of $D(t)$ vs. $E(t)$ and the maximum error. Similarly, with different welding current values, the mathematical models can also be expressed combining the results of $\mu(t)$ obtained from curve fitting with Eq. (16). With a welding current of 7,500 A, the mathematical model could be expressed as:

$$D(t) = \begin{cases} (0.7741E(t) + 2.265)E(t)^{1/3} & 0 < E < 1.9895 \\ 3.8051E(t)^{1/3} & 1.9895 \leq E < 2.4 \end{cases} \quad (19)$$

The maximum error between this model and the actual experiment nugget diameters was 0.1914 mm. Figure 51 shows this relation and the maximum error. In addition, with a welding current of 8,000 A, the mathematical model could be expressed as:

$$D(t) = \begin{cases} (1.073E(t) + 1.957)E(t)^{1/3} & 0 < E < 1.4522 \\ 3.5152E(t)^{1/3} & 1.4522 \leq E < 2.1 \end{cases} \quad (20)$$

The maximum error between this model and the actual experiment nugget diameters was 0.1817 mm. Figure 52 shows this relation and the maximum error. Moreover, with a welding current of 8,500 A, the mathematical model could be expressed as:

$$D(t) = \begin{cases} (1.019E(t) + 2.033)E(t)^{1/3} & 0 < E < 1.4463 \\ 3.5068E(t)^{1/3} & 1.4463 < E < 2.0 \end{cases} \quad (21)$$

The corresponding maximum error was 0.1531 mm. This relation and the maximum error are depicted in Fig. 53. The errors of these four models may be caused by the nugget diameter measurement and the calculations of the time when the first melting point of the weld appears. The former type of error is limited and affects all of the data, while the latter is induced by data calculation because the peak of the first order derivative value may have been wrongly identified. The influence of these two errors would be very limited if all the experiment data had been obtained using the same criteria and conditions. If more experiment data are obtained, the influence of errors diminishes. Where the solid curves denote the relation obtained from actual experiment data, while the dashed curves denote the relation derived from the actual experimental data because it is hard for the experiments to obtain welds with

very tiny nugget diameters; the discrete circles denote the original measurement values of the welds. In addition, Eqs. (18, 19, 20, and 21) have a similar format, which is:

$$D(t) = K_1E(t)^{4/3} + K_2E(t)^{1/3}$$

for the initial range, and then:

$$D(t) = K_3E(t)^{1/3}$$

for the other range. The corresponding coefficients of Eqs. (18, 19, 20, and 21) have small differences. Hence, Figures 50, 51, 52, 53 can be depicted in one figure as shown in Fig. 54.

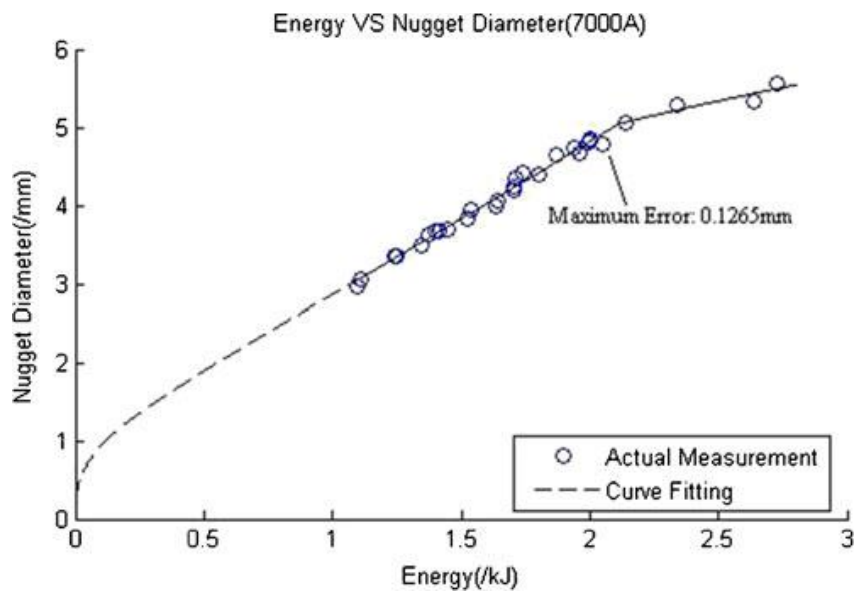


Figure 50. Relation between diameter and energy (7,000 A)

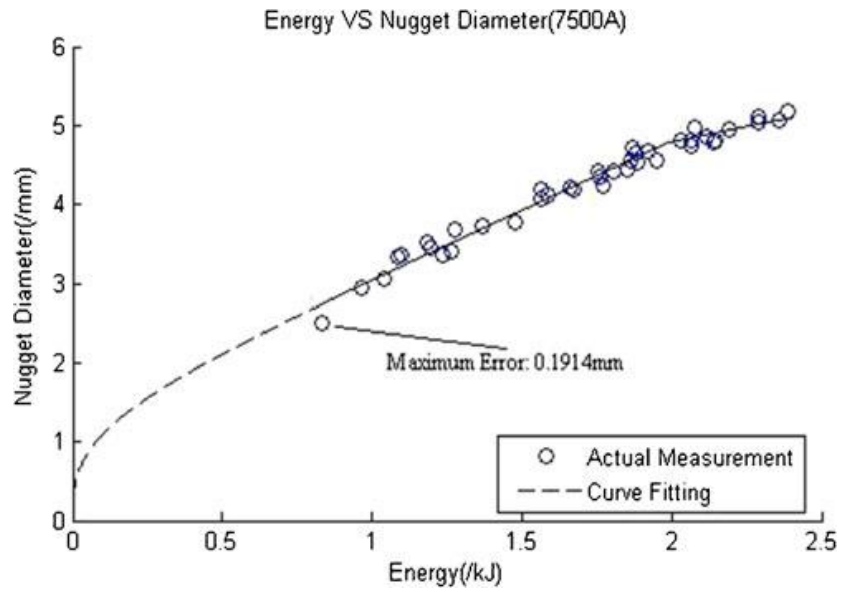


Figure 51. Relation between diameter and energy (7,500 A)

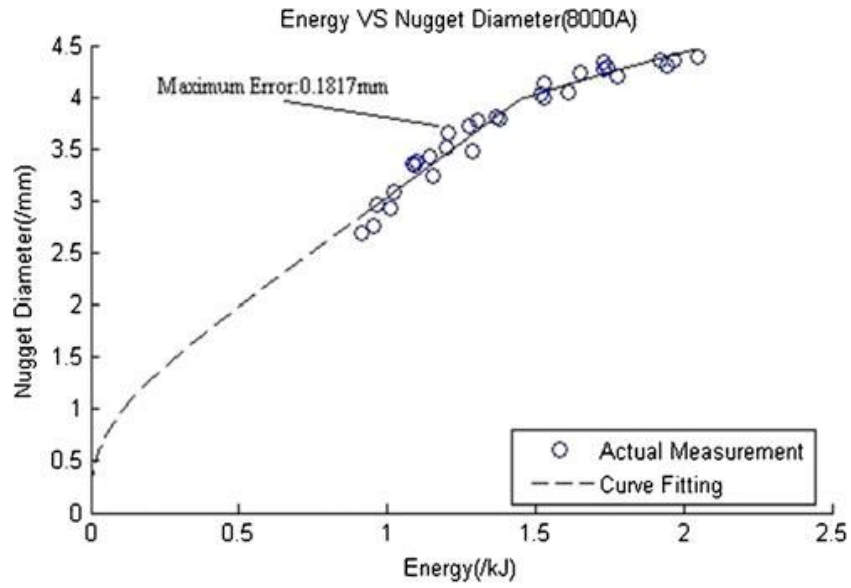


Figure 52. Relation between diameter and energy (8,000 A)

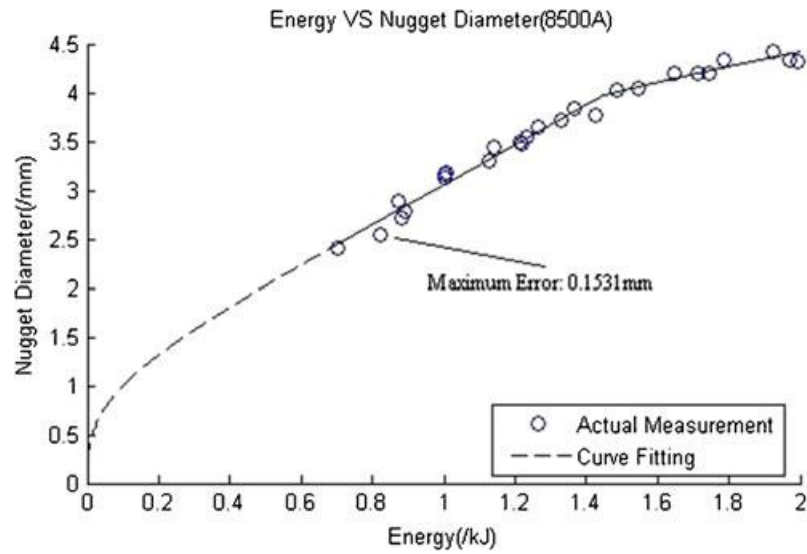


Figure 53. Relation between diameter and energy (8,500 A)

Then, the four equations can be described in one uniform format by averaging their corresponding coefficients K_1 and K_2 . However, to obtain smooth curves, the corresponding transition points of each equation should also be marginally adjusted. Equations (18, 19, 20, and 21) can be rewritten in uniform notation as shown in Eqs. (22, 23, 24, and 25) with the same values of K_1 and K_2 , respectively, when the heat energy is small.

$$D(t) = \begin{cases} (0.9569E(t) + 2.038)E(t)^{1/3} & 0 < E < 1.9772 \\ 3.93E(t)^{1/3} & 1.9772 \leq E < 2.8 \end{cases}, \quad (22)$$

$$D(t) = \begin{cases} (0.9569E(t) + 2.038)E(t)^{1/3} & 0 < E < 1.8467 \\ 3.8051E(t)^{1/3} & 1.8467 \leq E < 2.4 \end{cases} \quad (23)$$

$$D(t) = \begin{cases} (0.9569E(t) + 2.038)E(t)^{1/3} & 0 < E < 1.5437 \\ 3.5152E(t)^{1/3} & 1.5437 \leq E < 2.1 \end{cases} \quad (24)$$

$$D(t) = \begin{cases} (0.9569E(t) + 2.038)E(t)^{1/3} & 0 < E < 1.5350 \\ 3.5068E(t)^{1/3} & 1.5350 < E < 2.0 \end{cases} \quad (25)$$

where Eqs. (22, 23, 24, and 25) correspond to Eqs. (18, 19, 20, and 21), respectively. Although these four equations have the same K_1 and K_2 , the equations have different transition points and saturation values. To check the effectiveness of this uniform format, all the experiment data used before can also be used in checking for errors from the use of the uniform equations, with the scatter figure of errors as shown in Fig. 55.

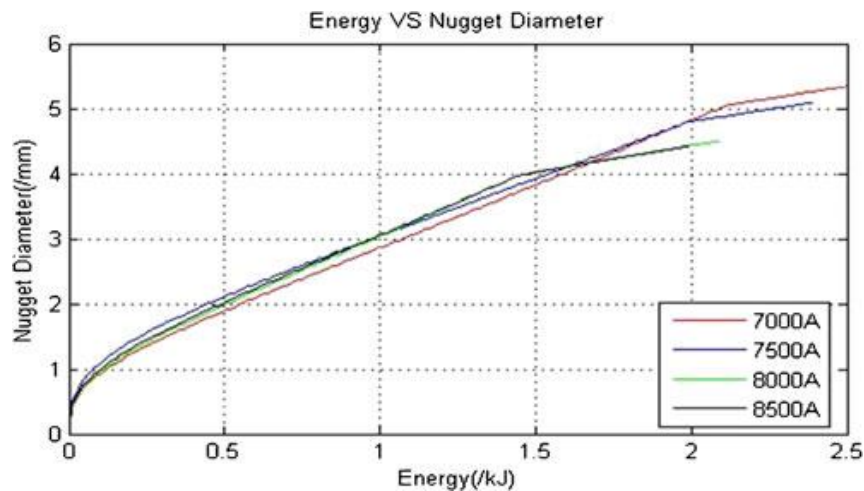


Figure 54. Integrated figure of four equations

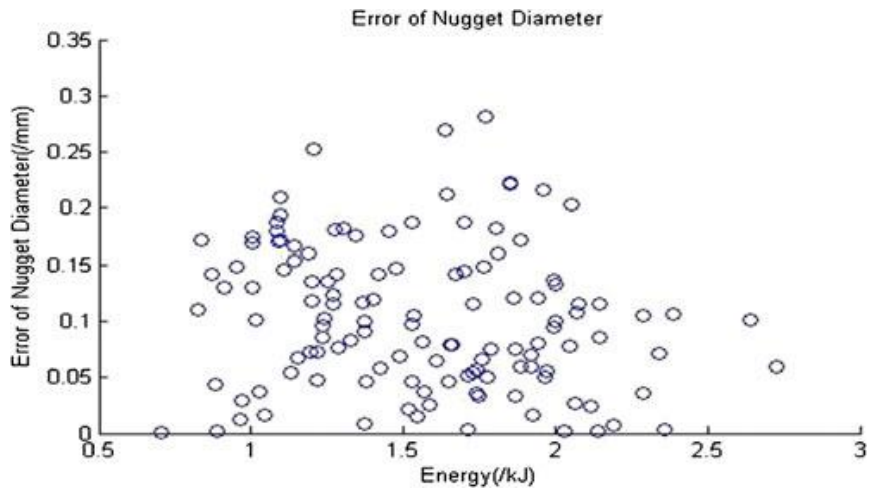


Figure 55. Errors of the model using the uniform equation

According to Fig. 55, though the uniform equations had larger errors than those using separated Eqs. (18, 19, 20, and 21), the maximum error was below 0.3 mm, and the majority of errors were below 0.2 mm. This means that the uniform equations can be used to describe the relation between nugget diameter and heat energy absorbed by the weld from the time when the first melting point appears. For different values of welding currents used, the relation was approximately the same when the values of heat energy are small; the sole difference being the curves may transit into the different $K_3E(t)^{1/3}$ at different points. Furthermore, some transition points were very close, such as when welding currents were 7,000 and 7,500 A, or when the welding currents were 8,000 and 8,500 A. The uniform format can supply a simple method for online measurement of nugget diameter. Obviously, if the predetermined nugget diameter is below 4 mm, the relation is the same when the uniform format is used, no matter which welding current is used. In addition, as shown in Fig. 54 and Eqs. (18, 19, 20, 21, 22, 23, 24, and 25), larger welding currents cannot produce welds with larger nugget diameters and even have lower saturation values, because the larger welding currents can easily induce expulsion at the later stage of the welding process. When an expulsion has occurred during the welding operation, the weld should be removed from the statistic process because the weld could not be a qualified one. As a result, 8,000 and 8,500 A welding currents can only produce welds with smaller nugget diameters than those welds produced using smaller welding

currents. The curve fitting results lead to two different results to express the nugget diameter using heat energy, either in terms of individual welding currents as shown in Eqs. (18, 19, 20, and 21) or the uniform way defined by Eqs. (22, 23, 24, and 25). Both can provide reasonable accuracy in the estimation of nugget diameter. As a result, nugget diameter becomes a measurable parameter during the welding process. However, there is a subtle difference between those two types of equations. In Eqs. (18, 19, 20, and 21), each equation corresponds to one welding current and has different coefficients from the other; while in Eqs. (22, 23, 24, and 25), the coefficients are the same when the value of heat energy is small, the differences being the different transition points and saturation values K_3 corresponding to different welding currents. If the central processing unit of the device allows, individual models of Eqs. (18, 19, 20, and 21) would be more beneficial, not only in terms of the more accurate measurement, but also in terms of energy efficiency, than using the uniform Eqs. (22, 23, 24, and 25). It is clear from Fig. 54 that, to achieve the same nugget diameter, a different amount of heat energy would be consumed for different welding currents, or for a given heat energy, different nugget diameters would be produced by different welding currents. Although the amount of the heat energy to be saved is very small for a specific weld, the total amount of heat energy saving would be very large for mass production, such as in the automobile manufacturing industry. Nevertheless, both types of equations are simple enough for any real-time application. The proposed model can be used as an online nugget diameter estimator in an actual control system for RSW.

3 Experimental verification

To take advantage of the online nugget diameter estimator and obtain welds with predetermined nugget diameters, the optimum control actions should be designed accordingly. Having obtained the actual value of nugget diameters from the estimator after each control cycle, the decision to continue or stop the welding action can be made. For example, to weld workpieces of the same materials as described in the above experiments, if the online estimated value of the nugget diameter is larger than the predetermined value, the welding

process should be terminated immediately. Additionally, if the online estimated value of the nugget diameter is smaller than the predetermined value but the error is within the nugget growth in a half cycle, meaning that the value after the next control cycle may be above the nugget diameter produced in a half cycle, the welding process should also be ceased. The information about nugget growth contributed by the amount of heat energy in a half cycle can be obtained from the preceding control cycle in real time. In addition to these two situations, the welding process should not be ceased because the predetermined goal has not been achieved. Using these measures, the error between the estimated value from Eqs. (18, 19, 20, 21, 22, 23, 24, and 25) and the predetermined value of nugget diameter can be limited to within a half control cycle in practical applications. In practice, to obtain one predetermined nugget diameter, the welding currents should be chosen carefully according to their corresponding mathematical models shown in Eqs. (18, 19, 20, 21, 22, 23, 24, and 25), which correspond to two types of mathematical models. Furthermore, each equation of the model has its own effective range because a higher welding current can induce expulsion more easily than using a lower welding current, which can reduce the weld strength and affect the final weld quality or seriously deteriorate the electrodes. On the other hand, different welding currents may achieve the same goal using different amounts of heat energy. Therefore, it is more efficient to use different welding currents for different nugget diameters. The models for different welding currents have different effective ranges. The heat energy used for predetermined nugget diameters using different welding currents based on Eqs. (18, 19, 20, and 21) is shown in Table 6. Equations (22, 23, 24, and 25) should have the same trends as shown in Eqs. (18, 19, 20, and 21). The unit of energy used was also kJ. To give clear results, the predetermined nugget diameters were from 2.8 to 5.4 mm, with the different intervals used shown in Table 6.

Nugget diameter D (mm)	Welding current I (A)			
	7,000	7,500	8,000	8,500
2.8	0.9690	0.8671	0.8895	0.8673
3.0	1.0734	0.9781	0.9856	0.9745
3.6	1.3850	1.3169	1.2724	1.2685
4.2	1.6920	1.6581	1.7057	1.7156
4.4	1.7930	1.7716	1.9611	N/A
4.5	1.8433	1.8282	N/A	N/A
4.8	1.9931	2.0074	N/A	N/A
5.4	2.5942	N/A	N/A	N/A

Table 6. Energy used for predetermined nugget diameter using different welding currents

Table 6 can be used to select the welding current for a given desired nugget diameter. Some particular nugget diameters can only be obtained using a few values of welding current. For example, to obtain very large nugget diameters, such as 5.4 mm, only a 7,000 A welding current can be used. On the other hand, if the desired nugget diameter can be obtained using more than one value of welding current, the welding current which uses the least heat energy to achieve the goal should be chosen. The percentages of energy saved can be also obtained. If the least heat energy is used, for the above seven different nugget diameters from 2.8 to 4.8 mm, the percentage of energy saved is 11.73, 10.15, 9.18, 3.47, 10.7, 0.83, and 0.72 %, respectively. In addition, though Table 6 provides an effective range for different welding currents, expulsion may occur especially when the welding current is large or if some unexpected phenomena appear. In practical applications, if expulsion occurs, the welding operation should be terminated immediately so as to avoid further risk. The investigation of expulsion can be realized by monitoring the variation of dynamic resistance. Dynamic resistance has a sudden drop when expulsion occurs because all the expulsions, no matter whether a surface expulsion or an internal expulsion, are induced by expelling some molten metals. This characteristic can be used for online investigation of the expulsion. Figure 56 shows a dynamic resistance profile when expulsion occurs.

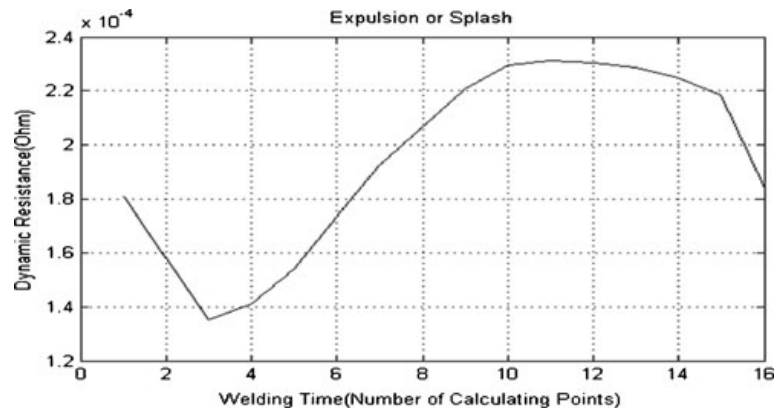


Figure 56. Dynamic resistance profile when expulsion occurs

It can be seen from Fig. 56 that the expulsion occurred at the 16th control cycle; therefore, the welding operation should be terminated immediately. This action can be used in the proposed control system to protect the RSW machine and maintain a safer operation. Experiments were conducted to validate the effectiveness of the proposed online nugget diameter control system in Fig. 34. The online nugget diameter estimator used the Eqs. (18, 19, 20, and 21). Although the model includes complex power formulas, they can be easily realized using the DSP internal library functions, which are written using the C language directly. The proposed control scheme and estimation were executed in real time. Corresponding experiment results are shown in Table 7.

Welding current I (A)	Predetermined nugget diameter D (mm)	Calculated nugget diameter D (mm)	Measurement of nugget diameter D (mm)	Calculated energy used E (kJ)
7,000	3.8	3.87	3.84	1.5257
7,000	4.7	4.73	4.68	1.9595
7,000	4.8	4.78	4.79	1.9852
7,000	5.0	5.06	5.06	2.1363
7,500	3.5	3.51	3.49	1.2663
7,500	4.5	4.56	4.56	1.8622
7,500	4.8	4.88	4.86	2.1155
7,500	5.0	4.94	4.95	2.1924
8,000	3.6	3.56	3.51	1.2538
8,000	4.0	3.91	4.03	1.4167
8,000	4.1	4.12	4.05	1.6099
8,000	4.2	4.22	4.27	1.7304
8,500	2.8	2.81	2.76	0.8817
8,500	3.5	3.53	3.54	1.2350
8,500	3.8	3.76	3.86	1.3442
8,500	4.1	4.15	4.19	1.6491

Table 7. Experiment results for actual control system using the separate functions

Where the calculated nugget diameters were the estimated values given by the model of Eqs. (18, 19, 20, and 21). The errors between the predetermined nugget diameter and the calculated nugget diameter were 0.1 mm in the experiments. The measurement of the nugget diameter was the actual measured value after conducting the destructive test and obtained as shown in Fig. 45.

Welding Current I (A)	Predetermined nugget diameter D (mm)	Calculated nugget diameter D (mm)	Measurement of nugget diameter D (mm)	Calculated energy used E (kJ)
7,000	3.5	3.50	3.36	1.2589
7,000	5.1	5.07	5.05	2.1577
7,500	3.5	3.55	3.58	1.2870
7,500	5.0	4.98	4.91	2.2373
8,000	3.5	3.50	3.62	1.2595
8,000	4.1	4.10	4.12	1.5876
8,500	3.5	3.61	3.68	1.3176
8,500	4.0	3.96	4.02	1.4966

Table 8. Experiment results for actual control system using the uniform functions

Despite the fact that it may have additional measurement errors, the overall errors between the predetermined nugget diameter and the actual measurement of nugget diameter were within about 0.1 mm in the above experiments. The results in Table 7 demonstrate that the proposed online nugget diameter control system can obtain satisfactory performance in actual welding operations. In addition, Eqs. (22, 23, 24, and 25) were also used in the experiments. These models were expected to yield slightly larger errors at some points before the transition points. The maximum error between the predetermined and the measurement value of nugget diameters was 0.2 mm. Table 8 shows the same experiments as Table 7, but the online nugget diameter estimator used the Eqs. (22, 23, 24, and 25). The experiment results validated the effectiveness of the mathematical models. Both types of models can produce welds with predetermined nugget diameter with very limited errors. According to the above experiment results, the model of Eqs. (18, 19, 20, and 21) can yield results with a higher accuracy than the model using Eqs. (22, 23, 24, and 25). However, the model of Eqs. (22, 23, 24, and 25) has the same coefficient for different welding currents when the heat energy is small, sometimes convenient to use on some particular occasions. In practical applications, which model should be used depends on the particular situation and task to be performed.

Chapter 5

Case study

The project consists in the correlation analysis between the result of the ultrasonic control and the welding output parameter. The object is to find a correlation that permits to evaluate the status of the single spot welding taking into account the welding parameter output only. Thanks to this project it is possible to eliminate the statistical control.

5.1. Project reason

The project was born from the manufacturing quality department with the aim to increase the robustness of control of RSW and to reduce the cost eliminating the ultrasonic control and hammer and chisel. These statistical controls are expensive for the plant because it has needed several workers only for this control. The plant has 3 insiders on average for each model on each shift. The plants have usually two or three shifts and so the cost is high. Also the cost of the tools must be considered and the cost of the worker training and learning. The other object is to increase the robustness of the control, nowadays for each turn is controlled only a car every two hundred and this system doesn't permit to find all the problem and only during the TDF (Test Dynamic Functional) or CPA (Costumer Product Audit) but this test can only find a vibration or noise issues. The statistical controls are only useful to evaluate the process drift and eventually correct the process with a new set up. If a critical issue is found like several near not welded point a line escalation starts to verify if other vehicles have the same problem to be repaired where necessary.

5.2. Preliminary

The first step of the project is to find the plant and the line where starts the analysis. The Melfi plant is chosen because it is the Italian plant with higher production of vehicles and with adaptive welding. Also it has a tool that permits to store the welding parameter on a server hard disk. This tool is present in the basted body line and side body line, but only the basted

body line has the CIS (“Codice identificativo scocca”/ body identification code) number to identify the vehicle and permits the correlation. The CIS is a number assigned at the end of chassis line with a joined plate and permits to identify the vehicle and assign the characteristic of the vehicle that in the following line permits the assembly of the correct configuration and optional (OPT). The Ultrasonic control station is positioned at the end of the line and the Q+ points are controlled. Then the worker saves the result of the control in a Ms. Excel file including the CIS and the data of control. The image below is an example of a Viscard of Jeep Renegade on basted body. In the Viscard all the spot-welds made in the line are represented together with the robot which carries out the operation.

5.3. Data collection

The data necessary for the project are the Ultrasonic results and the welding parameter. The Ultrasonic results are provided by the B.I.W. Quality leader in a different MS. Excel file for each CIS. The welding parameters are taken from the welding drawer hard disk (an XML file each week from a PC outside the line). The first problem is that each welding robot creates a single file for each CIS and this means that each robot generates more or less 1000 files per day. A line can have more than 20 robots. In the Body line that I have analyzed there are 25 robots for a total of 25,000 files each day, so this system requires a big data analysis and the hard disk must be often cleaned.

Each file has the parameters for the different spots weld done from the robot. Thanks to the Ultrasonic reports it is possible to know the identification number of the spot-weld and which robot makes it. Another solution to get the welding parameters is to go in line each day and take the data from the online computer. This system impacts on the production, so I did it fewer times to avoid the disturbance of the worker. From the XML file is not possible to have the curve of welding but only the average of the parameters and this causes a bad accuracy of the analysis. The useful parameters taken from the XML file are resistance, current, time, force and Quality Index. Thanks to auto-adaptive welding the current is variable depending on the calculated resistance, time and force are constant. The most important parameter is the Quality Index which calculates the quality of the welding thanks to an algorithm. The algorithm is a secret of the machine supplier GFWELDING, but after a meeting, the supplier explained this function that is illustrated in the next chapter. This parameter is a result of a comparison between the actual welding curve and the reference curves, so it evaluates the deviation from the reference curves taken in the start-up phase. Thanks to this information it is easy to determine the quality of the welding. The problem is that only in a few welding points this parameter works well. Probably during the start-up the reference curve wasn't taken or during the years some modifications are included in the line without updating the curves.

SWI-RP Sommario: Tutti Punti				CIS:	63908362						
Operatore:	MARIO ROSSI	Modello:	JEEP 520	Disegno:		Provati:	141/141				
Turno:	PRIMO TURNO	Gruppo:	SCOCCA 520	Progetto:	SCOCCA	Salt/Man:	0/10				
Data:	12/05/2018 8.43.25	Parte:	SCOCCA	Note:		Buoni:	138(97,9%)				
Prova:	12.05.2018 08.43.25					Scarto:	3(2,1%)				
	Punto	Descrizione	Risultato	Categoria	Spessore	Echi	Calo	Gain	Sonda	File UPR	File SWD
	Numero					Multipli	dB/mm	[dB]			
1	WP050355Q	OP070R05	Buono	Buono	1,55	4	2,66	35	N20S4.5W	SpotWeld	0,7+1,1_CMU
2	WP050357Q	OP130R07	Buono	Buono	2,46	2	2,31	35	N20S4.5W	SpotWeld	0,7+1,1+1,5_CMU
3	WP050599Q	OP070R05	Buono	Buono	3,69	2	2,63	35	N20S4.5W	SpotWeld	1,1+1,3+1,5_CMU
4	WP050597Q	OP070R05	Buono	Buono	3,54	2	3,4	35	N20S4.5W	SpotWeld	1,1+1,3+1,5_CMU
5	WP050363Q	OP130R07	Buono	Buono	3,16	2	2,45	35	N20S4.5W	SpotWeld	1,1+1,1+1,3_CMU
6	WP052963Q	OP070R11	Buono	Buono	2,02	3	1,67	35	N20S4.5W	SpotWeld	0,8+1,5_CMU
7	WP053031Q	OP070R11	Buono	Buono	1,99	4	2,32	35	N20S4.5W	SpotWeld	0,8+1,5_CMU
8	WP053117Q	OP090R13	Buono	Buono	2,08	4	2,1	35	N20S4.5W	SpotWeld	1,1+1,5_CMU
9	WP053121Q	OP070R07	Buono	Buono	2,11	4	1,92	39	N20S4.5W	SpotWeld	1,1+1,5_CMU
10	WP053107Q	OP090R13	Buono	Buono	1,93	2	6,64	37	N20S4.5W	SpotWeld	1,1+1,5_CMU
11	WP053109Q	OP090R13	Buono	Buono	2,14	3	3	35	N20S4.5W	SpotWeld	1,1+1,5_CMU
12	WP053113Q	OP070R07	Buono	Buono	2,28	2	4,32	35	N20S4.5W	SpotWeld	1,1+1,5_CMU
13	WP053119Q	OP090R13	Buono	Buono	4,01	2	2,26	35	N20S4.5W	SpotWeld	1,1+1,5+2,0_CMU
14	WP053115Q	OP090R13	Buono	Buono	2,14	2	4,32	35	N20S4.5W	SpotWeld	1,1+1,5_CMU
15	WP053123Q	OP030R03	Buono	Buono	3,04	2	3,14	35	N20S4.5W	SpotWeld	1,1+1,4+1,5_CMU
16	WP053139Q	OP030R03	Buono	Buono	2,98	2	2,32	40	N20S4.5W	SpotWeld	1,1+1,4+1,5_CMU
17	WP053145Q	OP030R03	Buono	Buono	3,42	2	1,63	35	N20S4.5W	SpotWeld	1,1+1,4+1,5_CMU
18	WP053173Q	OP070R05	Buono	Buono	2,49	3	2,46	35	N20S4.5W	SpotWeld	0,67+1,1+1,4_CM
19	WP053169Q	OP090R13	Buono	Buono	2,43	4	1,41	35	N20S4.5W	SpotWeld	0,67+1,1+1,4_CM
20	WP053165Q	OP090R13	Buono	Buono	2,57	4	1,62	35	N20S4.5W	SpotWeld	0,67+1,1+1,4_CM
21	WP053161Q	OP090R13	Buono	Buono	2,28	4	1,84	40	N20S4.5W	SpotWeld	0,67+1,1+1,4_CM
22	WP053153Q	OP090R13	Buono	Buono	2,49	3	1,31	35	N20S4.5W	SpotWeld	0,67+1,1+1,4_CM
23	WP053149Q	OP070R05	Buono	Buono	2,63	2	1,49	35	N20S4.5W	SpotWeld	0,67+1,1+1,4_CM
24	WP053143Q	OP090R13	Buono	Buono	2,31	4	2,02	35	N20S4.5W	SpotWeld	0,67+1,1+1,5_CM
25	WP053141Q	OP090R13	Buono	Buono	2,19	4	1,63	39	N20S4.5W	SpotWeld	0,67+1,1+1,5_CM
26	WP053137Q	OP090R13	Buono	Buono	2,19	2	5,12	39	N20S4.5W	SpotWeld	0,67+1,1+1,5_CM
27	WP053135Q	OP020R03	Buono	Buono	2,28	2	4,83	42	N20S4.5W	SpotWeld	0,67+1,1+1,5_CM
28	WP053125Q	OP020R03	Buono	Buono	2,57	2	0,97	35	N20S4.5W	SpotWeld	0,67+1,1+1,5_CM
29	WP053127Q	OP020R03	Buono	Buono	2,34	3	1,59	40	N20S4.5W	SpotWeld	0,67+1,1+1,5_CM
30	WP053129Q	OP020R03	Buono	Buono	2,54	2	1,08	40	N20S4.5W	SpotWeld	0,67+1,1+1,5_CM
31	WP053131Q	OP070R05	Buono	Buono	2,75	2	2,19	40	N20S4.5W	SpotWeld	0,67+1,1+1,5_CM
32	WP053133Q	OP140R07	Buono	Buono	2,52	4	1,86	35	N20S4.5W	SpotWeld	0,67+1,1+1,5_CM
33	WP059275Q	OP090R07	Buono	Buono	2,52	3	2,69	37	N20S4.5W	SpotWeld	0,67+1,1+1,4_CM
34	WP053201Q	OP070R03	Buono	Buono	2,11	2	5,05	35	N20S4.5W	SpotWeld	0,67+1,1+1,2_CM
35	WP053205Q	OP040R03	Buono	Buono	2,34	5	1,48	35	N20S4.5W	SpotWeld	0,67+1,1+1,2_CM
36	WP052943Q	OP020R03	Buono	Buono	1,93	2	2,83	35	N20S4.5W	SpotWeld	0,8+1,5_CMU
37	WP052945Q	OP020R03	Buono	Buono	1,81	4	2,31	35	N20S4.5W	SpotWeld	0,8+1,5_CMU
38	WP052801Q	OP090R07	Buono	Buono	2,42	4	1,87	35	N20S4.5W	SpotWeld	1,2+1,4_CMU
39	WP052803Q	OP070R17	Buono	Buono	2,33	6	1,01	35	N20S4.5W	SpotWeld	1,2+1,4_CMU
40	WP052807Q	OP090R07	Buono	Buono	2,36	4	2,03	35	N20S4.5W	SpotWeld	1,2+1,4_CMU
41	WP052811Q	OP090R07	Buono	Buono	2,3	4	1,63	35	N20S4.5W	SpotWeld	1,2+1,4_CMU
42	WP052815Q	OP070R17	Buono	Buono	2,21	4	2,06	35	N20S4.5W	SpotWeld	1,2+1,4_CMU
43	WP052813Q	OP070R17	Buono	Buono	2,3	3	2,81	36	N20S4.5W	SpotWeld	1,2+1,4_CMU
44	WP052809Q	OP090R07	Buono	Buono	2,36	5	1,49	35	N20S4.5W	SpotWeld	1,2+1,4_CMU
45	WP052805Q	OP070R17	Buono	Buono	2,36	3	1,92	35	N20S4.5W	SpotWeld	1,2+1,4_CMU
46	WP052869Q	OP070R17	Buono	Buono	2,33	4	1,85	35	N20S4.5W	SpotWeld	1,2+1,4_CMU
47	WP052867Q	OP070R17	Buono	Buono	2,36	5	1,5	35	N20S4.5W	SpotWeld	1,2+1,4_CMU

Figure 58. Ultrasonic report

```

<?xml version="1.0"?>
- <FIELD_DATA xsi:noNamespaceSchemaLocation="SCH6109" xmlns:xsi="IST6109" CISNUM="37906351" MSG_DT="2018-04-21T22:28:23" MSG_ID="MSG_610920180421222823_1110">
- <PROCESSING_DATA_SECTION>
- <TRACED_OPERATION OPERATOR="ope6109" OP_RESULT="OK" OPTYPE="WLD" OPCYCLE="1" OPCODE="SCC+ST090+090R13">
- <SINGLE_ITEM OPERATOR="ope6109" ITEM_RESULT="OK" ITEM_DESC="P001" ITEM_ID="1">
- <SINGLE_OP_RESULT TRY_RESULT="OK" TRY_ID="0">
- <MEASUREMENT UM="n.a." VALUE="0" MEASURE="STRING_VALUE" MEAS_DESCR="DEPCOD"> </MEASUREMENT>
- <MEASUREMENT UM="n.a." VALUE="0.0.53101" MEASURE="ABSOLUTE" MEAS_DESCR="SPOTNUM"> </MEASUREMENT>
- <MEASUREMENT UM="n.a." VALUE="1" MEASURE="ABSOLUTE" MEAS_DESCR="PRGNUM"> </MEASUREMENT>
- <MEASUREMENT UM="n.a." VALUE="21/04/2018 22:27:49" MEASURE="DATE_TIME" MEAS_DESCR="WELTIME"> </MEASUREMENT>
- <MEASUREMENT UM="DaN" VALUE="270" MEASURE="FORCE" MEAS_DESCR="WFORC1"> </MEASUREMENT>
- <MEASUREMENT UM="DaN" VALUE="0" MEASURE="FORCE" MEAS_DESCR="WFORC2"> </MEASUREMENT>
- <MEASUREMENT UM="n.a." VALUE="ON" MEASURE="STRING_VALUE" MEAS_DESCR="REGMOD"> </MEASUREMENT>
- <MEASUREMENT UM="n.a." VALUE="ON" MEASURE="STRING_VALUE" MEAS_DESCR="CLSMOD"> </MEASUREMENT>
- <MEASUREMENT UM="n.a." VALUE="0" MEASURE="ABSOLUTE" MEAS_DESCR="ALARMCODE"> </MEASUREMENT>
- <MEASUREMENT UM="n.a." VALUE="2" MEASURE="STRING_VALUE" MEAS_DESCR="WELMOD"> </MEASUREMENT>
- <MEASUREMENT UM="n.a." VALUE="0" MEASURE="STRING_VALUE" MEAS_DESCR="CURMOD"> </MEASUREMENT>
- <MEASUREMENT UM="n.a." VALUE="0" MEASURE="COUNT" MEAS_DESCR="WELCNT"> </MEASUREMENT>
- <MEASUREMENT UM="n.a." VALUE="33" MEASURE="COUNT" MEAS_DESCR="WDRSCNT"> </MEASUREMENT>
- <MEASUREMENT UM="n.a." VALUE="6.000" MEASURE="QUALITY_INDEX" MEAS_DESCR="WCLSRES"> </MEASUREMENT>
- <MEASUREMENT UM="uOHM" VALUE="258.3" MEASURE="RESISTANCE" MEAS_DESCR="WELR"> </MEASUREMENT>
- <MEASUREMENT UM="%" VALUE="10" MEASURE="PERCENTAGE" MEAS_DESCR="TOLDINF"> </MEASUREMENT>
- <MEASUREMENT UM="%" VALUE="5" MEASURE="PERCENTAGE" MEAS_DESCR="TOLDSUP"> </MEASUREMENT>
- <MEASUREMENT UM="ms" VALUE="460" MEASURE="TIME" MEAS_DESCR="WELTIME1_S"> </MEASUREMENT>
- <MEASUREMENT UM="ms" VALUE="460" MEASURE="TIME" MEAS_DESCR="WELTIME1_M"> </MEASUREMENT>
- <MEASUREMENT UM="kA" VALUE="7.41" MEASURE="CURRENT" MEAS_DESCR="WELCUR1_S"> </MEASUREMENT>
- <MEASUREMENT UM="ms" VALUE="0" MEASURE="TIME" MEAS_DESCR="WELTIME2_S"> </MEASUREMENT>
- <MEASUREMENT UM="ms" VALUE="0" MEASURE="TIME" MEAS_DESCR="WELTIME2_M"> </MEASUREMENT>
- <MEASUREMENT UM="kA" VALUE="0.00" MEASURE="CURRENT" MEAS_DESCR="WELCUR2_S"> </MEASUREMENT>
- <MEASUREMENT UM="ms" VALUE="0" MEASURE="TIME" MEAS_DESCR="WELTIME3_S"> </MEASUREMENT>
- <MEASUREMENT UM="ms" VALUE="0" MEASURE="TIME" MEAS_DESCR="WELTIME3_M"> </MEASUREMENT>
- <MEASUREMENT UM="kA" VALUE="0.00" MEASURE="CURRENT" MEAS_DESCR="WELCUR3_S"> </MEASUREMENT>
- <MEASUREMENT UM="ms" VALUE="0" MEASURE="TIME" MEAS_DESCR="WELTIME4_S"> </MEASUREMENT>
- <MEASUREMENT UM="ms" VALUE="0" MEASURE="TIME" MEAS_DESCR="WELTIME4_M"> </MEASUREMENT>
- <MEASUREMENT UM="kA" VALUE="0.00" MEASURE="CURRENT" MEAS_DESCR="WELCUR4_S"> </MEASUREMENT>
- </SINGLE_OP_RESULT>
- </SINGLE_ITEM>
- <SINGLE_ITEM OPERATOR="ope6109" ITEM_RESULT="OK" ITEM_DESC="P006" ITEM_ID="2">
- <SINGLE_OP_RESULT TRY_RESULT="OK" TRY_ID="0">
- <MEASUREMENT UM="n.a." VALUE="0" MEASURE="STRING_VALUE" MEAS_DESCR="DEPCOD"> </MEASUREMENT>
- <MEASUREMENT UM="n.a." VALUE="0.0.53117" MEASURE="ABSOLUTE" MEAS_DESCR="SPOTNUM"> </MEASUREMENT>
- <MEASUREMENT UM="n.a." VALUE="6" MEASURE="ABSOLUTE" MEAS_DESCR="PRGNUM"> </MEASUREMENT>
- <MEASUREMENT UM="n.a." VALUE="21/04/2018 22:27:51" MEASURE="DATE_TIME" MEAS_DESCR="WELTIME"> </MEASUREMENT>
- <MEASUREMENT UM="DaN" VALUE="270" MEASURE="FORCE" MEAS_DESCR="WFORC1"> </MEASUREMENT>
- <MEASUREMENT UM="DaN" VALUE="0" MEASURE="FORCE" MEAS_DESCR="WFORC2"> </MEASUREMENT>
- <MEASUREMENT UM="n.a." VALUE="ON" MEASURE="STRING_VALUE" MEAS_DESCR="REGMOD"> </MEASUREMENT>
- <MEASUREMENT UM="n.a." VALUE="ON" MEASURE="STRING_VALUE" MEAS_DESCR="CLSMOD"> </MEASUREMENT>
- <MEASUREMENT UM="n.a." VALUE="0" MEASURE="ABSOLUTE" MEAS_DESCR="ALARMCODE"> </MEASUREMENT>
- <MEASUREMENT UM="n.a." VALUE="2" MEASURE="STRING_VALUE" MEAS_DESCR="WELMOD"> </MEASUREMENT>
- <MEASUREMENT UM="n.a." VALUE="0" MEASURE="STRING_VALUE" MEAS_DESCR="CURMOD"> </MEASUREMENT>
- <MEASUREMENT UM="n.a." VALUE="1" MEASURE="COUNT" MEAS_DESCR="WELCNT"> </MEASUREMENT>
- <MEASUREMENT UM="n.a." VALUE="33" MEASURE="COUNT" MEAS_DESCR="WDRSCNT"> </MEASUREMENT>
- <MEASUREMENT UM="n.a." VALUE="5.645" MEASURE="QUALITY_INDEX" MEAS_DESCR="WCLSRES"> </MEASUREMENT>
- <MEASUREMENT UM="uOHM" VALUE="255.4" MEASURE="RESISTANCE" MEAS_DESCR="WELR"> </MEASUREMENT>
- <MEASUREMENT UM="%" VALUE="10" MEASURE="PERCENTAGE" MEAS_DESCR="TOLDINF"> </MEASUREMENT>
- <MEASUREMENT UM="%" VALUE="5" MEASURE="PERCENTAGE" MEAS_DESCR="TOLDSUP"> </MEASUREMENT>
- <MEASUREMENT UM="ms" VALUE="460" MEASURE="TIME" MEAS_DESCR="WELTIME1_S"> </MEASUREMENT>
- <MEASUREMENT UM="ms" VALUE="460" MEASURE="TIME" MEAS_DESCR="WELTIME1_M"> </MEASUREMENT>
- <MEASUREMENT UM="kA" VALUE="7.41" MEASURE="CURRENT" MEAS_DESCR="WELCUR1_S"> </MEASUREMENT>
- <MEASUREMENT UM="ms" VALUE="0" MEASURE="TIME" MEAS_DESCR="WELTIME2_S"> </MEASUREMENT>
- <MEASUREMENT UM="ms" VALUE="0" MEASURE="TIME" MEAS_DESCR="WELTIME2_M"> </MEASUREMENT>
- <MEASUREMENT UM="kA" VALUE="0.00" MEASURE="CURRENT" MEAS_DESCR="WELCUR2_S"> </MEASUREMENT>
- <MEASUREMENT UM="ms" VALUE="0" MEASURE="TIME" MEAS_DESCR="WELTIME3_S"> </MEASUREMENT>
- <MEASUREMENT UM="ms" VALUE="0" MEASURE="TIME" MEAS_DESCR="WELTIME3_M"> </MEASUREMENT>
- <MEASUREMENT UM="kA" VALUE="0.00" MEASURE="CURRENT" MEAS_DESCR="WELCUR3_S"> </MEASUREMENT>
- <MEASUREMENT UM="ms" VALUE="0" MEASURE="TIME" MEAS_DESCR="WELTIME4_S"> </MEASUREMENT>
- <MEASUREMENT UM="ms" VALUE="0" MEASURE="TIME" MEAS_DESCR="WELTIME4_M"> </MEASUREMENT>
- <MEASUREMENT UM="kA" VALUE="0.00" MEASURE="CURRENT" MEAS_DESCR="WELCUR4_S"> </MEASUREMENT>
- </SINGLE_OP_RESULT>
- </SINGLE_ITEM>

```

Figure 59. Output parameters

5.3.1. Quality Index

Quality index is a dimensionless number patented by ISI-welding to evaluate the quality of the welding. This welding quality system (WQS) control is useful to setup the correct welding and self-regulate the welding during the process thanks to adaptive control. The main features are:

- the reduction in setup time to optimize parameters of welding programs;
- reduction in analysis time and understanding of welding problems during production;
- decrease in the number of incorrect points;
- constant monitor the quality of welding points.

The principle of operation of this WQS is based on algorithms measurement of current and secondary voltage, the software computes dynamic resistance, power, electrode force, energy, resistances (mean, minimum and maximum), climb rate and other characteristic events that occur during each welding point.

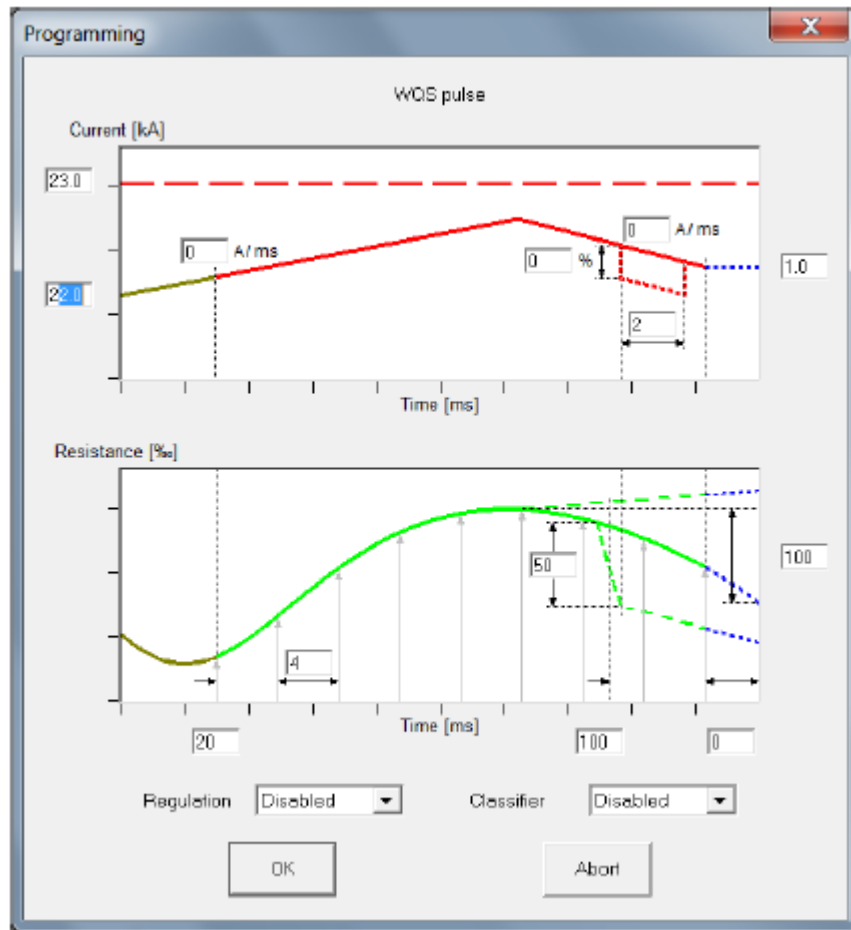


Figure 60. Resistance and current pulse analysis

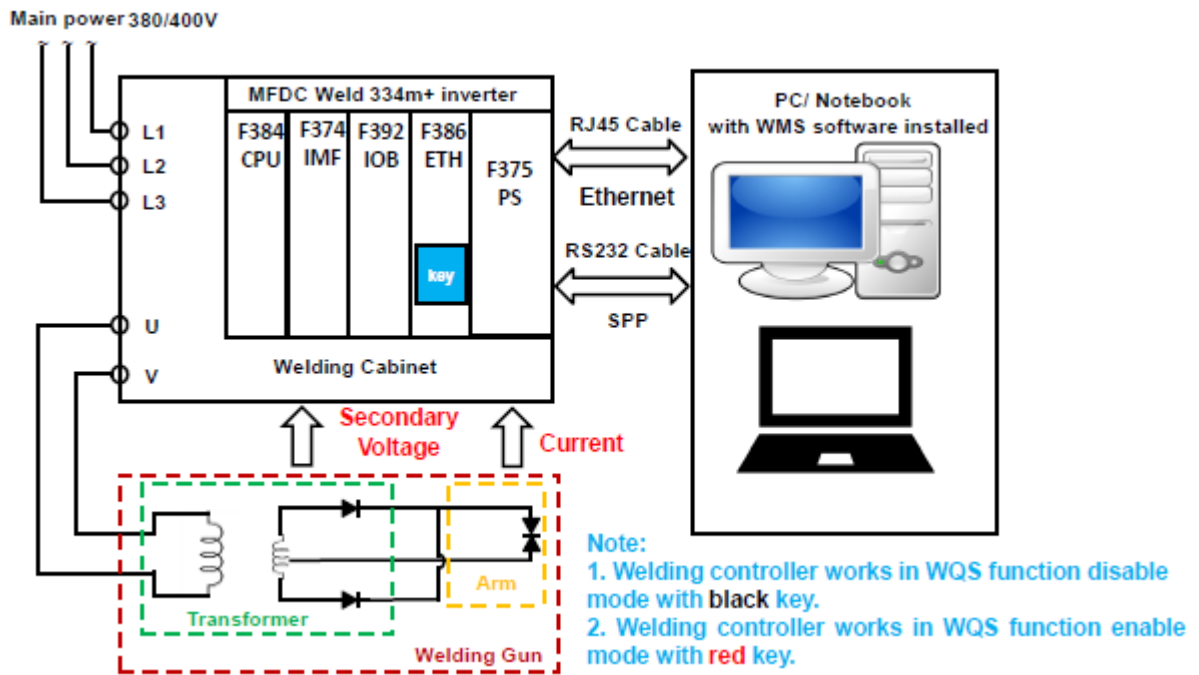


Figure 61. Schematization of welding component and circuit

The WQS interprets welding in three different modes:

1. **Oscilloscope**, welding parameter monitor. Graphic viewing of all fundamentals parameters;
2. **Classifier**, welding parameter monitor and classifier. Make classification of welding point after learning;
3. **Regulator**, welding parameter monitor and self-regulation. Modulation of the welding current in accordance with programming, to replicate the reference resistance profile. Welding time adjustment programmable.

The possibility to save all the data in a database for all welding points for later evaluate the problem of the welding and correct the process if necessary.

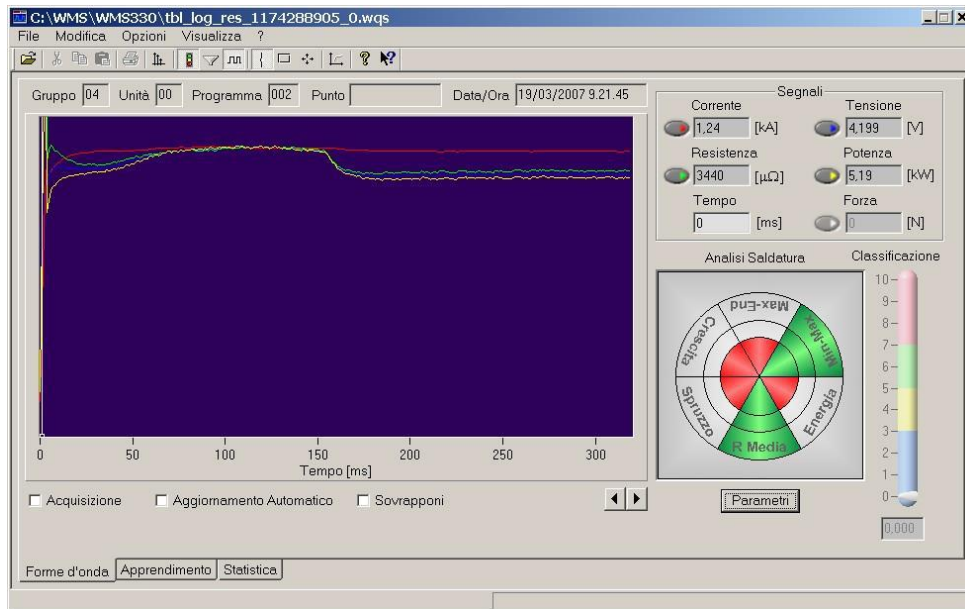


Figure 62. Curves of the parameters

The oscilloscope displays in real time the data measured during the welding process: current (red), voltage (blue), resistance(yellow), power(green). The real time monitoring is a tool for the analysis of the weld and the search for anomalies that may arise during production: welding spatter, glued welds, diagnostic alarms.

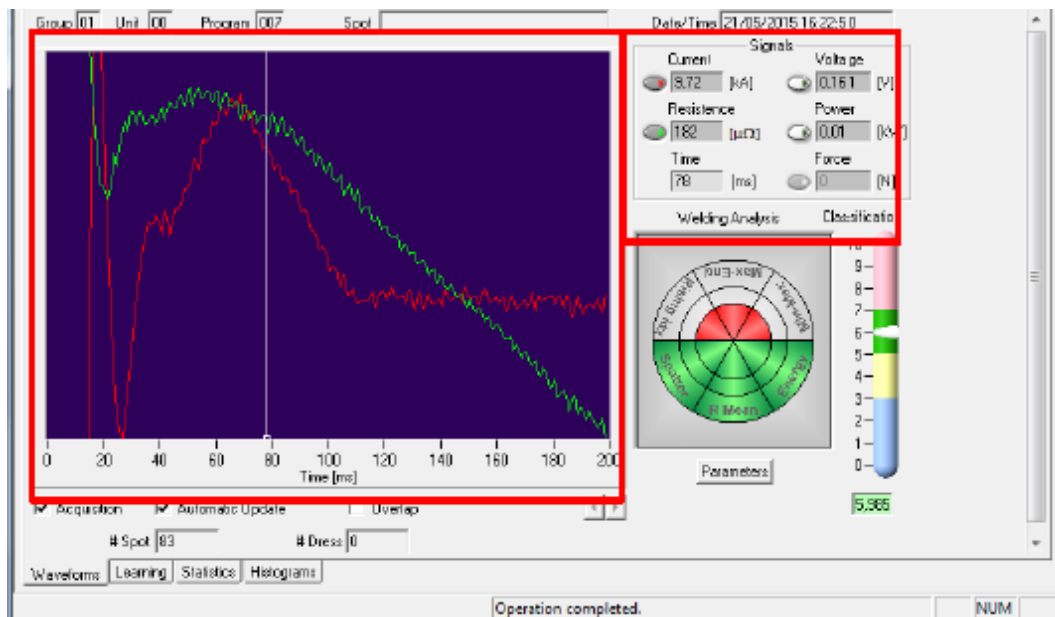


Figure 63. Oscilloscope analysis

The Regulator is a controller of the welding parameters current and welding time for:

- Obtaining a constant quality level of welding points;
- Compensate the electrode wearing;
- Compensate for external events such as welding on the edge, the shunt effect, the gripper misalignment;
- Compensate for the variation of the thickness of the sheet metal.

The controller may operate to automatically compensate for the change in thickness of the sheet metal with the aim to have always a good welding point thanks to the automatic regulation of the current and the welding time depending on the thickness of the plates.

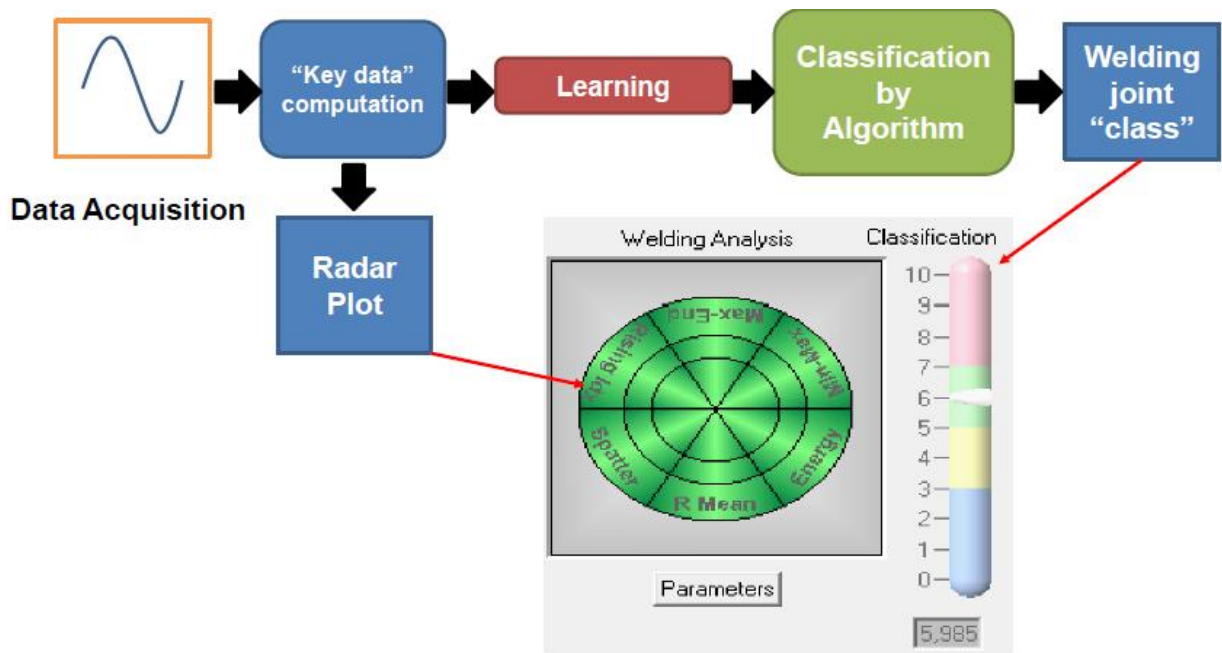


Figure 64. Regulator loop

The Learning phase is the step during the start-up wherein the reference curves of welding are taken to permit the evaluation of the selected point. To do that, after the welding process, the quality is controlled by the ultrasonic sensor and if it is ok the curve is certified. This process must be repeated for at the last fifteen curves for each point to have a good quality evaluation.

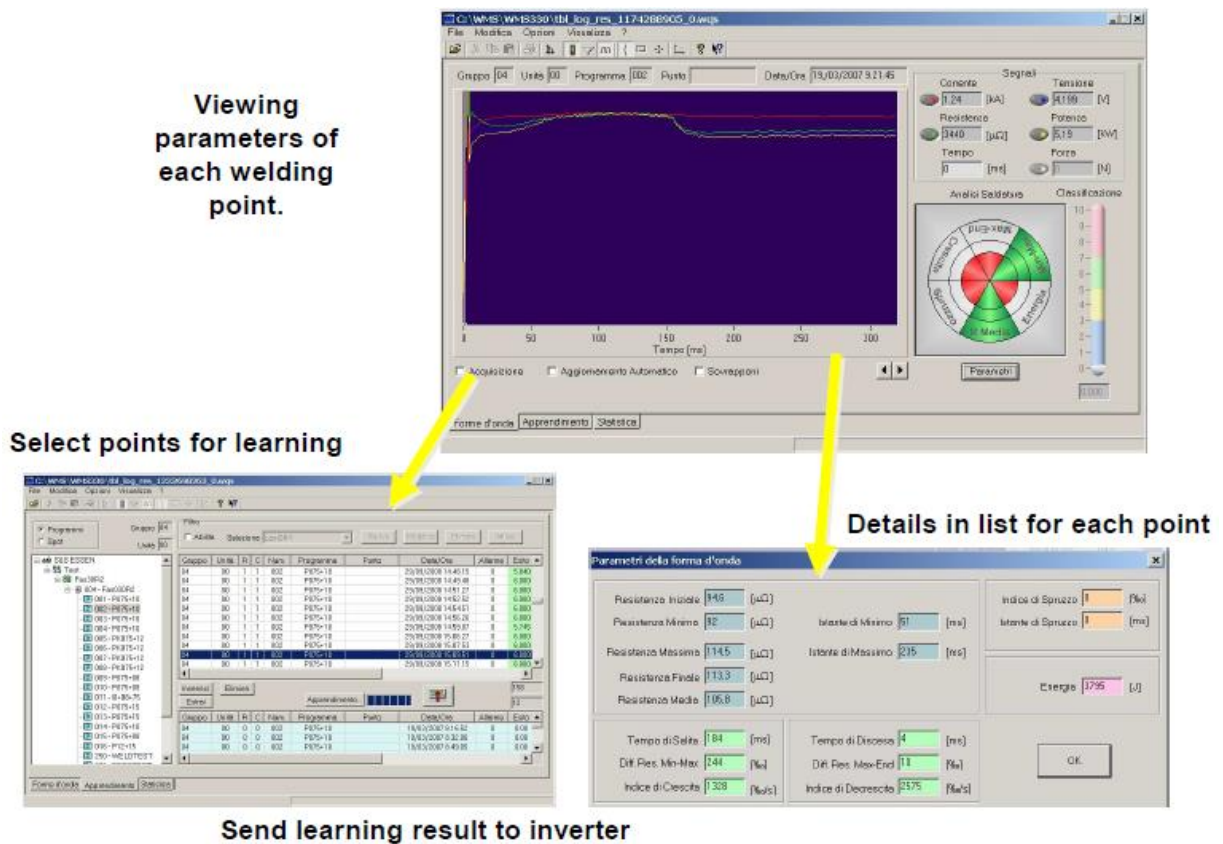
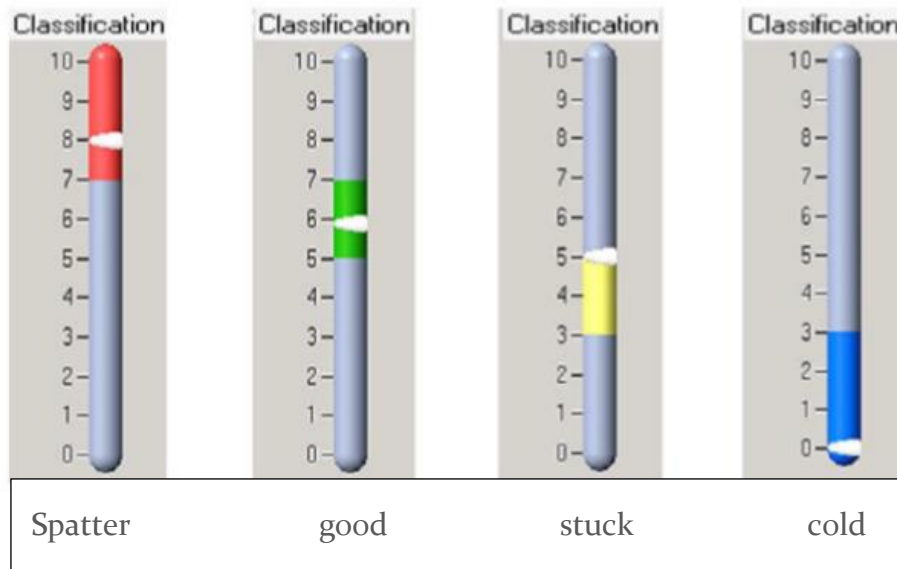


Figure 65. Learning phase

Classification of the welding result is the quality index that varies from 0 to 10 with a good result between 5 to 7.

- 0→3: very bad result probably the point is missed or “cold” (nugget not sufficient fused and cohesively);
- 3→5: bad result probably with defects of stuck welding or little diameter or thin nugget (undersized);
- 5→7: good result, the spot-weld is ok.
- 7→10: probably there is presence of aesthetics defects such as spatter or burnt (surface of the point dirty with burnt powder) but the weld is good.



The classification is the result of a complex comparison algorithm and simultaneous assessment of lots of electrical quantities and events that occur during welding. The classification is performed in real time by the welding control, and is also active even with the WMS disconnected.

The online advanced process diagnostic reduces or even eliminates the number of non-conformity welding points like spots without parts, glued spots or spatter spots. It is useful for a fast and easy statistic of the production conformity and preventing the critical situation with the aim of reducing line stops. It increases the efficacy of the dressing diagnosis thanks to the verification of proper programming.

All welds are stored in the database that permits a rapid evaluation of each singular spot-weld for each CIS number with the possibility of off-line analysis of the production and the quality traceability.

5.4. Correlation between welding parameter and U.S. control

The correlations between the parameters of the welding taken from the XML file with the corresponding results of the ultrasonic control are summed up in a MS Excel file. The correlations are made comparing ten different CIS number of Jeep Renegade model 520 considering only the body line. They take into account only the points where a non-conformity was found in the ultrasonic test. The correlations are illustrated in the following table.

The table is divided into twelve columns:

- **CIS**, the number to identify the examined body;
- **Point**, Spot-weld under investigation and comparison for the different CIS;
- **Robot**, to identify the robot and the station where the point is made, to easily find the respective parameter.
- **Results/Category**, the evaluation of the RSW by the ultrasonic control;
- **Thickness**, the thickness of the nugget calculated by the ultrasonic control;
- **File SWD**, the theoretical thickness of welded layer of the sheet metal ;
- **Force**, setup force of the electrode (constant parameter);
- **Quality index**, quality of the welding parameter (see the previous chapter);
- **Time**, setup time of welding (constant parameter) ;
- **Resistance**, calculated by the welding software (variable parameter);
- **Current**, mean value of the current regulated to compensate for the resistance variation (variable parameter).

A different color is used to underline the gravity of the non-conformity:

yellow → aesthetics defect (burnt, spatter);

orange → middle gravity defect (Thin, Undersized);

red → high gravity defect (Missed, Cold, Detached)

Missed	Cold	stuck	Thin	Undersized	Spatter	Burnt
--------	------	-------	------	------------	---------	-------

CIS	point	robot	Results	thickness	File SWD	force [DaN]	quality index	time [ms]	resistance [uOHM]	current [kA]
64051782	WP050303Q	OP120R05	OK	2,78	0,67+0,75+1,8_CM	280	6000	380	315,7	8,99
64318975	WP050303Q	OP120R05	OK	2,78	0,67+0,75+1,8_CM	280	6000	380	310,4	9,21
64319809	WP050303Q	OP120R05	OK	2,75	0,67+0,75+1,8_CM	280	6000	380	307,7	9,41
64319932	WP050303Q	OP120R05	OK	2,81	0,67+0,75+1,8_CM	280	6000	380	312	9,03
63051247	WP050303Q	OP120R05	OK	2,78	0,67+0,75+1,8_CM	280	6000	380	307,7	9,35
64359938	WP050303Q	OP120R05	OK	2,81	0,67+0,75+1,8_CM	280	6000	380	312,6	9,25
64301195	WP050303Q	OP120R05	Thin	1,87	0,67+0,75+1,8_CM	280	6000	380	310,2	9,23
63902324	WP050303Q	OP120R05	OK	2,78	0,67+0,75+1,8_CM	280	6000	380	313,8	9,12
63906002	WP050303Q	OP120R05	OK	2,75	0,67+0,75+1,8_CM	280	6000	380	311,8	9,20
64356629	WP050303Q	OP120R05	OK	2,78	0,67+0,75+1,8_CM	280	6000	380	308,1	9,34
63909501	WP050303Q	OP120R05	OK	2,81	0,67+0,75+1,8_CM	280	6000	380	317	9,05
64291719	WP050303Q	OP120R05	OK	2,78	0,67+0,75+1,8_CM	280	6000	380	311,7	9,28
63908362	WP050303Q	OP120R05	OK	2,37	0,67+0,75+1,8_CM	280	6000	380	319,8	8,94

Table 9. Correlation 1

In table 9 the spot WP050303Q is analyzed and in the examined CIS it is possible to see only one incorrect point for the CIS 64301195 which shows a low Thin defect. The Quality Index remains constant for all the point, probably the reference curves are not well taken and the control is ineffective. Also the resistance and the current are in the normal range of the other CIS. This first comparison is not significant for the analysis.

CIS	point	robot	Results	thickness	File SWD	force [DaN]	quality index	time [ms]	resistance [uOHM]	current [kA]
62852546	WP052823Q	OP070R15	OK	2,8	0,9+1,0+1,7_CMU	330	0	480	290,1	8,07
62857008	WP052823Q	OP070R15	Thin	1,95	0,9+1,0+1,7_CMU	330	0	480	285,4	8,04
62958939	WP052823Q	OP070R15	Thin	2,24	0,9+1,0+1,7_CMU	330	0	480	286,4	8,05
63044671	WP052823Q	OP070R15	Thin	2,04	0,9+1,0+1,7_CMU	330	0	480	286,6	8,04
63260095	WP052823Q	OP070R15	Thin	1,86	0,9+1,0+1,7_CMU	330	0	480	283,8	8,04
63322556	WP052823Q	OP070R15	OK	2,51	0,9+1,0+1,7_CMU	330	0	480	284,8	8,05
63513790	WP052823Q	OP070R15	OK	2,57	0,9+1,0+1,7_CMU	330	0	480	286,4	8,05
63565394	WP052823Q	OP070R15	OK	2,42	0,9+1,0+1,7_CMU	330	0	480	287,9	8,05
63776793	WP052823Q	OP070R15	OK	2,54	0,9+1,0+1,7_CMU	330	0	480	284,3	8,04
64051782	WP052823Q	OP070R15	OK	2,8	0,9+1,0+1,7_CMU	330	0	480	292,7	8,05
64318975	WP052823Q	OP070R15	OK	2,48	0,9+1,0+1,7_CMU	330	0	480	290,2	8,05
64319809	WP052823Q	OP070R15	OK	2,45	0,9+1,0+1,7_CMU	330	0	480	284	8,05
64319932	WP052823Q	OP070R15	OK	2,6	0,9+1,0+1,7_CMU	330	0	480	288,3	8,05
63051247	WP052823Q	OP070R15	OK	2,45	0,9+1,0+1,7_CMU	330	0	480	285,2	8,05
64359938	WP052823Q	OP070R15	OK	2,68	0,9+1,0+1,7_CMU	330	0	480	283,7	8,04
64301195	WP052823Q	OP070R15	Thin	2,21	0,9+1,0+1,7_CMU	330	0	480	282,5	8,04
63902324	WP052823Q	OP070R15	Burnt	3,22	0,9+1,0+1,7_CMU	330	0	480	282	8,04
63906002	WP052823Q	OP070R15	OK	2,33	0,9+1,0+1,7_CMU	330	0	480	283,5	8,04
64356629	WP052823Q	OP070R15	OK	2,48	0,9+1,0+1,7_CMU	330	0	480	287,2	8,04
63909501	WP052823Q	OP070R15	OK	2,71	0,9+1,0+1,7_CMU	330	0	480	287,8	8,04
64291719	WP052823Q	OP070R15	OK	2,42	0,9+1,0+1,7_CMU	330	0	480	287,2	8,04
63908362	WP052823Q	OP070R15	Thin	2,15	0,9+1,0+1,7_CMU	330	0	480	283,2	8,04

Table 10. Correlation 2

In table 10 the spot WP052823Q is analyzed and in the examined CIS it is possible to notice seven incorrect points which show principally a low Thin defect. The Quality Index is 0 for all the points, probably the reference curves are not taken or the control is disabled. It possible to see that some defective points has a lower resistance than others. Nevertheless other defective points have the value of resistance aligned. This table is also not significant.

CIS	point	robot	Results	thickness	File SWD	force [DaN]	quality index	time [ms]	resistance [uOHM]	current [kA]
62852546	WP053118Q	OP090R14	OK	2,6	1,0+1,1+1,5_CMU	280	7210	480	216,5	8,22
62857008	WP053118Q	OP090R14	OK	2,36	1,0+1,1+1,5_CMU	280	6000	480	215,4	8,25
62958939	WP053118Q	OP090R14	OK	2,71	1,0+1,1+1,5_CMU	280	6000	480	219,4	8,25
63044671	WP053118Q	OP090R14	OK	2,6	1,0+1,1+1,5_CMU	280	6000	480	215,8	8,25
63260095	WP053118Q	OP090R14	OK	2,6	1,0+1,1+1,5_CMU	280	6000	480	213,9	8,25
63322556	WP053118Q	OP090R14	Undersized	2,68	1,0+1,1+1,5_CMU	280	6000	480	213,1	8,25
63513790	WP053118Q	OP090R14	Cold	2,86	1,0+1,1+1,5_CMU	280	6000	480	213,8	8,25
63565394	WP053118Q	OP090R14	OK	2,42	1,0+1,1+1,5_CMU	280	6000	480	215,4	8,25
63776793	WP053118Q	OP090R14	OK	2,57	1,0+1,1+1,5_CMU	280	6000	480	212,1	8,24

Table 11. Correlation 3

In table 11 the spot WP053118Q is analyzed and in the examined CIS it is possible to see two incorrect points which show a serious defect (Cold) and an undersized defect respectively. The Quality Index remains constant for all the points except the first one. Also here the reference curves are not taken in a proper way or must be updated. In this case, the resistance is low for both the cases, but it has not a significant deviation from the regular one.

CIS	point	robot	Results	thickness	File SWD	force [DaN]	quality index	time [ms]	resistance [uOHM]	current [kA]
62852546	WP053119Q	OP090R13	OK	3,86	1,1+1,5+2,0_CMU	320	8010	480	280,4	7,69
62857008	WP053119Q	OP090R13	OK	4,07	1,1+1,5+2,0_CMU	320	8010	480	275,3	7,68
62958939	WP053119Q	OP090R13	OK	3,98	1,1+1,5+2,0_CMU	320	8010	480	275,8	7,66
63044671	WP053119Q	OP090R13	OK	4,25	1,1+1,5+2,0_CMU	320	8010	480	273,3	7,68
63260095	WP053119Q	OP090R13	OK	3,81	1,1+1,5+2,0_CMU	320	8010	480	271,2	7,68
63322556	WP053119Q	OP090R13	OK	4,07	1,1+1,5+2,0_CMU	320	8010	480	277,4	7,69
63513790	WP053119Q	OP090R13	OK	4,16	1,1+1,5+2,0_CMU	320	8010	480	271,4	7,7
63565394	WP053119Q	OP090R13	OK	4,04	1,1+1,5+2,0_CMU	320	8010	480	279,3	7,68
63776793	WP053119Q	OP090R13	Burnt	4,25	1,1+1,5+2,0_CMU	320	8010	480	281,6	7,68
64051782	WP053119Q	OP090R13	OK	3,89	1,1+1,5+2,0_CMU	320	8010	480	272,8	7,68
64318975	WP053119Q	OP090R13	OK	3,95	1,1+1,5+2,0_CMU	320	8010	480	273,2	7,66
64319809	WP053119Q	OP090R13	OK	3,89	1,1+1,5+2,0_CMU	320	8010	480	273,4	7,69
64319932	WP053119Q	OP090R13	OK	4,13	1,1+1,5+2,0_CMU	320	6000	480	274,5	7,7
63051247	WP053119Q	OP090R13	OK	4,01	1,1+1,5+2,0_CMU	320	8010	480	267,9	7,68
64359938	WP053119Q	OP090R13	OK	3,89	1,1+1,5+2,0_CMU	320	8010	480	266,9	7,7
64301195	WP053119Q	OP090R13	OK	4,13	1,1+1,5+2,0_CMU	320	6000	480	267,6	7,73
63902324	WP053119Q	OP090R13	OK	3,81	1,1+1,5+2,0_CMU	320	8010	480	267,7	7,68
63906002	WP053119Q	OP090R13	Burnt	3,66	1,1+1,5+2,0_CMU	320	8010	480	268,8	7,66
64356629	WP053119Q	OP090R13	OK	4,4	1,1+1,5+2,0_CMU	320	6000	480	266,8	7,71
63909501	WP053119Q	OP090R13	OK	4,01	1,1+1,5+2,0_CMU	320	6000	480	276,2	7,7
64291719	WP053119Q	OP090R13	OK	3,89	1,1+1,5+2,0_CMU	320	8010	480	272	7,68
63908362	WP053119Q	OP090R13	OK	4,01	1,1+1,5+2,0_CMU	320	8010	480	270,1	7,69

Table 12. Correlation 4

In table 12 the spot WP053119Q is analyzed and in the examined CIS it is possible to notice two incorrect points which show aesthetics defects. The Quality index assumes two values of 6,00 and 8,01. From the theory about the quality index, the value 8,01 should highlight the presence of an aesthetics defect. There is the probability that spatter is not reported by the worker that makes the ultrasonic control because the point is not located in an aesthetic position.

CIS	point	robot	Results	thickness	File SWD	force [DaN]	quality index	time [ms]	resistance [uOHM]	current [kA]
62852546	WP053136Q	OP090R14	OK	2,16	0,67+1,1+1,5_CM	300	8010	660	226,5	7,62
62857008	WP053136Q	OP090R14	OK	2,22	0,67+1,1+1,5_CM	300	8010	660	227,8	7,62
62958939	WP053136Q	OP090R14	OK	2,34	0,67+1,1+1,5_CM	300	5380	660	231,1	7,64
63044671	WP053136Q	OP090R14	OK	2,28	0,67+1,1+1,5_CM	300	8010	660	227	7,62
63260095	WP053136Q	OP090R14	OK	2,22	0,67+1,1+1,5_CM	300	8010	660	225,6	7,62
63322556	WP053136Q	OP090R14	OK	2,54	0,67+1,1+1,5_CM	300	8010	660	226,9	7,62
63513790	WP053136Q	OP090R14	OK	2,49	0,67+1,1+1,5_CM	300	8010	660	225,5	7,62
63565394	WP053136Q	OP090R14	Thin	2,05	0,67+1,1+1,5_CM	300	8010	660	223,9	7,62
63776793	WP053136Q	OP090R14	OK	2,57	0,67+1,1+1,5_CM	300	8010	660	226,1	7,62

Table 13. Correlation 5

In table 13 the spot WP053136Q is analyzed and it is possible to see a Thin defect. The Quality index is 8,01 for all the CIS except for one that is 5,38. From the theory about the quality index, the value 8,01 should highlight the presence of an aesthetics defect. There is the probability that spatter is not reported by the worker that makes the ultrasonic control because the point is not located in an aesthetic position. The incorrect point shows a low resistance with respect to the others. This can be due to the incorrect thickness of the metal sheet.

CIS	point	robot	Results	thickness	File SWD	force [DaN]	quality index	time [ms]	resistance [uOHM]	current [kA]
62852546	WP053137Q	OP090R13	OK	2,19	0,67+1,1+1,5_CM	330	7740	600	244,6	7,98
62857008	WP053137Q	OP090R13	OK	2,34	0,67+1,1+1,5_CM	330	5460	600	243,4	7,98
62958939	WP053137Q	OP090R13	OK	2,14	0,67+1,1+1,5_CM	330	8010	600	243,9	7,97
63044671	WP053137Q	OP090R13	OK	2,34	0,67+1,1+1,5_CM	330	5715	600	241,6	7,97
63260095	WP053137Q	OP090R13	OK	2,46	0,67+1,1+1,5_CM	330	5995	600	241,3	7,97
63322556	WP053137Q	OP090R13	OK	2,31	0,67+1,1+1,5_CM	330	6455	600	244,5	7,97
63513790	WP053137Q	OP090R13	OK	2,49	0,67+1,1+1,5_CM	330	8010	600	240,5	7,96
63565394	WP053137Q	OP090R13	OK	2,16	0,67+1,1+1,5_CM	330	6660	600	246,8	7,97
63776793	WP053137Q	OP090R13	Thin	1,96	0,67+1,1+1,5_CM	330	6190	600	240,6	7,97
64051782	WP053137Q	OP090R13	OK	2,25	0,67+1,1+1,5_CM	330	6720	600	245,9	7,97
64318975	WP053137Q	OP090R13	Thin	2,02	0,67+1,1+1,5_CM	330	8010	600	241,8	7,96
64319809	WP053137Q	OP090R13	OK	2,25	0,67+1,1+1,5_CM	330	6000	600	245,2	8
64319932	WP053137Q	OP090R13	OK	2,11	0,67+1,1+1,5_CM	330	8010	600	242,1	7,97
63051247	WP053137Q	OP090R13	OK	2,19	0,67+1,1+1,5_CM	330	6465	600	245,5	7,98
64359938	WP053137Q	OP090R13	OK	2,16	0,67+1,1+1,5_CM	330	6015	600	242,9	7,97
64301195	WP053137Q	OP090R13	OK	2,14	0,67+1,1+1,5_CM	330	7390	600	240,4	7,97
63902324	WP053137Q	OP090R13	OK	2,19	0,67+1,1+1,5_CM	330	8010	600	241,9	7,97
63906002	WP053137Q	OP090R13	OK	2,25	0,67+1,1+1,5_CM	330	6410	600	240,5	7,98
64356629	WP053137Q	OP090R13	OK	2,28	0,67+1,1+1,5_CM	330	8010	600	242,3	7,98
63909501	WP053137Q	OP090R13	OK	2,16	0,67+1,1+1,5_CM	330	8010	600	244,9	7,97
64291719	WP053137Q	OP090R13	OK	2,16	0,67+1,1+1,5_CM	330	8010	600	244,7	7,97
63908362	WP053137Q	OP090R13	OK	2,19	0,67+1,1+1,5_CM	330	8010	600	242,4	7,97

Table 14. Correlation 6

In table 14 the spot WP053137Q is analyzed and it is possible to see two Thin defects. The Quality index for these points assumes different values, but all the values are in the good range or in the aesthetic range. The incorrect point shows a low resistance with respect to the others. This can be again attributed to the incorrect thickness of the metal sheet.

CIS	point	robot	Results	thickness	File SWD	force [DaN]	quality index	time [ms]	resistance [uOHM]	current [kA]
62852546	WP053140Q	OP090R14	OK	2,22	0,67+1,1+1,5_CM	300	5965	660	228,5	7,62
62857008	WP053140Q	OP090R14	OK	2,25	0,67+1,1+1,5_CM	300	5995	660	229,1	7,62
62958939	WP053140Q	OP090R14	OK	2,34	0,67+1,1+1,5_CM	300	6110	660	232,4	7,62
63044671	WP053140Q	OP090R14	OK	2,22	0,67+1,1+1,5_CM	300	5955	660	228	7,62
63260095	WP053140Q	OP090R14	OK	2,11	0,67+1,1+1,5_CM	300	8010	660	226,4	7,62
63322556	WP053140Q	OP090R14	OK	2,28	0,67+1,1+1,5_CM	300	5995	660	226,7	7,62
63513790	WP053140Q	OP090R14	OK	2,43	0,67+1,1+1,5_CM	300	8010	660	227,5	7,63
63565394	WP053140Q	OP090R14	Thin	1,96	0,67+1,1+1,5_CM	300	8010	660	225,1	7,62
63776793	WP053140Q	OP090R14	OK	2,4	0,67+1,1+1,5_CM	300	5920	660	227,3	7,62

Table 15. Correlation 7

In table 15 the spot WP053140Q is analyzed and it is possible to see a Thin defect. The Quality index for this point assumes a different value but all the values are in the good range or in the aesthetic range. The incorrect point shows a low resistance with respect to the others. Once again this can be due to the incorrect thickness of the metal sheet.

CIS	point	robot	Results	thickness	File SWD	force [DaN]	quality index	time [ms]	resistance [uOHM]	current [kA]
64051782	WP053200Q	OP070R04	Thin	1,81	0,67+1,1+1,2_CM	260	8010	500	159,2	8,71
64318975	WP053200Q	OP070R04	OK	1,93	0,67+1,1+1,2_CM	260	8010	500	161,2	8,71
64319809	WP053200Q	OP070R04	OK	2,22	0,67+1,1+1,2_CM	260	8010	500	160,3	8,71
64319932	WP053200Q	OP070R04	OK	2,54	0,67+1,1+1,2_CM	260	6820	500	160,7	8,71
63051247	WP053200Q	OP070R04	OK	2,02	0,67+1,1+1,2_CM	260	8010	500	160,6	8,71
64359938	WP053200Q	OP070R04	OK	2,57	0,67+1,1+1,2_CM	260	8010	500	162,9	8,71
64301195	WP053200Q	OP070R04	OK	2,25	0,67+1,1+1,2_CM	260	8010	500	158,5	8,71
63902324	WP053200Q	OP070R04	OK	2,19	0,67+1,1+1,2_CM	260	8010	500	162	8,7
63906002	WP053200Q	OP070R04	OK	2,22	0,67+1,1+1,2_CM	260	8010	500	159,3	8,71
64356629	WP053200Q	OP070R04	OK	2,19	0,67+1,1+1,2_CM	260	8010	500	161,7	8,71
63909501	WP053200Q	OP070R04	OK	2,4	0,67+1,1+1,2_CM	260	8010	500	161,4	8,71
64291719	WP053200Q	OP070R04	OK	2,31	0,67+1,1+1,2_CM	260	6820	500	161,8	8,71
63908362	WP053200Q	OP070R04	OK	2,14	0,67+1,1+1,2_CM	260	6000	500	158	8,73

Table 16. Correlation 8

In table 16 the spot WP053200Q is analyzed and it is possible to notice a Thin defect. The Quality index for this point assume a different value, but all the values are in the good range or

in the aesthetic range. The incorrect point shows a low resistance with respect to the mean of the group, but there are other CIS with a lower resistance. So, in this case, the value of the resistance is not sufficient to evaluate the quality of the point.

CIS	point	robot	Results	thickness	File SWD	force [DaN]	quality index	time [ms]	resistance [uOHM]	current [kA]
62852546	WP053201Q	OP070R03	OK	2,16	0,67+1,1+1,2_CM	260	8010	620	161,9	8,73
62857008	WP053201Q	OP070R03	OK	2,14	0,67+1,1+1,2_CM	260	7140	620	159,2	8,73
62958939	WP053201Q	OP070R03	OK	2,16	0,67+1,1+1,2_CM	260	6060	620	164,1	8,74
63044671	WP053201Q	OP070R03	OK	1,93	0,67+1,1+1,2_CM	260	8010	620	160,6	8,73
63260095	WP053201Q	OP070R03	Burnt	1,58	0,67+1,1+1,2_CM	260	5995	620	161,8	8,74
63322556	WP053201Q	OP070R03	OK	1,99	0,67+1,1+1,2_CM	260	8010	620	158,5	8,73
63513790	WP053201Q	OP070R03	OK	2,14	0,67+1,1+1,2_CM	260	8010	620	156,7	8,73
63565394	WP053201Q	OP070R03	OK	2,02	0,67+1,1+1,2_CM	260	8010	620	157,7	8,73
63776793	WP053201Q	OP070R03	OK	2,02	0,67+1,1+1,2_CM	260	8010	620	158,4	8,73

Table 17. Correlation 9

In table 17 the spot WP053201Q is analyzed and it possible to see a Burnt defect. The Quality index for the defected point is in the good range and in the aesthetic range. Also here the quality index probably is not setup in a proper way.

5.5. End of Analysis

The analysis shows bad results considering the single parameter of the welding, but for critical defects a significant deviation of the parameters is not found. The good result is taken from the analysis of the quality index. Before the start of the project, is the quality index was not used in the plant to evaluate the welding, also because it did not have a correct setup and thus it was not able to detect a good result. From this analysis, a new project starts concerning the correct setup and implementation of the Quality Index which is based on the comparison of

the actual welding curve with the reference curve. It is therefore of paramount importance to take a significant and correct reference curve to achieve good results.

The new work starts taking a new reference curve for a welding point with high frequency of defects to check whether with the process increases the quality with the new curve. In the first two weeks of implementation, the point does not show defects because the curve is the same used by the adaptive welder system.

5.6.Future of project and implementation

It is important to correctly set up the reference curve and implement the online control quality system in all the lines where this technology is present. This could help increasing the quality of the RSW thanks to the Quality Index for ISI-Welding or other types of control index for the station with different welding system manufacturers (e.g. BOSCH).

The first goal is to finally eliminate the high-gravity defects from the line. This can be done with the correct setup of the reference curve. Changes in the process like new material, new sheet metal thickness, influence of the welding process and of the reference curve must be considered again to guarantee the robustness of the welding process. It is also important to implement an alert that reports if the points have high-gravity defects for quickly fixing and repair of the problem.

The second goal is to implement an automatic analysis of the process by evaluating for each point the result of Quality Index. This step is useful to understand if the welding process has a deviation with respect to the perfect welding. To do this it is important that the value of quality index is automatically stored in a table and for each day or shift the software evaluates the deviation and an operator can understand if the process must be modified or updated. For example, it is possible to understand if the Quality Index shows a bad result near the change of an electrode and the solution could be to anticipate the substitution.

5.7. Cost analysis of solution implementation

The project starts to increase the quality control of the RSW and removes the statistical control of the welding which are expensive for the plant. The cost analysis takes into account the elimination of the ultrasonic control and hammer/chisel check thanks to the online control that automatically stores the result of the welding in a database. The economic investments are on time and people to take the reference curve for Quality Index. This technology can be applied to all the new manufacturing lines because it does not have an extra cost since it is already included in the adaptive welding system. On the contrary the replacement of the actual line without the Quality control system is not considered because it would be too expensive.

The benefit/cost (B/C) analysis calculates the cost saving only by eliminating the worker that is in charge of the Ultrasonic control. The analysis takes into account the time that an operator needs to evaluate a single point and the total controlled points on a vehicle. The evaluation is done for the Jeep Renegade 520 model considering the total points controlled in 2017.

Time estimate to control a single point	1,134 min
Total time used to control the points in 2017 considering that 1272001 is the total number of controlled point in the year (data taken from ultrasonic reports)	24.040 hours
Hourly labor cost	24 €/h
Total labor cost in 2017 to control the RSW for Jeep Renegade	576.000 €

Table 18. Cost analysis

In the automotive industry is important to reduce the costs where it is possible without decreasing the quality. This control system for the RSW increases the quality of the welding by control of each point for each vehicle as an alternative to statistical control that cannot detect all welding defects.

Chapter 6

Conclusion

The quality of the resistance spot welding is important for the final product and the process must guarantee a point without serious defects which may endanger the quality of the vehicle. The correlation between the output parameter of the welding system and the ultrasonic control reports doesn't show good results. Thanks to the analysis presented in this thesis a solution already included in the system was found through the use of the so-called Quality Index. This solution must be correctly implemented to improve the quality of the weld. New reference curves are taken for some example points with a greater number of defects from the beginning of the year, to check if the system can work better with the correct setup. In two months these points have never shown a defect, because the reference curves also helped the adaptive system during welding. It is important to take new reference curves after the "slow build" (run-up of process industrialization), when the process is stabilized. Thanks to this project the plant takes care of properly set up the tools where this control is already present but doesn't work in the correct way. In the near future new lines must include this tool for a better process control. The statistical control cannot be removed yet, until the welding system automatic generates an alert if a serious defect occurs, but the number of offline control can be reduced if the process guarantees good results with the decrease of the non-compliances. This project is not over and it will continue with the verification of other production lines.

References

Sites:

- <https://www.rofin.com> (laser technology)
- <https://www.sciencedirect.com>
- <https://www.ieeexplore.ieee.org>
- <https://www.geschmidt.com/weldhelp-resistance-welding-troubleshooting/>
- www.varendt.co.uk/.../GE-Krautkramer-USM...perator-Manual.pdf
- www.milinc.com/.../nondestructive-testing-ndt/ultrasonic-inspection
- <https://www.fcagroup.com/plants/en-US/Melfi/Pages/default.aspx>

Books:

- Okan Okay Koçak. (2003). Defect assessment of spot welds by ndi. Ankara, Turkey. The Middle East Technical University
- Kang Zhou & Lilong Cai. (2013). Online nugget diameter control system for resistance spot welding. London, UK. Springer-Verlag

Standard FCA norms:

- Conformity checks for welds and mechanical joints
- Metals joining design
- Electric welding for lap resistance
- Ultrasound control of the weld points